

Computer Modelling of Complex Systems with Applications in Physical and Related Areas

Yu Feng B.Eng M.Sc.

Submitted in fulfilment of the requirements for a

Ph D Degree, 1997

School of Computer Applications

Dublin City University

Dublin 9

Supervisor Dr Heather J Ruskin

July 1997

Declaration

I hereby certify that this material, which I now submit for assessment on the programme of study leading to the award of Ph.D. is entirely my own work and has not been taken from the work of others save and to the extent that such work has been cited and acknowledged within the text of my work.

Signed: YWTg Date: 14/09/97

Acknowledgements

I would like to express my heartfelt gratitude to my supervisor, Dr Heather J Ruskin, for her supervision, guidance, encouragement and support over the last four years. At every stage of development, she was generous with her time and comments. Her faith, patience and understanding helped make it possible for me to finish.

I would like to express my sincere thanks to Prof Michael Ryan, for his help whilst I was studying in the school of Computer Applications. Many thanks are also expressed to Dr David Sinclair, Dr James Power, Mr Jim Doyle and Ms Anne O'Brien for all the invaluable help they gave me.

I would also like to thank all the former and current postgraduates whom I have met in the computer lab and the Irish girls with whom I have been lived in Cremore Heights. Especially to Sandra Ward, Gary Leeson, and Dara Mahon, who helped me to know Irish humour and Ireland, improve my English, and have provided much support, patience and encouragement since I studied here.

I would also like to thank my family and relations for all their love, expectation and encouragement they have shown over the years. I would like to thank my Chinese friends for their help and understanding while I have been away from home.

Finally, I would like to thank the school of Computer Applications for providing me with the opportunity and the funding to undertake this research. This has also given me the opportunity to learn western culture and enjoy my Irish student life style in Dublin.

Abstract

Computational modelling techniques have been applied in physics, biology and other fields for decades to investigate the scale-invariant properties in non-equilibrium complex (many-cell) systems. Specific examples have been considered to underpin the simulation of cellular systems, i.e. sandpiles as simple models of transport phenomena, and soap froths as models of many-cell cellular networks. A number of characteristic properties have been investigated to explore common features of complex systems. Particularly interesting for the simple sandpile automaton is the achievement of the critical state through the phenomenon known as self-organised criticality (SOC).

Various simulation algorithms e.g. cellular automata, direct simulation and Monte Carlo have been used to model the sandpile and froth systems respectively. The studies of a directed and dissipative CML sandpile model provide evidence for the occurrence of SOC, with the system characterised by simple power-law distributions. For the soap froth model, the effect on the evolution of the presence of defects is investigated, together with the implications of varying the amount of disorder. Scaling properties obtained, for various initial conditions, are given in detail. The improvements on methods of computational modelling, and the limitations of software and hardware implementation are also briefly discussed.

Table of Contents

Chapter 1 Introduction to the Nature of Complex Systems	1
1 1 Brief Review of "Cellular" Systems	1
1 2 Type of Systems and Applications	1
1 3 Computational Modelling Techniques	2
1 4 Scope of Thesis	4
Chapter 2 Computational Science (Scientific Computing) and Simulation Techniques	6
2 1 Introduction	7
2 1 1 Computational Science / Scientific Computing	7
2 1 2 Model, System, and Simulation	7
2 1 3 Computational Model	9
2 1 4 Complex (Many-body) Systems	10
2 1 5 Why do we Need Computer Simulation?	11
2 2 Computing Environment	12
2 2 1 Hardware Capability	12
2 2 1 1 Overview on Architecture Principles	12
2 2 1 2 Storage and Parallelism	13
2 2 1 3 Parallel Architectures	14
2 2 1 4 Dedicated Machines	15
2 2 2 Machine Performance--an Illustration	16
2 2 3 Current software Techniques for Handling Updating	17
2 2 3 1 Algorithm Requirements	17
2 2 3 2 Updating Algorithms Sequential Updating	17
2 2 3 3 Simultaneous (Parallel) Updating	18
2 2 3 4 Language Compilation	19
2 3 Simulations for Complex Systems	20
2 3 1 Simulation Classifications	20
2 3 1 1 Discrete and Continuous Models	20
2 3 1 2 Stochastic and Deterministic System Problems	21

2 3 1 3	Equilibrium and Dissipative Systems	22
2 3 2	Direct and Indirect Simulation Methods	22
2 3 3	Cellular Automata, Monte Carlo and Molecular Dynamics	24
2 4	Simulation Techniques Cellular Automata	25
2 4 1	Cellular Automata Description of Mechanism	25
2 4 2	Background	27
2 4 3	Classification	28
2 4 4	Applications	29
2 5	Simulation Techniques Monte Carlo	30
2 5 1	Introduction	30
2 5 2	General Principles of the MC Methods	31
2 5 3	Metropolis Method	32
2 5 4	Applications	32
2 6	Other Simulation Techniques e.g. Molecular Dynamics	33
2 6 1	Introduction	33
2 6 2	Applications	34
2 6 3	Monte Carlo and Molecular Dynamics	35
2 7	Applications of Simulation Methods- Specific Cases	36
2 7 1	CA Models and the Phenomenon of SOC Building Piles of Sand	36
2 7 2	Cellular Networks, Froth Evolutionary Behaviour	37
2 8	Summary	38
Chapter 3 Simple Dynamical Cellular System Models		39
3 1	Simple Cellular Automata System and SOC	39
3 1 1	Simple Cellular Systems	39
3 1 2	Models and Applications	40
3 1 3	Scale-Invariance and Self-Organised Criticality (SOC)	41
3 2	Sandpile Automata and SOC	43
3 2 1	Basic Sandpile Driven Model	43
3 2 1 1	Discrete Driven Models	43
3 2 1 2	Catalogue of Sandpile Models	47

3 2 2	Current Studies on Sandpile and SOC	48
3 2 2 1	Theoretical Results	48
3 2 2 2	Experimental Results	49
3 2 2 3	Computer Simulation Results	51
3 3	Studies of Sandpile Models	51
3 3 1	Simple Sandpile Height Models and SOC ..	51
3 3 2	Results and Conclusions	52
3 3 3	The Directed Sandpile Model with Holes Introduction for a Preliminary Note	54
3 4	Dissipative Sandpile Models	57
3 4 1	Nonconservative Sandpile Model	57
3 4 2	Various Dissipative Models	58
3 4 2 1	BTW and Zhang Dissipative Models	58
3 4 2 2	CA and CML Dissipative Models	59
3 4 3	Results for CA and CML Models	60
3 4 3 1	Dissipative Sandpile, CA Model	60
3 4 3 2	Dissipative Sandpile, CML Models	61
3 4 3 3	Conclusion	64
3 5	SOC and Complex Systems	65
3 6	In Summary	66
Chapter 4 Cellular Network Models		68
4 1	Background and Introduction	68
4 1 1	Cellular Structures	68
4 1 1 1	Introduction	70
4 1 1 2	History	71
4 1 2	Applications Soap Froth Model	71
4 1 2 1	Basic Geometrical Relations and Topological Processes	73
4 1 2 2	Von Neumann's Law and Scaling State	74
4 1 2 3	Lewis and Aboav-Weaire Laws	75
4 1 2 4	Simple Soap Froth Model	76

4 2	Current Studies of Froths	76
4 2 1	Experimental Studies and Results	77
4 2 2	Theoretical Results	79
4 2 3	Computer Simulation Algorithms and Early Results	80
4 2 3 1	Direct Simulation	80
4 2 3 2	Monte Carlo Method	83
4 2 3 3	Topological Analysis (Vertex Model)	84
4 2 3 4	The Potts model	85
4 3	2D Froth Models- Implementations via Direct Simulation Methods	86
4 3 1	2D Froth with Voronoi Network	86
4 3 1 1	Voronoi Network	86
4 3 1 2	Voronoi Froth Models- Large Scale Systems	87
4 3 2	Defective 2D Froth Models The Simple Case	88
4 3 2 1	Ordered and Disordered Froth	88
4 3 2 2	Single Defect 2D Froth Model	90
4 3 3	Multiple Defects in an Ordered / Disordered Froth	92
4 3 3 1	Multiple Defects in an Ordered Froth	92
4 3 3 2	Multiple Defects in a Disordered Froth	92
4 4	Results and Discussion	95
4 4 1	Voronoi Disordered Froth	95
4 4 1 1	Additional Notes on Direct Simulation Implementation- Performance	95
4 4 1 2	Results of Froth Simulation	96
4 4 2	Froth with a Single Defect	98
4 4 3	Monodisperse and Polydisperse	104
4 4 3 1	Results and Discussion	104
4 4 3 2	Conclusions on Single/Multiple Defect(s)	112
4 4 4	A Note on Stages of Evolution in a 2-D Froth	113
Chapter 5 MC Simulations and other Considerations		119
5 1	System Simulation with MC Introduction	119
5 1 1	Simple Systems	120

5 1 2	MC for Froths General Points	120
5 1 3	Implementation for 2D Froth	121
5 1 4	Froth Coarsening	124
5 1 4 1	Notes by MC	123
5 1 4 2	Performance under Different Choices for $\langle A \rangle$ and λ	126
5 1 4 3	Performance of Bubble Area	127
5 1 4 4	Summary	129
5 1 5	Technical Implications of 3D Froth	130
5 1 5 1	Theoretical Implication	130
5 1 5 2	Technical Implications for Froth by MC Method	134
5 2	Other Techniques	136
5 2 1	CA for Grain Growth	136
5 2 2	Molecular Dynamics on Wet Foam	138
5 3	Computer Simulation Implementation	138
5 3 1	Simulation Approaches	138
5 3 2	Languages Requirement	149
5 3 3	Algorithms Limitation	140
5 3 4	Limitation of Simulation Methods	141
Chapter 6 Conclusions and Comments		143
6 1	Introduction	143
6 2	Techniques Implementation	143
6 3	Cellular systems and Phenomena Exhibited	146
6 3 1	SOC and Simple Systems	146
6 3 2	Cellular Networks	147
6 3 3	Common Features .	148
6 4	Suggestions for FutureWork	149
References		152

Chapter 1 Introduction to the Nature of Complex Systems

1.1 Brief Review of "Cellular" Systems

Traditional mathematics offers few methods for building a comprehensive theory of complex dynamical systems. A broad research program to study such systems grows naturally out of studies on complex (many-cell) systems. The prototypical examples are cellular automata and random cellular networks, that appear to be analytically less tractable. Studies of these systems lead naturally to consideration of the geometry of the systems' parameter space and the effects of parameter changes on system behaviour.

Cellular Automata were invented by John Von Neumann (1966), who was interested in connections between biology and the new science of computational devices, i.e. automata theory. This was pursued by the mathematician Stanislaw Ulam, who suggested using cellular automata as a framework to solve self-reproduction problems, (Burks (1966)). The Game of Life was created by John Horton Conway to demonstrate universal computation in cellular automata, (Berlekamp et al (1982)). Attention has been attracted to the Game of Life and its relation to some scientific problems, Poundstone (1985), and in this context Wolfram (1984) (1986) proposed a classification of cellular automata. A characteristic feature of these cellular automata systems is that they consist of large numbers of simple identical "units" with local interaction. For a review, see Gutowitz (1990), Mitchell (1996).

Materials consisting of cellular network structures such as metal grains and biological tissues are common in nature, where the surface energy of the boundaries makes the pattern unstable, causing certain grains to shrink and eventually to disappear, Weaire and Rivier (1984). In cellular network systems, individual interaction has a strong influence not only on its near-neighbours and next-neighbours, but extending to all the individuals within the system. For a review, see Glazier and Weaire (1992), Stavans (1993).

1.2 Type of Systems and Applications

The study of cellular systems in nature has been a major subject in physical, chemical, biological and related sciences over decades. Its applications cover a wide range of phenomena and may broadly include, but are not limited to

- Simple cellular systems e.g. model of transport phenomena, earthquake occurrences, traffic jam, forest fire, spin glasses, turbulence, Biological evolution and ecological balance, simple epidemic models, immunological reactions models and financial market fluctuations
- Cellular networks e.g. structure and evolution of froths and foams, modelling of polycrystalline alloys, ceramics structures and lipid monolayers, grain growth problems and physics of garnet films

In most cases, the simple cellular system is defined as a lattice in position space. Sites may represent points in a crystal lattice, with values given by some quantified observable or corresponding to types of units. The sandpile model, the dynamical Ising model and other lattice spin systems are simple types of such single cellular automata system models. Many share the characteristic behaviour of Self-organised Criticality (SOC), a concept introduced to describe the process of achieving a critical state through dynamic adjustments intrinsic to the system as opposed to governed by an external parameter, Bak (1996)

We concentrate predominantly on simulations of physical and related systems, where a satisfactory "run" requires the computation of billions of events to describe formation, growth or evolution. While both experimental and theoretical methods offer basic approaches to understanding complex phenomena, some systems are difficult to characterise precisely because they are of large size and involve complex interactions. Experimental work is typically difficult to perform, due to the many parameters involved and theoretical solutions are similarly not usually feasible or are limited to extreme or equilibrium behaviour for simplified or approximated systems. The rapid growth in power and availability of modern computers means that, in a simulation, the size of the system may be varied and

complex interactions controlled with relative ease. This not only serves to stimulate experimental work and develop new insights to the theoretical system, but also provides a means of filling the gap between them, Heermann (1990)

1.3 Computational Modelling Techniques

The interdisciplinary area of computational science has grown from the recognition that physics, chemistry, biology and related fields have a common need for efficient algorithms, together with sophisticated hardware and software to address complex problems, Wilson (1987). Simulation techniques form one of the most important tools in computational modelling and can be used to study a diverse range of phenomena.

Computational modelling can be used in a variety of different ways. The traditional methods of direct simulation solve equations numerically in a straightforward way, providing a direct computer analogue of the physical system under study. Examples are discussed e.g. by Koonin and Meredith (1990), and by Gould and Tobochnik (1996). More recently, simplified computational models and indirect simulations have been used more extensively, where those include enhancements of early Monte Carlo methods, (based on hypothetical statistical populations), direct modelling of discrete system elements (using e.g. cellular automata), modelling of system interactions through molecular dynamics simulations, neural network, and other augmented techniques such as genetic algorithms and so on. Recent references include Wolfram (1983) (1986), Jam (1992), Gaylord and Wellin (1995), Frankel and Smit (1996), Crandall (1996) and Giordano (1997).

The choice of methods is clearly wide and simulations have been applied in many research fields. The choice of a particular method depends both on the details of the system and the information sought, but also on practical limitations, since the more detail retained on the system, the more all the demands made of the simulation. Physicists may wish to provide analogies to the behaviour of non-linear dynamical systems and to explain the complex natural phenomena, computer engineers may desire to improve the power of a given device; biologists may wish to model the spread of an epidemic or assess macroscopic behaviour.

from studies of molecular dynamics and so on, nevertheless the principles of such simulations remain the same

Specific examples focussed on in this thesis, to underpin the simulation of cellular systems, are the sandpile automaton and the 2D soap froth, which provide simple models of complexity with different interaction features and system constraints. These also provide idealised models for a number of more sophisticated applications and as such, merit attention both in their own right and for the insight they afford. Furthermore scale-invariance in non-equilibrium complex systems is common and the sandpile automaton as a paradigm for SOC provides a means of investigating this property through numerical simulations. Implementation details of the different simulation approaches are discussed in the context of these real problems.

1.4 Scope of Thesis

The arrangement of the material in this thesis is as follows

Chapter 2 defines what is meant by a simulation and why we need to use computer simulation to deal with complex systems. The various categories of simulation methods are described and distinguished, e.g. cellular automata, Monte Carlo and Molecular Dynamics.

Chapter 3 reviews the cellular automata method applied to scientific systems. Sandpile models and the phenomenon of self-organised criticality, (SOC), are discussed in this context. Numerical simulations of a directed sandpile model and dissipative sandpile models are analysed and reported with simulation statistics used to provide evidence of the occurrence of SOC.

Chapter 4 focuses on a model for 2D froth, exploring via direct simulation, the effect on froth evolution of the presence of defects, large amounts of disorder and so on. The strengths of the direct method are discussed in some detail, together

with practical considerations for extending the size of the systems investigated where a large amount of information on the system structure must be retained

Chapter 5 discusses further the increase in complexity involved in simulating a real network and considers alternative modelling technique. Hardware and software limitations are considered briefly, together with the improvements which might reasonably be expected through upgrading

Chapter 6, in the final chapter, we comment on some of the implications for simulating complex physical systems. A synopsis of system type, methodology and performance is given and recommendations for further methodological studies and improvement are made, together with suggestions for extending work on the problems considered at relatively low computational expense

References and appendices are given at the end of the thesis, where the latter include copies of published papers, algorithm details, detailed figures and a table of example statistics of froth evolution and a diskette containing full details of the programmes used

Chapter 2 Computational Science (Scientific Computing) and Simulation Techniques

Scientific problems nowadays are not solved solely by the means of conventional experiments and theoretical considerations. A major new ingredient is the use of computers to aid research. It is well-known that physics, chemistry, medicine, astronomy and other sciences share a common need for efficient algorithms, system software, and computer architecture to address large computational problems. A new interdisciplinary science, *computational science (or scientific computing)*, which is focused on using computers to analyse scientific problems has been devised to meet the need and has attracted much attention, Wilson (1986) and references therein. Simulation techniques have played and continue to play an important role in computational science studies.

Simulation is a process which allows us to understand the behaviour of an existing or potential system by observing the behaviour of a model representing the system. With the advance of simulation approaches in recent years, it provides increased efficiency in implementation of a complex system without actually constructing or physically dealing with the system itself. All the old investigation problems and some completely new concepts, such as the fractal behaviour of nature are now studied through computer simulation techniques. The applications include a diverse array of phenomena, in fields ranging from physics and other natural sciences, from meteorology to social, arts, political and economic processes.

In this chapter, we first introduce the notion of computational science and its components: model, system, and simulation. Then, we categorise the simulation classification and discuss simulation as a methodology for focusing predominantly on the application to complex physical and related systems. We present the architecture needed and distinctive features of the software and describe various types of simulation techniques and their applicability. A discussion of the underlying theoretical basis for the different techniques is also given in general terms. Specific details are developed for the problems of interest in subsequent chapters.

2.1 Introduction

2.1.1 Computational Science / Scientific Computing

Computational science relates to the knowledge and techniques required to perform computer simulations and other computationally intensive problems through model analysis in the respective disciplines, Wilson (1986) Its characteristics include

- having a precise mathematical statement,
- being intractable by traditional methods,
- having a significant scope,
- requiring an in-depth knowledge of science, engineering (or the arts)

Thus, computational science, involving mixed areas of an applied discipline, seeks to obtain an improved understanding of some complex phenomena through the implementation of the problem by a suitable computer architecture and algorithms. In short, it means to investigate a complicated system by an appropriate computational model usually via computer simulation. Various research fields, e.g. biology, physics, economics, have established branches of scientific computing endeavour and have emerged as recognised topics in computational science. Unfortunately, the computer science community has been slow to meet this development, so that redundancy of effort has ensued.

The use of simulation in research and development is now established as a third basic methodology, complementing traditional theory and experimentation, Decker and Johnson (1993). The importance of simulation is illustrated by results achieved for fundamental problems in science and engineering that could be advanced only by applying computational techniques. Some examples include global climate modelling, turbulence, and biomolecular modelling, Wilson (1987). A detailed description follows of what is involved in simulation of a system.

2.1.2 Model, System, and Simulation

The application of modelling techniques for analysis of *system dynamics* is a popular methodological approach in various areas. For the solution and flexible

application of such models, simulation is of increasing importance. It has been defined by Naylor et al (1986)

“*Simulation* is a technique for conducting experiments on a digital computer, this technique involves certain types of mathematical and logical models that describe the behaviour of business, economic, physical or chemical systems or some component thereof over periods of time ”

In general terms, *simulation* is a form of experimentation that involves asking decisions in a simulated environment - a laboratory setting that replaces real world conditions In scientific terms, *simulation* refers to the process of designing a *model* of a real *system* and conducting experiments with the model for a better understanding of the behaviour of the system, or evaluating various patterns for the operation of the system, Bratley et al (1983), Fishwick (1995)

Here, a *system* can be defined as the understanding of the relationship between things which interact For example, a pile of sand is a system, in which grains interact based upon how they are piled If the pile is unbalanced, the interaction results in movement of the grains until they find a new condition under which they are in balance, (either dynamic or static) Isolated groups of sands which do not touch one another are not a system, because there is no interaction

A system can be *modelled*, i.e. one can create another system that supposedly replicates the behaviour of the original system. Theoretically, e.g. it is assumed that if conditions for a second group of sand grains replicate the first set, then, we can predict that they will achieve a new configuration that is the same as the first one Alternatively, we can use the mathematical representation of sand grains by appropriate laws, to predict how future piles of the same or different types of sand will interact Mathematical modelling is thus fundamental to the description of system behaviour

A *model* is therefore, a simplified representation or description of the real system intended to be understood As some complex systems may be beyond our intuitive knowledge, we seek to study and analyse the real thing by constructing models In most areas of science and engineering, physical laws are applied to obtain mathematical models for analysing systems Model building is relatively easy if the physical laws are known and the system is compact and well-behaved However,

the modelling of complex, large-scale systems is difficult since many procedural elements can not be described directly. Simulation approaches are used to overcome these difficulties.

Generally speaking, simulation modelling assumes that a system is computable. Here a system is characterised by a number of variables, where each variable value represents a unique state of the system. The dynamic behaviour of the system is observed under different states. Thus, the outstanding advantage of simulation is not only to fully obtain the system's variability and sensitivity with changing conditions, but also to increase its safety and productivity. Furthermore, whenever results obtained by simulation modelling are different from those obtained by other methods, it is the only approach that allows a re-test of system behaviour. Therefore, it is capable of providing insight into aspects of transient misbehaviour, such as temporary influences by external constraints, which is not available for any other techniques.

2.1.3 Computational Model

A *computational model* of some process is, essentially, no more than a computer program. It is a program for which claims are made, DeVries (1994). The structure of the program reflects that of the mechanisms assumed by theory for the process under study. A computational model may be a mechanistic model, or an input/output functional model, or both. Observation of a particular model's behaviour can provide precise information on the long-term effects of the system. Thus, computational models can be a source of significant insights for other similar systems as a new methodology to deal with complex systems.

A computational model can also be very effective at driving theory development. Usually, it is not the case that a written program for a model is based on a well-understood or completely perfect theory. However, by exploring computational variants, the theoretical details can be developed to a deep level, which otherwise is unattainable. For example, Partidge et al (1984) used a computational model to refute a widely-held theoretical belief, and hence presented a revision of the acceptance of a class of theories of habitation behaviour.

2.1.4 Complex (Many-body) Systems

Complex systems span physical science, mathematics, computation and biology. In general terms, a complex system is defined as a network of interacting objects, agents, elements or processes that exhibit a dynamic, aggregate behaviour, Bonabeau and Theraulaz (1994). The action of an object possibly affects subsequent actions of other objects in the network, so that the action of the whole is more than simple sum of the actions of its parts. In other words, a system is complex if it is not reducible to a few degrees of freedom by statistical description, i.e. forms a so-called *many-body* system.

For instance, a sandpile can be built in the process of adding grains of sand into a pile. With the sand slides become bigger, the pile becomes steeper, and eventually, some of grains topple till they fall out of the boundary. At this point, the system is far away from equilibrium, and its behaviour and properties can no longer be understood in terms of those of the individual grains. The sandpile generates a new dynamic, which can be investigated through the whole pile rather than every single grain. Therefore, the sandpile is a complex system.

In general, we are interested in predicting, both qualitatively and quantitatively, the behaviour of a complex system by means of a few relevant physical elements. It is assumed that a large number of independent agents are interacting with each other in many different ways. Accordingly, system function may reflect various relationships between them, e.g. the billions of interconnected neurones make up a brain. Waldrop (1992) has pointed to four aspects of systems which characterise complexity.

- 1 Systemic interactions can lead the system to spontaneous self-organisation.
- 2 Complex systems do not just *respond* to events. For example, recent research has found that species in biology evolve for better survival in a changing environment.
- 3 Distinction between complicated and unpredictable. Complexity has its dynamic aspect. Every complex, self-organising, adaptive system possess a kind of dynamism that makes it qualitatively different from static objects, e.g. snowflakes, which are merely complicated.

4 Complex systems are more spontaneous, disorderly and alive. However, their unusual dynamism may also be far from the unpredictable circuit known as chaos.

It was difficult to study complex system in detail until recent decades because of the high computational power required. For complex systems in any specified area, the whole system may demonstrate a global dynamic which is not easily predicted from those of the individual components, thus, much research tends towards using discrete rather than continuous modelling and corresponding simulation approaches. It is also possible to analyse the behaviour of individuals based on a large scale network. Most investigations are concentrated on considering the behaviour and properties of interconnected groups.

2.1.5 Why do we Need Computer Simulation?

Computer simulation provides a powerful way of solving problems. For some exactly soluble problems, e.g. in physics, a complete specification of a system's microscopic properties leads directly and easily to an explanation of macroscopic properties. One example is that of idealised models like the perfect gas or crystal, where the Hamiltonian directly gives the state equation, Baxter (1982). In studies of more complex systems, however, there are no exact solutions available, and in reality it is too costly to examine every possibility and too difficult to analyse their behaviour based on a straightforward approximation scheme. Computers typically are used for incidental calculation in this type of work.

For scientific problems, the computational aspect becomes more important because computer simulation has the flavours of both theoretical and experimental features. A good theoretical background is the premise to studying a subject by simulation methods. On the other hand, analytical results do not provide solutions to diverse problems. Pure theoretical approaches tend to be applicable only to very simplified models. Simulations are a useful learning tool for a system under many and varied conditions, Wagner (1975). e.g. describes setting up a simulation of a loading dock with ships moving in and out at specified tides more cheaply and easily than having the ships physically moving in and out. A forest fire simulation is more easily and

less dangerously observed than firing the nearest forest, Ball and Guertin (1992), Duarte et al (1994)

The results of computer simulations may also be compared with those of theory and real experiments. They provide a test of the underlying model used and, eventually, if the model is a good one, the simulator hopes to offer insights into the limitations of theory and experiment to assist the interpretation of new results. This dual role of simulation serves as a bridge between models and theoretical calculations, and between models and experimental results. When dealing with non-linear phenomena, computer simulation of an idealised model of interest enables sensitivity analysis via a specified algorithm, Binder (1986). Given this connecting role, and the way in which simulations are analysed, those techniques are often called computer experiments as well, Allen and Tildesley (1990). Furthermore, an important fraction of the human knowledge about critical phenomena and phase transitions is due to computer simulations performed on statistical models, Stanley and Ostrowsky (1986). The study of some new research field, like aggregation phenomena, is wholly based on computer simulation and experimental data without theoretical understanding to date. More details on computing environments, simulation techniques and applications are discussed in the next Section.

2.2 Computing Environment

2.2.1 Hardware Capability

2.2.1.1 Overview on Architecture Principles

In the hardware processing for large scale simulations, it is important to tune the machine to the needs of the problem being investigated. We consider the structure of the hardware with respect to storage organisation, processor organisation, connectivity etc.

Vector computers have been used for scientific computing since their development in the 1970s. The first supercomputer architectures included one or a few fastest available processors to increase the packing density, minimise switching time, pipeline the system, and apply vector-processing techniques. The main task is to

repeatedly use a small set of program instructions repeated for multiple data elements, Hwang (1993) Vector processing has proven to be highly effective for numerically intensive applications, but not for more commercial uses, such as online transaction processing or databases

2.2.1.2 Storage and Parallelism

In order to obtain as much memory as possible, it is desirable to introduce a parallelism concept and construct a parallel approach. In general, approaches to parallelism are classified into the following categories: event, geometric, and algorithmic parallelism, where event parallelism is the most straightforward and easily applicable.

Parallelism has played an important role in computer development in recent years. It is a popular approach for the designers of current supercomputers. This provision in a computer system allows us to utilise the maximum amount of concurrency and treat the problem with the minimum programming. Apart from the computational power and acceleration of algorithms, parallelism brings with it a new view on scientific and other processes. Generally, various levels of parallelization can be identified. These are respectively

(i) Instruction level parallelism which is the heart of all "multispin" coding algorithms. This can turn a normal scalar computer into a mini-parallel computer, and also provides the basic programming tool for SIMD (Single Instruction Multiple Data) machines.

(ii) The chaining level of parallelism, which is closely associated with vector computers and which typically, can execute a multiplication instruction and an addition instruction simultaneously. More sophisticated machines such as the CRAY YMP can execute logical and shift operations simultaneously.

(iii) Parallelism can also be introduced at a higher level in the form of multiple vector processors which can execute different parts of a loop simultaneously and spread loops automatically. Such systems clearly represent the emerging trend in supercomputing architecture e.g. CRAY XMY.

The parallelism approach is considered an appealing one because it can accelerate the execution of a single program and increase throughput and reliability. The existence of an independent control unit makes possible to execute parallel loops with branching, subroutine calls and random memory activity as compared to single processor vector machines which have insufficient computational resources to handle the complexity of the problems and achieve the accuracy required.

2.2.1.3 Parallel Architectures

In the 1980s, the first massively parallel processors began to appear with the single goal of achieving far greater computational power than vector computers by using low cost standard processors. Theoretical models of parallel computing illustrate a number of possible parallel computer architectures, but not all of these have physical realisations. The limitation includes the number of processors, their mode of operation, the memory organisation and the connectivity between the processors. The number of possible combinations is quite large.

There are two main categories of structures on most existing parallel machines. On the one hand, there are machines with a small number of very powerful processors, similar to the CRAY and Alliant which have only two, four or eight processors. On the other hand, there are machines with a very large number of processors, each of which is much less powerful and indeed some of which have only bit-level capabilities. Examples include the Connection Machine, Heermann (1991).

A further classification on the various types of machines include Single Instruction Multiple Data (SIMD) and Multiple Instructions Multiple Data (MIMD). The instruction of SIMD is broadcasted by an external controller and executed by the processors. This type of architecture is most effective when it can exploit parallelism at the level of the data on which it operates, this means that the problem can be solved by simultaneous operation on all of the data elements involved. The Connection Machine is an example of SIMD type. One of these, the CM-2, is considered, for example, to be a very good tool for cellular automata simulation and in addition, provides a useful means of exploiting the natural parallelism of the spatial grid as well as its capacity to perform efficient communications with neighbouring data points. In terms of the cellular automata example, one of the

main virtues of the CM-2 is that it has a Boolean hypercube configuration which means that it allows using a code indexing scheme to embed multi-dimensional grids into the hypercube so that nearest neighbours are naturally preserved

Machines such as the CRAY (mentioned previously) have the feature that each of the powerful processors can operate more or less as a conventional computer independent of the other processors and these thus belong to the MIMD class

2.2.1.4 Dedicated Machines

For some problems, such as many which arise in statistical physics, the computer time required for the solution is *prohibitively large* for a conventional computer. This is an obvious and important reason why we do not use a general purpose computer but endeavour rather to create special purpose machines in order to make best use of the time and substantial computing power which is available. As an example, again taken from physical applications, the investigation of the spin glass problem on a special purpose computer used the equivalent of one year of CRAY time!

A dedicated machine which can match either the problem itself or the particular algorithm can be used to solve the problem in a relatively short time. Moreover, the price of a dedicated machine may be cheaper than a conventional one because although it needs more silicon chips these are inexpensive and readily available.

There are several specific machine types that have been tried on cellular automata since these were first introduced by von Neumann (1951). The first CA machine was created by Toffoli et al (1981). Designated CAM-6, it provided an array of 256 by 256 locally connected cells, each one with four bits of state. The state of every cell is updated 60 times per second. Although it is a sequential machine, its execution is very fast with a performance comparable to a supercomputer. The cellular computer is used for its computational capacity because it is comparable to the case for a general-purpose computer. In particular its capacity means that it can be used as an experimental environment for modelling abstract or real physical and related phenomena.

The main drawback of this kind of architecture is the increasing size of the look-up table. For instance, if we have three planes with 9 bits per plane, the look-up table should store $2^{27} \times 3$ bits, i.e. ≈ 50 Mbyte of information.

Another dedicated machine is the Réseau d'Automate Programmables 1 (RAP 1), which is used for modelling fluid dynamic behaviour and cellular networks, Manneville (1989). Such machines can be considered as simplified versions of the Connection Machine. The disadvantage of a special purpose machine lies in its inflexibility. It is difficult to use it directly for a new system involving new techniques and modified algorithms.

2.2.2 Machine Performance--an Illustration

Considerations of applications of large-scale simulations on general purpose machines can be illustrated by a review of the results of implementations of selected programs on two scalar mainframe machines, a vector computer, and on a SIMD and MIMD computer by Kohring (1991). The speeds achieved are described in terms of the MUPS (millions of sites updated per second). This is a convenient measure of performance, given that such programs typically consist almost entirely of integer and logical instructions and not of floating point operations. Kohring gives an example of cellular automata. On the scalar computer, SUN Sparc-1 and IBM-3090, the MUPS speed was 1.6 and 2.7 alternatively. On the CRAY XMP where the individual processor is a high-performance vector machine, the speed was 233. For the Connection Machine, CM-2 16(384-processors, SIMD computer), the speed was 270, compared to 1690 on the MIMD computer CRAY YMP/832 8-processors. This last is clearly faster than all others to date and has considerable implications for researchers hoping to achieve comparable performances on less-sophisticated systems for similar classes of problems.

2.2.3 Current Software Techniques for Handling Updating

2.2.3.1 *Algorithm Requirements*

In large scale simulations of representations of real systems, it is obvious that the development of the basic hardware has been insufficient, in part because problems which are challenging in their own right must be solved in order to *construct* the machines as well as achieving more computational power. Rather than relying on new hardware developments, therefore, we need to improve the software techniques so that the hardware can run the simulations with maximum efficiency given the current provision. Furthermore, it is also necessary to develop algorithms which can be efficiently implemented on a *variety* of machines with only minor programming changes. We next discuss some algorithms and how these handle the updating of results in fixed provision hardware.

2.2.3.2 *Updating Algorithms: Sequential Updating*

Many problems that are of interest in numerical investigations, for example the solution of systems in statistical physics, require the simulation of a large number of simple variables, each of which is represented by a small number of bits or single bits. General-purpose computers usually provide complicated operations on long data words. The sequential updating procedure consists of updating the variables, one by one, in either a random or a prescribed periodic order. The simple implementation of this process can be carried out on any computer with, for example, a FORTRAN 77, or FORTRAN 90 compiler since all the sites have to be updated at the same time.

It is clear that sequential updating of the code is extremely inefficient. The ideal rule we take should be inherently parallel and simultaneously applied to all the sites for a complete realisation of the system. The obvious failing, therefore, is that this implementation wastes *enormous* amounts of memory. In this case, it involves a large number of useless computations since the CPU operates on overall words rather than those bits which contain the relevant information. The states of the system are typically binary 0 or 1, thus it is sufficient to use one word for several bit variables.

2.2.3.3 *Simultaneous (Parallel) Updating*

Parallel dynamics consist in updating all the variables synchronously, where this is known as the multi-spin or multi-bit coding method. It makes an efficient use of the computer memory and gives some degree of parallelism to the *scalar* processor. Multi-spin coding is an effective approach to implementing large size simulations of real systems.

Many bits are stored in a single computer word so that if e.g. the word length is 32 bits, we can clearly save 32 one bit variables in one word. We can then use a logical method of counting the neighbouring bits and updating the sites, e.g. the logical bitwise EOR and bitwise AND to sum over neighbouring sites. It is thus possible on serial machines to treat several variables at the same time and achieve partial parallelism. Oliveira (1990) has discussed the application of computing Boolean (only two states) statistical models by Boolean operations AND, OR and XOR.

On vector machines, we can exploit, in part, the inherent parallelism by considering the data structure. The processing of the code requires that we only need to change the names of the bitwise intrinsic SHIFT and the definitions of left, right and circular shift functions which may vary on different machines, Stauffer (1991). However, we can use the bit-by-bit handling functions, where IOR can produce logical OR operations in parallel. The first bit of IOR (N1, N2) is the logical OR of the first bit of N1 and the first bit of N2, the second bit applies similarly to the second bits of N1 and N2 and so on.

On MIMD machines, the hardware architecture is different, but can similarly be used to handle many bits simultaneously and multi-bit coding is applicable. For this reason, the speed of MIMD machines is faster than any others.

The advantage of multi-spin or multi-bit coding is clearly that it saves on the memory and increases the speed by exploiting parallelism and updating each bit on the whole word. For most usual general-purpose machines, best performances are obtained with vector computers. For example, on the CRAY computer, one bit is used for one spin and 64 bits in a word are updated simultaneously with a speed of

340 spin updates per microsecond for the YMP/832 processor for the hydrodynamic example of Kohring (1991)

2.2.3.4 Language Compilation

Both machine architecture and computer language have considerable influence on the way in which the user perceives a particular problem and formulates algorithms to solve it numerically. The hardware and the software having been discussed in general terms, and we now consider the relation between them, i.e. explore the potential of the inherent parallelism of the machine together with the encoded language.

Traditionally, large amounts of code for scientific and engineering computations have been written in FORTRAN. Unfortunately, it is necessary to adjust the programs to the compiler one is using due to the fact that different FORTRAN compilers treat the functions differently and have different organisation of the memory. For example, ISHFT is not yet a standardised FORTRAN function, but is implemented in some form on most machines. ISHFT(N1, N2) shifts the bits of word N1 by N2 positions to the left or N2 positions to the right when N2 is negative. The rightmost N2 bit positions of N1 should then be filled with zeros or the leftmost N2 bits when N2 is negative. The circular shifts are not available, and the bit-by-bit functions vary and have different definitions.

New FORTRAN versions constantly attempt improvement on this, but the standardisation of regular functions typically needs a long time to be accepted by all users. This is particularly the case where large elaborate programs have been constructed and are in use for complex problems, using a given set of functions. However, programs written in other languages such as C and PASCAL, are more standardised on bit operation and are gradually becoming more widely used in scientific applications. One such is C, which has the advantage that FORTRAN and C interface very readily and efficiently, so that a FORTRAN program can use C routines, and vice versa, with little programming effort.

2.3 Simulations for Complex Systems

2.3.1 Simulation Classifications

When we attempt simulation of a system, similar considerations arise, irrespective of the nature of the application. In what follows, we concentrate on some well-established simulation approaches and some application areas, in particular of physical and related many-body complex systems. We classify the simulation by the types of computational models, system characteristics and simulation methods, as indicated in Section 2.1.2.

2.3.1.1 Discrete and Continuous Models

Models can be broadly divided into two categories based on the types of system variables, namely continuous and discrete. When the predominant activities of the system cause smooth changes in the attributes of its entities, the system is represented by a continuous model. If the system changes occur discontinuously, it is described as a discrete one, Kaplan and Glass (1995).

Both ordinary and partial differential equations formalism are used to define simulation models of continuous systems. Difference equations, cellular automata, and Markov chain models are used to specify discrete-time systems, (where time is represented by integer numbers).

Continuous simulations were traditionally carried out through the medium of analogue computation, Bennett (1976). With the appearance of the digital computer in the early sixties, the digital processor was seen to be a superior simulation tool. Further the mathematical modelling of complex systems has in the past been implemented by various standard programs to solve those ordinary and partial differential equations. The programs are usually written in FORTRAN, PASCAL and C. Consequently, a researcher with modest modelling needs has had little option but to produce his own program. This has effectively prevented the development of mathematical models in many areas of scientific research. Recently, several software products have been developed which strip away the veils of mathematical complexity and provide the modeller with tools, Stauffer et al (1988).

In discrete models, the interactions can in general be viewed as discrete events undergoing local state changes to neighbours in some space. e.g. calculable by means of discrete event, object-oriented simulation of collections of subsystems.

The concept of an event driven simulation contains the most general updating scheme for a simulation, since an event can be either externally or internally generated. In a special case, an event can be a time step, so a time stepped simulation is named a discrete event simulation, Vesely(1994).

2.3.1.2 Stochastic and Deterministic System Problems

A *deterministic* system is referred to as based on a Newtonian vision of cause-effect as found mostly in physics. Change in the state of a system can occur continuously over time or at discrete instants in time. The discrete instants can be established deterministically or stochastically depending on the nature of model inputs. Systems exhibiting deterministic characteristics are predictable, linear, and controllable. Therefore, small stimuli cause small outcomes, and large stimuli will have large outcomes. All the events are ahistoric which means experiences do not change the result.

The simulation problem is defined to be either *probabilistic* or *deterministic* depending on whether or not they are directly concerned with the behaviour and outcome of random processes. A *stochastic* model or probabilistic model has at least one random variable and therefore, at a given instant in time the next state of the model is not uniquely determined. Deterministic models (also called state-determined models) are those where the current state and current input, if any, uniquely determine the next values of state variables, e.g. molecular dynamics, Heermann (1990).

Although the procedure for describing the dynamic behaviour of discrete and continuous model changed differ, the basic concept of simulating a system by portraying the changes in the state of the system over time remains the same.

In a simulation, we usually try to ignore the uncertainties of model in order to treat the models as deterministic ones if the uncertainties are of little importance compared with the general behaviour of the model. However, a large class of

problems are stochastic in nature. Topics such as percolation and Monte Carlo methods of modelling systems are of this type, Janke (1995)

2.3.1.3 Equilibrium and Dissipative Systems

A system in equilibrium is stable in the sense that while perturbations can move the system away from stability, at least temporarily, coping mechanisms exist to restore stability after such a shock. In addition, in an equilibrium system, primary emphasis is placed on the relations among separate components of the systems under analysis.

Dissipative systems abound in complexity theory and involve complicated yet deterministic interaction between agents. These systems are open to environmental influences and undergo real change and restructuring based on inherent stability. Unlike an equilibrium system, a dissipative system when perturbed will undergo changes which create a new equilibrium, different from previous points in time. Equilibrium systems, by contrast, show only momentary fluctuations before settling back into the previous state.

Toffler (1984) has discussed how a dissipative system on the edge of chaos undergoes change. He suggested that all systems contain subsystems which are continually fluctuating. At times, a single fluctuation or a combination of those fluctuations may become so powerful, as a result of positive feedback, that it shatters the existing organisation. However, at this revolutionary moment, which is designated the *singular moment* or a *bifurcation point* by the author, it is impossible to determine in advance which direction change will take, i.e. whether the system will dissipate into chaos or leap to a new, more differentiated, higher level of order or organisation, called a dissipative structure. This phenomenon contains a very attractive and important question, i.e. whether disorder arises out of order or order out of disorder. Simulation of a complex system may also provide some insight to this question for specified systems (see Ch 4).

2.3.2 Direct and Indirect Simulation Methods

Direct simulation methods refer to the simulation of numerical equations in a straightforward manner to obtain the solution. Use of numerical simulation

methods include solving linear equations, eigenvalue problems, differential equations and partial differential equations, and others. In the traditional study of physical and related systems, most applications of computer simulation concentrate on these methods which describe the underlying system models directly and provide solutions to the equations that govern the physical processes.

A mathematical model is introduced to describe, as far as possible, the physical system for which a set of assumptions apply which make the solution of the problem somewhat more tractable. The model is essentially an idealised version of the system and the aim is to obtain parameters of the model which relate directly to properties of the system that we wish to measure. Hence, the simulation corresponds to reproducing computationally as many of the actual system features as possible, then recording the effects of change or inducing changes to occur, where these closely mimic real changes in the system. This approach defines so-called *direct simulation*.

However, the investigation of non-equilibrium, complex (many-body) systems, which cannot be described by a set of linear differential equations is subject to limitations when using the conventional direct simulation approaches. No general solution is known when the number of interacting bodies is greater than two. Useful results are sometimes obtained by making some simplifying approximations, (e.g. the simplest one consists of neglecting interactions altogether), or by reducing the problem to an effective one-body problem. Nevertheless, all known approximate schemes are of limited applicability. Direct simulation meets with difficulties since equations used to describe the system model are difficult to solve without further simplifying assumptions or possibly more advanced computing techniques if available. The alternative general approach to handling problems involving complex many-body dynamics is typically based on discretization of the system processes, so that these can be broken down into a series of small steps. This principle underlies *indirect* simulation in that a slightly *different* problem to the actual one of interest is actually modelled. Such methods rely on reproducing system properties through either aggregate or ensemble behaviour, rather than implementing them straightforwardly, Jain (1992), Thompson (1992). Monte Carlo methods, cellular automata models, molecular dynamics, neural networks and

related techniques have become more widely used as indirect simulation approaches to formal mathematical models, in order to investigate the evolutionary properties of these complex systems

Indirect methods tend to deal with simpler aspects of a system, and are thus particularly suitable for problems requiring computation of millions or even billions of similar types of events, such as e.g. growth or division of cells in molecular biology, re-orientation of spin in the Ising model of a ferromagnet, and others, since the difficulty lies in achieving simulated behaviour which in the limit approaches that of the real systems. Thus a satisfactory run will require the computation of billions of events to describe formation, growth or evolution. Some illustrations are given subsequently.

2.3.3 Cellular Automata, Monte Carlo and Molecular Dynamics

Cellular automata, Monte Carlo Methods and molecular dynamics are three important indirect simulation techniques which are currently enjoying considerable popularity in the modelling of physical and related complex systems. Typically, MC is unsurprisingly used as a stochastic method, MD as a relatively deterministic one, whereas CA is used in both ways. To distinguish more clearly between the methods, we have

Cellular automata (CA) form a class of mathematical systems characterised by discrete local interaction and an inherently parallel form of evolution. CA provide prototypical models for complex processes consisting of a large number of simple locally connected components. Examples of phenomena that have been modelled using CA include turbulent flow caused by the collisions of fluid molecules, growth of crystals and patterns of electrical activity in simple neural networks, Wolfram (1984) (1986).

Monte Carlo (MC) is a numerical analysis technique that uses random sampling of distributions to estimate the solution of physical and mathematical problems, i.e. it is roughly one of the statistical simulation methods, Landau (1994).

Molecular Dynamics (MD) provides the methodology for detailed microscopic modelling on the molecular scale. The system can consist of few or many-bodies, with the motion of each individual atom or molecule described according to e.g. a

Hamiltonian, (usually describe aggregate energy of a system) MD usually involves calculations on a number of particles, from a few tens to a few thousands, or even several millions. Macroscopic quantities are extracted from the microscopic trajectories of particles. It is a tool which we can use to understand macroscopic physics from an atomic point of view. The applications of MD include the thermodynamic properties of gas, liquid, and solid, plasma and electrons, transport phenomena etc, Haile (1992)

2.4 Simulation Techniques: Cellular Automata

Cellular Automata (CA) is an important area in the field of complexity which is linking different domains of traditional sciences. One main achievement is that CA focuses on system global phenomena through local simple individual interaction. Such phenomena occur in many fields and at many levels of description, e.g. ants interact to form a colony, or water molecules interact to make a fluid, or sandpiles interact to create avalanches. As we discussed in the last section, it is necessary to choose a simulation model which accurately reflects these aspects of a complex system that we wish to study. Many such systems share the common features above and CA models, because of their simplicity, have performed well in terms of representing these. Not all systems are best represented by the same type of CA and there are numerous variants.

2.4.1 Cellular Automata: Description of Mechanism

A cellular automaton (CA) is a discrete dynamical system. Space, time and the states of the system are discrete. Each point in a regular spatial lattice, called a cell, can have any one of a finite number of states. The states of the cells in the lattice are updated according to a local rule. That is, the state of a cell at a given time depends only on its own state at one previous time step, and the states of its nearby neighbours at the previous time step. All cells on the lattice are updated synchronously. Thus, the state of the entire lattice advances in discrete time steps (Gutowitz (1996))

In mathematical terms, a cellular automata is described as a lattice of finite state automata with N states, and K neighbours for each cell. The state S of each cell is

updated in discrete time steps as a function of state transitions defined for the alphabet NK the combination of states for each cell and its neighbours

$$S(NK) \rightarrow S(i) \quad (2.3.1)$$

one-dimensional CA is an elementary cellular automata with $N=2$, $K=2$

$$S(i-1), S(i), S(i+1) \rightarrow S(i) \quad (2.3.2)$$

Shown in Fig 2.3.1, the neighbourhood of each cell consists of itself and its two nearest neighbours with periodic boundary conditions. The CA rule is often displayed as a lookup table, or rule table, which lists each possible neighbourhood together with its output bit, (the update value for the state of the central cell in the neighbourhood)

Rule table:

neighbourhood	000	001	010	011	100	101	110	111
output bit	0	1	1	1	0	1	1	0

Lattice

t=0 10100110010

t=1 11101110111

Fig 2.3.1 one-dimensional, binary-state CA with periodic boundary conditions shown iterating for time step

The behaviour of a CA is often illustrated using space-time diagrams in which the configuration of states in the d-dimensional lattice is plotted as a function of time. Fig 2.3.2 shows the behaviour of a CA with $N=200$, iterated over 200 time steps. This is a basic CA architecture and it can be modified in many ways, such as for higher dimensions, different boundary conditions, stochastic rather than deterministic CA rule and so on.

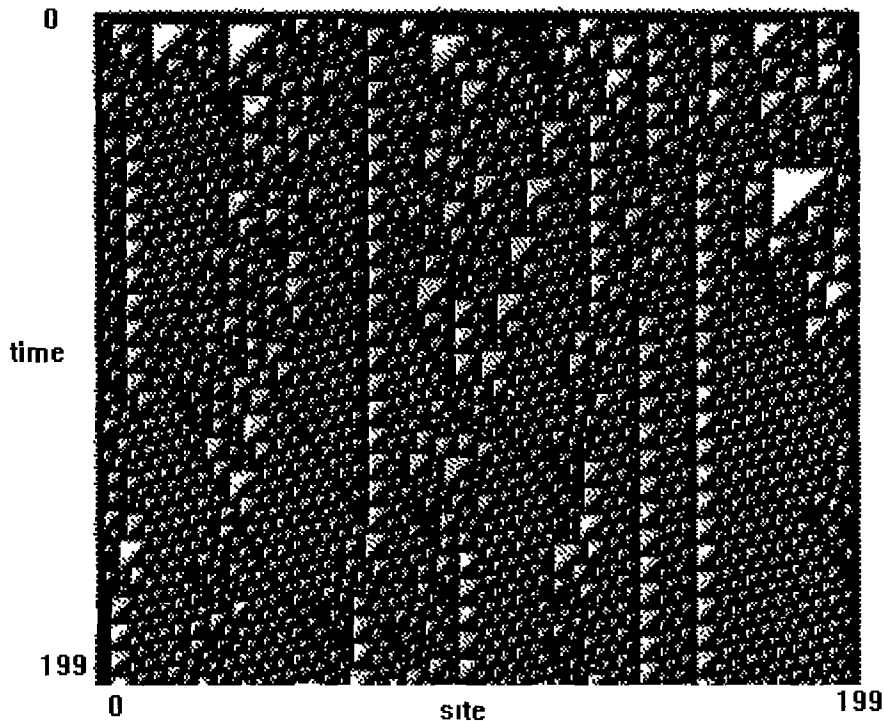


Fig 2 3 2 a space-time diagram, showing the typical behaviour of CA. Cells in state 1 are displayed as black, and cells in state 0 as white, Mitchell et al (1996)

2.4.2 Background

CA were first described by Von Neumann and Ulam, who studied the behaviour of models of coupled masses and springs, resulting in the first computational evidence of chaotic behaviour in dynamical systems, Von Neumann (1966). Conway developed the Game of Life system, which is a simple 2-D analogue of basic processes in living systems, which is the most widely known example of a CA. The game consists in tracing changes through time in the patterns formed by sets of "living" cells arranged in a 2D grid. The rules governing these changes are designed to mimic population change. Wolfram (1984) (1986) was the first to point out the potential for extensive use of CA models in statistical physics and later a number of authors, e.g. Stauffer (1990), developed the links between physical systems and CA-like structures in nature so that numerous biological examples are now to be found in the physical literature. These include e.g. immunological and ecological studies. For a further review, see Manneville et al (1989).

The essential feature of a cellular automaton lies in the fact that its state variable takes a different separate value for each cell. The state can be either a number or a property. Its neighbourhood is the set of cells that it interacts with. So, a CA model usually is used to describe the system in terms of relations between cells. Some complex systems fit easily and perfectly into the framework of cellular automata, for others these simplifying assumptions are too restrictive for real modelling. CAs are used not only as models in natural sciences, but are also appropriate models of parallel computation features due to their complete space-time and state discreteness.

2.4.3 Classification

Several researchers have been interested in the relationships between the generic dynamical behaviour of CA and their computational abilities. Despite the computational simplicity of CA, they are capable of a variety of behaviour. An important property is that they tend to be self-organising, i.e. starting from complex, random cell configurations, the rules governing the system cause patterns to occur from initial chaos. Wolfram (1984) suggested that CA rules can be classified into four qualitative classes, based on the space-time pattern demonstrated by CA at long times.

- 1 Spatio-temporally uniform state. The automata reaches a homogeneous state regardless of initial conditions.
- 2 Separated simple or periodic structures. The automata reach a state after some relatively small transient period consisting of space-time separated configurations. The configurations vary in detail depending on the initial configuration, but may have overall behaviour which is independent of the initial state.
- 3 Chaotic space-time patterns. The automata reach a chaotic evolution pattern starting from random initial conditions.
- 4 Complex localised structure. Properties vary with initial conditions.

The disadvantage of Wolfram's classification is that class membership is *undecidable*, Culik and Yu (1988). After Wolfram's work, several researchers have queried the relation of static properties of CA rules to their dynamical

behaviour Langton (1990) studied the relationship between the average dynamical behaviour of cellular automata and a particular statistic (λ) of a CA rule table Langton selected a number of two-dimensional CA *samples* Starting with $\lambda=0$ and gradually increasing to $\lambda=1-1/k$, he found that the *average behaviour* of a CA undergoes a phase transition from ordered behaviour, which has a fixed or limiting cycle after a short transient period, to chaotic behaviour As λ reaches a critical value λ_c , those rules tend to have longer transient phases Moreover, Langton indicated that CA close to λ_c tend to exhibit long-lived, complex pattern, i.e. non-periodic, but non-random, where the λ_c stage roughly corresponds to Wolfram's fourth class of CA For a review of the relationships between λ and dynamical and computational properties of CA, see Mitchell et al (1994)

2.4.4 Applications

The nature of CA is to provide a convenient abstraction of continuous phenomena Models of this type are thus useful for studying problems of energy transfer and biological growth pattern, fluid flow, and earthquake evolution, Gutowitz (1990) The properties being observed normally correspond to patterns that are coherent over a large array of cells, although the cells are not co-ordinated with a specific set of cells In simulations, the elemental level of CA allows us to get more information for the processes occurring within the system. This breakdown of the statistics into detailed structured information is one of the additional objectives of the thesis In the most direct cases, the cellular automata lattice is in position space This sites may represent points in a crystal lattice, with values given by some quantified observable or corresponding to the types of units The sandpile model, dynamical Ising model and other lattice spin systems are simple types of CA models

Furthermore, CA provides a computational and analytical development for general-purpose ideas on the studies of complex systems, e.g. Forrest (1990) has used CA as abstract models to study emergent behaviour These systems are inherently difficult to analyse due to their complexity. The discreteness of CA is expected to

make the analysis simpler. The ideas can be used in generalising more continuous systems, such as Coupled Map Lattices, which are discrete in time and space, but have a continuous state variable.

Cellular automata can be considered as parallel processing computers. The computational capabilities of CA have been used extensively, Toffoli (1987), and it has been shown that some CA could be used as general purpose computers, and may therefore, be considered as general *paradigms* for parallel computation, (as Turing machines provide a paradigm for *serial* computation). The local and uniform nature of the laws governing cellular automata means that a hierarchy of structures and phenomena may be represented, including operation at molecular level.

2.5 Simulation Techniques: Monte Carlo

2.5.1 Introduction

The name Monte Carlo was applied to a class of mathematical statistical simulation methods first used by scientists working on the development of nuclear weapons in Los Alamos in the 1940s. The principle of this method is the invention of games of chance whose behaviour and outcome can be viewed as relating to competition and evolutionary behaviour in real world systems. The effectiveness of numerical or simulated gambling as a research effort was developed by digital computer, (e.g. Kalos and Whitlock (1986) for commentary), where, in particular, these simulations deal with a large number of chances or events. The treatment of the probability of event occurrence, the aggregation of results and their statistical analysis together with methods of dealing with bias and errors are all core features of the MC approach.

Statistical methods are then used to obtain microscopic properties from averages of mechanical variables of molecules. The Monte Carlo (MC) method is defined by representing the solution of a problem as a parameter of a hypothetical population, and using a random sequence of numbers to construct a sample of the population, from which statistical estimates of the parameter can be obtained, Binder (1986).

MC methods are thus stochastic rather than deterministic procedures, where atoms are moved more or less randomly during the course of the simulation. In MC, a number of molecules (or ions) are confined within a region, then at each step, a randomly chosen molecule is moved to a new randomly determined location. The computer then determines whether to accept or reject this movement depending on whether the energy change of the resulting system state is acceptable according to some predetermined criterion. This process is repeated many times until there is no further change in the energy and other captured properties of the system, at which point the system is deemed to have reached thermodynamic equilibrium. Usually, a large number of molecular states are generated and the corresponding physical properties of these states are averaged to obtain macroscopic properties of the system, such as energy and entropy, Binder (1992).

2.5.2 General Principles of the MC Methods

The random nature of a Monte Carlo simulation means that, in the long run, the simulation will approach equilibrium values, while an individual move has a realistic chance of taking the simulation away from equilibrium. As MC typically uses pseudo random number generators to generate the element of chance, its applications are enormous and provide insight in many fields. Many problems, which at first glance do not seem to fit the MC criteria, can have behaviour which is related to some stochastic element of the system to which a solution is sought.

MC can be considered in either direct or indirect terms. The direct application, is less commonly used but as would be expected, concentrates on a straightforward simulation of the original problem. It relies on the numerical solution of equations defining the system, which can be used to predict the model properties at different stages. Indirect methods solve a related problem which uses random numbers to generate different states of the related system. It is obvious that the level of sophistication varies according to the type of problem considered. Indirect methods only will concern us in the examples used for illustration in later Chapters.

2.5.3 Metropolis Method

The MC technique is now used in many disciplines, with different variants and specific algorithms, depending on the nature of the problem addressed. An extremely important Monte Carlo algorithm for molecular systems was developed by Metropolis et al (1952), which is commonly used in large scale statistical physics simulations. This has been applied to lots of problems where molecular just implies small unit rather than a biological molecule. It specifies conditions under which a system is allowed to move to a new configuration, and because of its importance, we reproduce the steps here in brief.

- 1 Specify an initial configuration
- 2 Generate a new configuration
- 3 Calculate a new configuration and energy change ΔE
- 4 For $\Delta E \leq 0$ accept the new configuration. Return to 2
- 5 calculate $\exp(-\Delta E/kT)$
- 6 Generate a random number $R \in [0,1]$
- 7 For $R < \exp(-\Delta E/k_B T)$, accepted the new configuration and return to 2
- 8 Otherwise, retain the old configuration as the new one. Return to 2

Where E is the system energy, k_B is Boltzmann constant and T is temperature. Clearly, certain assumptions are required to model a given system even if it is quite easy to include a Boltzmann distribution of energies. A system described by a Boltzmann distribution e.g. a gas, will have elements which are not in a minimum energy state due to the thermal change of the system. The Metropolis algorithm steps above ensure that the system will evolve into one which includes excited elements, which may lead to expansion or other macroscopic properties.

2.5.4 Applications

Applications of MC simulation include calculations in statistical mechanics, radiation transport, elementary particle interactions, computer operating systems, biological evolution and so on. Popular application to surface behaviour includes the Ising model, percolation model, spin glasses, and random walks. Of interest

typically are insights on critical phenomena, i.e. establishment of scaling laws and universality of behaviour of complex systems both in equilibrium and in non-equilibrium, Gould and Tobochnik (1989), Binder and Heerman (1992)

2.6 Other Simulation Techniques: e.g. Molecular Dynamics

2.6.1 Introduction

The essence of MD is to numerically solve the N-body problem of classical mechanics. The N-body problem attempts to relate collective dynamics to single-particle dynamics and the puzzling behaviour of large collective particles by examining the motions of individual particles.

Molecular-scale computer simulation involves a three-step procedure,

- 1 model individual particles,
- 2 simulate the movements of a large number of the model particles,
- 3 analyse the simulation data for the required collective phenomenon.

MD simulations are used to compute the motions of individual molecules in models of solids, liquids and gases, Miller (1976). The key word is *motion*, which describes how positions, velocities and orientation change with time. The behaviour of a system can be computed if for the system's elements, a set of initial conditions and forces of interaction are defined, Bekey (1985), Hoover (1991). Tremendous improvements in computer power and computational methodology have accelerated the development towards simulation of larger and larger systems, so that today MD simulations of a million particles is possible. Such advances have also enabled researchers to obtain much information and accurate calculation of physical properties and longer-lived dynamical processes.

The simplest calculation in molecular mechanics is a calculation of the potential energy of the system, which is performed by summing the numerous energy terms for the given conformation of the system using the given set of potential energy functions and parameters. Optimising the structure of system structure can be done by energy minimisation which improves the conformation by reducing the energy of the system. More information about a system can be obtained from molecular dynamics simulations. In these calculations, the motions of the particles are

followed by calculating the forces produced by applied field and, from this, the accelerations and velocities. Careful control of the energy and temperature of the system ensures that the conformations, which are produced form a statistical ensemble, from which thermodynamic and other properties can be calculated, Hu et al (1984)

2.6.2 Applications

MD has some computational advantages because of the deterministic way in which it generates trajectories. The presence of an explicit time variable can be used to *estimate* the time needed for a run, with the duration time several multiples of the relaxation time for the slowest phenomenon being studied. This convenient feature is not available for estimating the time required for other methods.

In addition to equilibrium molecular dynamics, nonequilibrium methods have been developed, Hoover (1986), Evan and Morriss (1990). These methods appeared as alternatives to equilibrium simulations for computing transport coefficients. In these methods, an external force is applied to the system to establish the nonequilibrium situation of interest, and the system's response to the force is then determined from the simulation. Nonequilibrium MD has been used to obtain quantities such as the shear viscosity, bulk viscosity and diffusion coefficients, Hoover (1983) (1991).

However, MD simulations are *limited*, largely by the speed and storage constraint of available computers. They are usually performed on systems containing 110 - 1000 particles, although calculations involving as many as 10^6 particles have been performed presumably when systems were slightly simpler to specify. Due to the *size* limitation, simulations are confined to system of particles that interact with relatively *short-range* forces, (i.e. intermolecular forces should be small when molecules are separated by a distance equal to half of the smallest overall dimension of the system). Due to the *speed* limitation, simulations are confined to studies of relatively *short-lived* phenomena, (roughly those occurring in less than 1100-1000 psec). The characteristic relaxation time for the phenomenon under investigation must be small enough so that one simulation generates several relaxation times, Ciccotti and Hoover (1986).

2.6.3 Monte Carlo and Molecular Dynamics

Monte Carlo (MC) and molecular dynamics (MD) represent very different types of simulation. Being a deterministic method, MD simulations have been applied to investigate the physical properties of a system directly, e.g. co-ordinates, interatomic forces etc. and to determine its time evolution. On the other hand, MC simulations are stochastic and use random numbers to generate a sample population of the system from which properties can be determined. Meanwhile, MC simulations are by no means limited to molecular systems, e.g. in studies of gases and fluids, where the random nature of the technique is applied, but are used in diverse areas.

MC is usually easier than MD to code in a high-level language such as Fortran and C. MC is also easier to implement for systems in which it is difficult to extract the intermolecular force law from the potential function. Systems having this difficulty include those composed of molecules that interact through discontinuous forces, Haile (1995).

For determination of simple equilibrium properties such as the pressure in atomic fluids, MC and MD are *equally effective*, both require about the same amount of computer time to attain a *similar* level of *statistical precision*. However, from the simulation examples, Binder (1986) has found that MD more efficiently evaluates some system interfacial properties than MC. Besides the configurational properties, the MD method also provides access to dynamic quantities, such as transport coefficients and time correlation functions. Such dynamics quantities cannot generally be obtained by MC, although certain kinds of dynamics behaviour may be deduced from MC.

The random nature of Monte Carlo simulations makes them useful for sampling space. Although MC are generally not as efficient as MD simulations, MC simulations can incorporate large structure changes which cannot be simulated by MD. For instance, some variant MC methods can implement some functions without considering the factor of an energy barrier, which might prevent the same role in MD. In general, MC simulations are useful for coarse-grained complex

systems while MD are good at performing the complementary role of local optimisation

2.7 Applications of Simulation Methods- Specific Cases

Over the past decade, much progress has been made in the understanding of complex systems, particularly in areas relating to their dynamical features, computational properties, structure of their rule space, relationship between single cellular system and cellular networks, and so on. Computational advances, such as more powerful processors, have led to increased ability to handle these problems. In particular, it is clear that simulation methods provide valuable insight into the analysis of disordered dynamical systems, with the potential for answering fundamental questions, such as the way in which a process evolves and in what way its behaviour depends on system features.

In this thesis, we discuss applications of simulation techniques to physical and related complex systems. Two typical examples of cellular systems, namely a sandpile automaton model, and a cellular network model for soap froth, are used as illustrations of systems under different levels of constraint and are analysed using various computer simulation methods. A brief introduction to these problems follows.

2.7.1 CA Models and the Phenomenon of SOC: Building Piles of Sand

Bak and co-workers (1987) (1988) investigated a sandpile CA as a model for transport phenomena in order to gain insight into spatio-temporal complexity. In this context, they introduced the concept of self-organised criticality (SOC), where this phenomenon is defined for a class of dynamical systems obeying simple rules which naturally lead to a state presenting unique scale-invariant correlations. This is in contrast with the criticality conventionally defined for physical systems, where achievement of a critical state is controlled by an external parameter.

In a simple sandpile, random movement of grains of sand in the pile represents the interactions between different sites. The addition of grains of sand transforms the system from a state in which the individual grains follow their own local dynamics to a critical state where the emergent dynamics are global. Relaxation of the system

creates spatial and temporal self-similarities, which give rise to fractal patterns or $1/f$ noise. The character of SOC is lack of any characteristic scale. In other words, it means that in a complicated dynamical system in which many elements influence each other with short-range interaction, the system will naturally evolve to a critical state where small perturbations could lead to either minor or catastrophic events.

Several sandpile cellular automata models exhibiting SOC have been studied. In the original model of Bak et al (1987), the system is perturbed externally by random addition of sand grains. Different dynamical rules have been investigated leading to several universality classes. Some variants include directed flows, Kadanoff et al (1989), and induction of "turbulence", Ruskin (1993), piles with threshold conditions imposed on the height, on the local gradient or even on the Laplacian, Manna (1991), whilst others have also looked at general slope gradient e.g. Dhar (1989), Mehta (1990). Continuous variables with a full transfer of energy of the sand from a cell instead of a fixed discrete amount have also been studied e.g. Zhang (1989), Pietronero et al (1991), Fodor and Janosi (1991) and Diaz-Guilera (1992). Other authors have considered deterministic perturbations in a nonconservative system Christensen et al (1992), Olami and Christensen (1992) (in a earthquake modelling) and so on. Further details on this and some results for a specific class of dissipative systems are given in Chapter 3.

2.7.2 Cellular Networks; Froth Evolutionary Behaviour

Cellular patterns are common in nature, e.g., magnetic domains in magnetic systems, crystalline domains in ceramics and alloys, cells in biological tissues or bubbles in a soap froth. Their statistical behaviour can be investigated by monitoring the network evolution through time. The two-dimensional soap froth, as an idealised cellular structure, has recently attracted much attention following the work of Weaire and Kermode (1983)(1984), Weaire and Rivier (1984), Rivier (1985). A froth has all boundaries equivalent and surface-energy-driven diffusion leads to the motion of bubble boundaries. The basic mechanism of froth evolution is the gas diffusion across its membranes, due to the different pressures between neighbouring cells. Early work on 2-D froths found dynamic scaling properties to

be *universal* in the sense that they are independent of the system and specific initial conditions, Stavans and Glazier (1987)

Various computational techniques have been applied to problems of froth behaviour. Those include direct simulation of the system equations, Weaire and Kermode (1983) (1984), indirect simulation (Monte Carlo and variants such as the Potts model), Wejchert et al (1986), Glazier et al (1990), and the vertex model of Kawasaki et al (1989)(1990). Further details of the algorithms are reviewed in Chapter 4 and 5.

2.8 Summary

It is evident that computer simulations provide a valuable complement to experimental and theoretical work in the modelling of complex systems. The speed, reliability and convenience of modern computers have ensured considerable success for these methods in recent years, and conversely, the need to produce and handle large numbers and millions of events have impacted on the developments in computing techniques. In the next three chapters, we give details of simulations, (the algorithms and the analysis), applied to systems of particular interest.

Chapter 3 Simple Dynamical Cellular System Models

As described in Chapter 2, cellular automata provide an important tool in large-scale simulation, and constitute a bridge between physical and computational realisations. Physical and related complex systems, containing many discrete elements with local interactions, are thus often conveniently modelled as simple cellular automata. A wide variety of examples may be considered, with several CA representing different competing units. Use of "simple" here usually means a single type of basic element or unit and we use the terminology interchangeably in what follows.

In this chapter, we concentrate on illustrations of one type of two-dimensional cellular structure: the sandpile models of a single cellular system. We initially review the literature on the theoretical and experimental background to these systems by computer simulation. Sandpile models have been studied as a paradigm of self-organised criticality (SOC), defined in the previous chapter, and have been used to describe characteristic spatio-temporal behaviour in many fields. In particular, we look at sandpile models of dissipative systems. These include both discrete CA systems and counterparts which depend (in part) on continuous state functions, the so-called Coupled Map Lattices.

3.1 Simple Cellular Automata System and SOC

3.1.1 Simple Cellular System

While physical laws such as Newton's, explain many simple phenomena, more complicated systems must usually be studied by treating them as a collection of simple systems, i.e. so-called reductionism, Bak and Chen (1990). However, many phenomena in nature are so complicated that even reductionism can not help and the macroscopic behaviour can not be predicted in terms of the microscopic changes.

There are many such examples of systems with complex behaviour. Much effort has been spent on understanding the underlying mechanisms of this behaviour, but it is difficult to form general rules for spatio-temporal complexity, Anderson (1991). The analysis of the time evolution of an isolated simple dynamical

cellular system is a first step to explaining its complex behaviour. However, cellular systems consist of a *very large* number of individual units, where each unit is a dynamical system itself. The interaction between units can be very difficult to determine, even if all the units are identical. Under various situations, such as varying interaction, different boundary conditions, and the existence or absence of noise, the system completely changes its dynamic behaviour, Feder (1988).

Complex behaviour can be observed when intrinsic dynamics govern the temporal behavior of a system, or the interactions follow complicated rules. However, complexity may also arise as a result of continued local *simple* interactions between *all* individuals in an extended system. Some extended systems with complex local features may nevertheless lead to simple collective behavior. This is found in some biological systems, where after a transient period, a regime characterized by punctuated equilibria is achieved, Bak and Sneppen (1993).

3.1.2 Models and Applications

Cellular automata models apply iterative rules to build aggregates of a system, (Section 2.5.1, Wolfram (1986), Toffoli and Margolus (1987)). Such systems are typically placed on a 2D or 3D lattice. Using the defined rules, sites are populated, depopulated and the results are evaluated at various time steps. The final state provides interesting insights as to how similar systems in nature might perform. The sandpile model is a simple example of a cellular automata system, where each site or cell contains a column of grains, which topple according to prescribed rules applied at discrete time steps. At each step, the new value for a cell depends only on the current state of the cell itself and on neighbouring states or states of immediate neighbours. These systems are interesting in that simple rules can lead to extremely complex behaviour. Moreover, slight changes in the rules can change the behaviour radically so that even though the formulation of a cellular automaton may seem almost trivial, the large number of possible rules supports considerable sophistication in the systems that are modelled. More than one CA may be used for more complex systems, e.g. in competition studies.

Apart from their simplicity, sandpile automata have been studied as typical CA models for other important characteristics. For example, sandpiles are disordered

in their geometry, and this, together with their packing, has important consequences for granular static and dynamic properties. These systems also show complexity, in the occurrence and relative stability of a large number of *metastable configurational* states. Analogies between sandpiles and other complex systems, such as spin glasses, flux creep in superconductors and charge-density waves have been made. For example de Gennes (1966) has drawn analogies between vortex motion in superconductors and avalanches in sandpiles. A number of different dynamics for sandpile evolution have been considered, which depend on height, slope and other CA features. Following the introduction of the simple height model, Bak et al (1987) (1988) discussed some important features of the dynamics of sandpiles. These are considered in brief below.

3.1.3 Scale-Invariance and Self-Organised Criticality (SOC)

A common feature of complex systems is that they are driven slowly by small changes in energy, which is then dissipated rapidly in an *avalanche process*. This occurs because complex systems exist in metastable states and small increments of energy can trigger an arbitrarily sized avalanche, which may take the system far from an equilibrium state.

Equilibrium systems commonly show scale-invariant critical behaviour, with fluctuations in the order parameter of various sizes and durations at a phase transition. A critical point at which a phase transition occurs is normally reached in thermodynamic, critical processes by fine-tuning of a relevant physical control parameter, such as the temperature or the pressure.

As nature is neither ordered nor predictable, there are many scale invariant phenomena, e.g. fractals, earthquakes, $1/f$ noise, fluctuation of the stock market indices. Since nature cannot provide any fine-tuning of control parameters by itself, it is unlikely that the wide occurrence of scale-invariance is due solely to critical processes in equilibrium systems. Over the last decade, new concepts have been proposed to explore the complexity and dynamics of large nonequilibrium systems. Chaos has been used to predict irregular and unexpected behaviour, Gleick (1988), Eubank and Farmer (1993). Some apparently random behaviour indeed can be explained by deterministic nonlinear equations and provides one explanation for apparent chaos. The characteristics are described by strange

attractors and sensitivity depends on initial conditions. Conversely, self-organised criticality (SOC) is a paradigm used to explain scale-invariance in complex systems, which reach a critical state via their intrinsic dynamics. In other words, unlike conventional critical phenomena, this critical state is unique and independent of the initial conditions and does not require sensitive adjustment of a system control parameter. It is "self-organising". SOC was first referred to by Mandelbrot (1969) in relation to analysis of stock-market share prices, where "knock-on" effects are ruled by very complex connections between companies of either a financial or technical nature and vary considerably in terms of duration.

Bak, Tang, and Wiesenfeld (BTW) proposed SOC as an explanation of this spatio-temporal complexity illustrating the phenomenon through sandpile dynamics. A sandpile is built by random addition of grains, so that it "relaxes" to a stable (or metastable) state, from which the addition of a further grain causes further relaxation in the shape of toppling of grains to a lower level. The addition of a single grain causes a local disturbance but the size of the domain affected by the disturbance distributes over a wide range. There is no global communication within the pile at the early stage of building.

As the slope increases, a single grain is more likely to cause other grains to topple. Eventually the slope reaches a certain value and cannot increase any further, because the amount of sand added is balanced on average by the sand falling out of the pile. This is then a stationary state, since the average amount of sand and the average slope are a constant in time. It is clear that further addition create some communication throughout the whole system linking behaviour of individual grains through avalanches that may occasionally span the entire sandpile. Eventually, the system regains equilibrium and this is the self-organised critical state.

The sandpile is an open dynamical system, since sand is added from outside. It has many degrees of freedom, (or grains of sand). A grain of sand landing on the pile represents potential energy. When the grain topples, this energy is transformed into kinetic energy, and when the toppling is ended, the kinetic energy is dissipated, and transformed into heat in the pile, i.e. energy flows through the system. The critical state can be maintained only because of energy in

the form of new sand being supplied from the outside. Fluctuations are observed over a range of time as well as length scales, indicating considerable spatio-temporal complexity.

With respect to spatial aspects, Mandelbrot (1982) has used the word fractal for geometrical structures which span all length scales. Fractal structures appear in a variety of physical systems in nature, from the pattern in snowflakes to the distribution of galaxies, Feder (1988). It has been demonstrated that fractals can be explained by SOC, where size distributions have a power-law or multifractal form. Examples of physical phenomena displaying fractality include turbulence. Here the energy is clearly not dissipated uniformly in space but intermittently through cascades at all length scales, Family and Vicsek (1991).

Another example of a system demonstrating SOC is that of the energy-frequency relation of earthquake occurrence, which is related to the Gutenberg-Richter (power) law, Gutenberg and Richter (1944). An interesting aspect of earthquakes is their self-similarity. It has been found that a power-law distribution of size exists not only for individual earthquake events *within a system over time* but also for each earthquake event itself. Both short-range and long-range temporal correlation of fractal behaviour is, therefore, observed. In particular, the occurrence of large earthquakes tends to occur in temporal clusters, Kagan and Jackson (1991), where the seismographic analysis of the event shows the energy distribution at the stationary critical state, to be similar to that for SOC, Creutz (1994).

3.2 Sandpile Automata and SOC

3.2.1 Basic Sandpile Driven Model

3.2.1.1 Discrete Driven Models

The original one-dimensional sandpile model introduced by Bak et al (1987)(1988), has subsequently given rise to many variants. The simple model is a cellular automaton with each site i on a line of sites characterised by an integer variable h_i giving the height of the pile. The local slope of a site is given as

$$z_i = h_i - h_{i+1} \quad (3.2.1)$$

A sand grain added on a randomly chosen site i results in dropping movement

$$z_i \rightarrow z_i + 1 \quad (3.2.2)$$

$$z_i \rightarrow z_{i-1} - 1 \quad (3.2.3)$$

Grains topple when neighbouring sites have a local slope or gradient difference larger than some critical value, z_c , ($z_c = 2$ in 1D models) Excess grains are then transferred to its nearest neighbouring sites according to

$$z_i \rightarrow z_i - 2 \quad (3.2.4)$$

$$z_{i\pm 1} \rightarrow z_{i\pm 1} + 1 \quad (3.2.5)$$

The neighbours affected by the toppling can topple again, thus resulting in a chain reaction, or so-called *avalanche*. During the avalanche, no more grains are added. Separate time scales are involved in the dynamic evolution of the pile, one in terms of the addition of grains and the other is in terms of relaxation of grains in the pile. The avalanche ends when the system reaches a stable state with $z_i \leq z_c$ (for all i), and another grain is added according to Eqns 3.2.2 and 3.2.3 until a new avalanche is started. After a transient period, with duration dependent on the initial conditions, the system reaches a critical state, where for all i , $z_i = z_c$. This state is a fixed point since the system returns to this stable state after any perturbation. Further additions of a grain results in grains falling down the slope and finally off the pile. This state is critical in the sense that the avalanches have no characteristic size. The fixed point is an attractor for the dynamics, no matter which way the sandpile is built up. However, this state has no spatial structure, and correlation functions are trivial. The 1D sandpile is shown in Fig 2.1.1

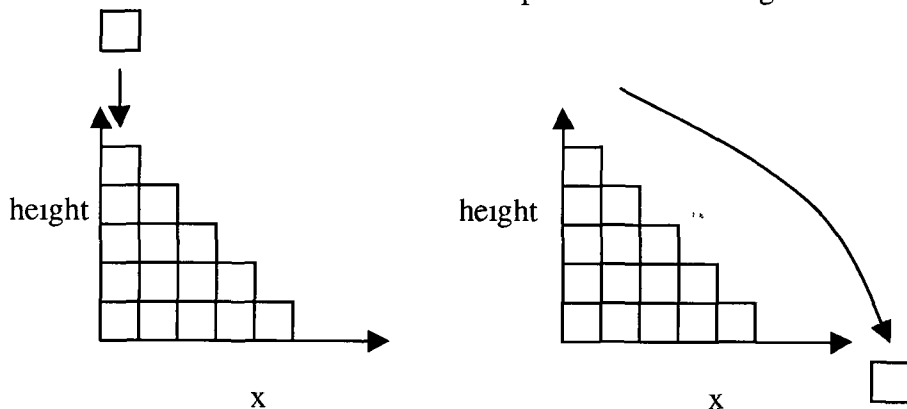


Fig 2.1.1 BTW 1-D sandpile model with closed and open boundary for the left and right boundaries

The situation is different for the two-dimensional model where parallel rules are applied. The 2D sandpile model is typically considered for a square lattice, with each lattice site (i,j) characterised by an integer $z_{(i,j)}$ (where $i,j = 1,2, \dots, L$). The integer $z_{(i,j)}$ can be taken to represent a dynamical variable such as height, slope etc. for a site (i,j) in a spatially extended system. Sand is added one grain at a time to a randomly chosen site, thus increasing the dynamical variable by one unit, $z_{(i,j)} \rightarrow z_{(i,j)} + 1$. Whenever the dynamical variable exceeds a threshold value $z_{(i,j)} > z_c$, at a given site, then the whole column of sand is redistributed among the neighbours, leading to a series of topples which may give rise to an avalanche and which subside after a finite period of time. The simple dynamical rules satisfy local conservation through

$$z_{(i,j)} \rightarrow z_{(i,j)} - 4 \quad (3.2.6)$$

$$z_{(i\pm 1, j\pm 1)} \rightarrow z_{(i\pm 1, j\pm 1)} + 1 \quad (3.2.7)$$

The pile eventually achieves a statistically steady state and any additional sand grain will fall off the open boundary. This is a *dissipative* relaxation mechanism since it is accompanied by loss of energy through the boundary.

Here we show a sequence of toppling events in a very small system for illustration, (Fig. 2.1.2). The number in the squares represents the heights. If a grain of sand is added to a site with height 3, it causes that site to topple. Eventually, as toppling diminishes, the system comes to rest. There are nine sites toppling in the example shown, so the avalanche has size $s=9$ for this particular perturbation. The total duration time, the number of update steps, $t=7$ of the avalanche.

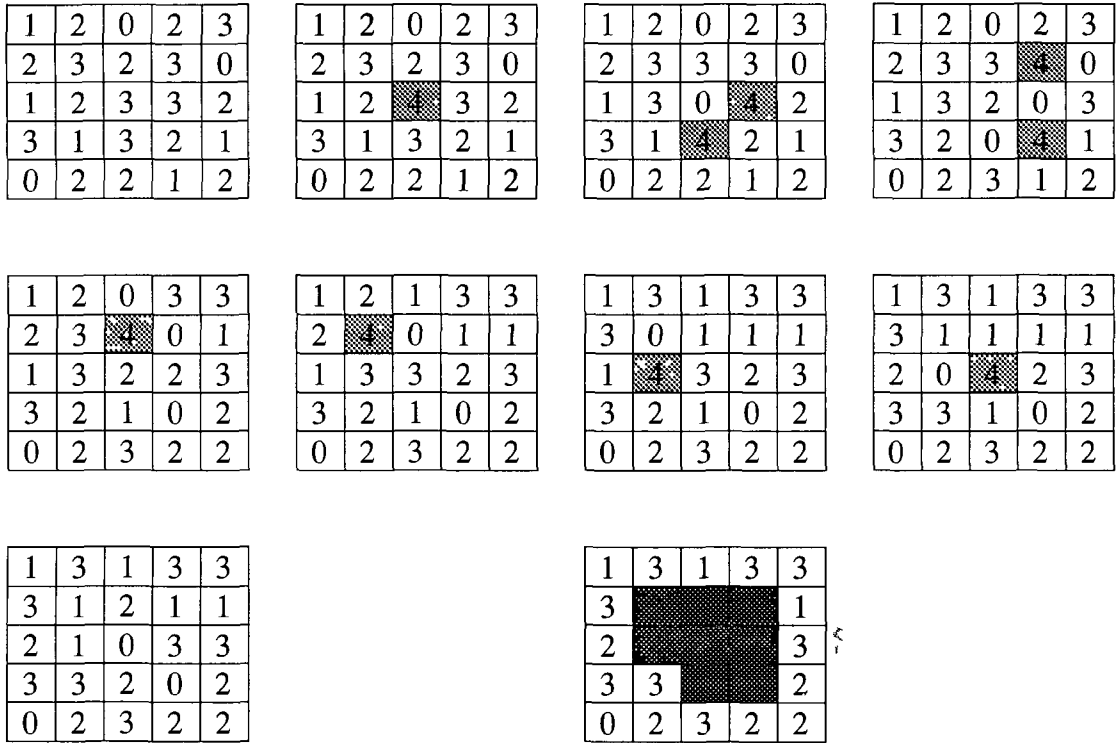


Fig 2.1.2 Illustration of topping avalanche in a small sandpile in a BTW 2-D model
 Within the avalanche of size 9, one site has toppled twice. The black squares indicate the eight sites that toppled.

For the 2D sandpile, the critical state for which all sites have exactly the critical slope is not stable any more due to small perturbations. An avalanche would spread into two directions on the lattice with more than one grain falling off the pile, and it is not a fixed point as in 1D. However, after a transient period, the system through a self-organizing process reaches a stable critical state where, *on average*, the rate of flow into the system equals the rate of flow out of the system across the boundary. The stationary state then responds to the addition of a sand grain with an avalanche. This is of unpredictable size, (number of toppled sites), and duration, (number of iterations needed to reach the stable state), so that size and lifetime distributions vary over large scales. Statistically, the probability distributions of the size s and lifetime t averaged over a large number of perturbations have been observed to follow power-laws

$$P(s) \sim s^{1-\tau} \tag{3.2.8}$$

$$P(t) \sim t^{-b'} \tag{3.2.9}$$

where τ and b' are defined to be the size and lifetime exponents respectively, with

no characteristic time and length scales. If we define $P(s, L)$ as the distribution function of avalanches s for a system of size L , then we have

$$P(s, L) = L^{-\beta} F(s/L^\gamma) \quad (3.2.10)$$

where β is a decay exponent, $\beta = \gamma(\tau - 1)$ (τ defined by Eqn(3.2.8)) γ is a critical index which represents how the cutoff scales with system size and F is a scaling function. When $L \rightarrow \infty$, the avalanche size distribution becomes independent of the system size L , and when $s/L^\gamma \rightarrow 0$, F approaches a power law and decays very quickly for $s \gg L^\gamma$, Tang (1988)

3.2.1.2 Catalogue of Sandpile Models

Many sandpile automata models have been studied to date. In the critical height model, the integer variable z represents the height of the sand column at the site (i, j) , i.e. is dependent on zero derivatives of the local sand height function being equal to zero. The critical slope model is defined to depend on the first derivatives of the local sand height function, i.e. strictly is a local gradient rather than overall slope and the critical Laplacian Model is dependent on the second derivatives of the local sand height function, Manna (1991). Of the various sandpile models the height version in particular has been intensively studied because of its intuitive form and the simplicity of its mathematical structure, Lubeck and Usadel (1996). However, the critical slope model even the local gradient version behaves in a way which is much closer to a real sandpile. Formulation of the model is similar to Eqn (3.2.6) but differs in that if the local *slope* in any direction exceeds the critical slope, then the sandpile topples. Early studies, e.g. Manna (1990), Ruskin and McCarren (1994) failed to find evidence for simple power-law behaviour, so that scaling in the avalanche cluster and duration distribution function does not appear to be satisfied. Here "scaling" means that distribution and correlation functions for all dimensionless quantities are constant in time. For additional work on the slope model see, e.g. Puhl (1992), Frette (1993) and references within. For the critical Laplacian model, studies by Kadanoff et al (1991) have shown, through a scaling analysis, that the exponents are different from the critical height model, and the model thus belongs to a different "universality" class. The key equation is

$$L_{(i,j)} = 4h_{(i,j)} - h_{(i+1,j)} - h_{(i,j+1)} - h_{(i-1,j)} - h_{(i,j-1)} \quad (3.2.11)$$

where $L_{(i,j)}$ is the local Laplacian

Zhang (1989) proposed a different stochastically driven *continuous* energy model. He considered a real number $E_{(i,j)}$ represented at each site (i,j) on a square lattice. The system is perturbed randomly by adding an amount to a randomly chosen site, i.e. $E_{(i,j)} \rightarrow E_{(i,j)} + \delta E$. If the value at any site exceeds the threshold value $E_{(i,j)} > E_c$, the system relaxes according to

$$E_{(i\pm 1, j\pm 1)} \rightarrow E_{(i\pm 1, j\pm 1)} + \varepsilon E_{(i,j)} \quad (3.2.12)$$

$$E_{(i,j)} \rightarrow 0 \quad (3.2.13)$$

ε is an exponent for energy dissipation. Similar to the 2D BTW model, when $\varepsilon=0.25$, the system is conservative and dissipation occurs only at the boundary, where the number of nearest neighbours is less than 4. Zhang has studied systems with $E_c = 1$ and δE chosen uniformly in the interval $[0, 0.5]$, and found that the same universality class as that for the BTW model applies, (i.e. values of critical exponents are in agreement with those obtained for the 2D BTW model).

Another *continuously driven dynamical system* was introduced by Olami et al (1992) (OFC) in terms of earthquake modelling. Though the dynamics of earthquakes are very complex, the event is driven by slow relative motion of tectonic plates, and the occurrence of abrupt shocks is intermittent. There are two time scales involved in the process, one is related to the stress accumulation, while the other is associated with the duration of the abrupt releases of stress.

3.2.2 Current Studies on Sandpile and SOC

3.2.2.1 Theoretical Results

Sandpiles with SOC have also been studied by several theoretical approaches. Mean-field theory has been used to neglect the effects of the fluctuations so that local variables are replaced by statistically averaged values, Tang and Bak (1988), Christensen et al (1993). One fundamental question of the mean-field approach is that of the upper critical dimension, i.e. the spatial dimension above which mean-field results are valid. In most SOC models, this dimension seems to be 4, Obukhov (1988), Diaz-Guilera (1994).

Theoretical work by Ding et al (1992) on alternative models with stochastic slide, however, has led to the conclusion that small and large sandpiles belong to different universality classes. This also provides some explanation for the apparent discrepancy observed with former experimental work, Held et al (1990). Another approach has been to investigate sandpile models where the rules are more suitable for obtaining analytic results, e.g. Abelian sandpile model, Dhar (1989), Creutz (1994). The renormalization group method is widely used in critical phenomena where the lack of characteristic scales is demonstrated frequently, Pietronero et al (1994).

There has been a lot of interest in constructing differential equations to describe the scale invariance of cellular automata models. For example, anomalous diffusion equations with singularities have been considered for studying the deterministic dynamics of the avalanches reached in the critical state, Carlson et al (1990), Chau and Cheng (1994), Kadanoff et al (1992). Additionally, nonlinear stochastic differential equations have been used by the dynamic renormalization group to analyse the earthquake models, Hwa and Kardar (1989), Grinstein et al (1990), Diaz-Guilera (1993).

3.2.2.2 Experimental Results

Real sandpiles of course present very complex behaviour so that they are difficult to explain fully in terms of simple interaction rules. For example it has been found that the existence of SOC in real sandpiles depends on how the pile is built. Two distinct types of experiments have been performed.

Jaeger et al (1989) used the method of rotating a semi-cylindrical drum partially filled with sand at a low constant velocity. In this experiment, the drop number (defined to be no. of grains tumbling at one time step) was found to be approximately periodic in time. Held et al (1990) considered the case of critical-mass fluctuations in an evolving sandpile, through an experimental study where the sandpile was built up to a steady state and then subsequently perturbed by the addition of a single grain at a time. After each grain was added, the size of the resulting avalanche was recorded. Repeated perturbations showed that avalanches were not predictable in terms either of their individual size (weight) or of their duration.

Held and his co-authors discovered that sufficiently small sandpiles showed broad scale-invariant distributions for avalanche sizes. For larger sandpiles, the avalanche distributions become sharply peaked, and the scale-invariance breaks down demonstrating finite-size scaling and the existence of SOC. Experiment shows that a single grain of sand can cause avalanches ranging from the extremely small to the system's finite limit.

However, the observed behaviour indicates that inertial effects play an important role, Dhar (1992), Prado and Olami (1992). Inertial effects lead to a nonlocal process, whereas in the numerical models, only the local geometry determines the dynamics. The relationship between the drop number of sand grains measured in experiments and the avalanche size measured in numerical models is unclear. Moreover, the work of Rosendahl et al (1993) deals with grain-by-grain quiescent perturbation of real sandpiles of various sizes for which it appears that power law behaviour is valid for all system sizes. Mehta and Barker (1994) have recently reviewed theoretical and experimental dynamics of granular material, which deals with some of these questions.

An experiment to investigate the relaxation dynamics of a sandpile was performed by Jaeger et al (1989). In their work, sandpiles initially at a given angle of repose were vibrated with varying degrees of intensity, and the relaxation of the average slope of the pile was monitored. It was found that for large intensities of vibration, the slope of the pile decayed to zero such that its relaxation was proportional to the logarithm of the time, whereas for smaller intensities, the slope of the pile stayed finite and the relaxation appeared slower than logarithmic.

In a more recent experiment, Frette et al (1996) have observed the internal *dissipated* energy in a slowly driven one-dimensional 1D rice pile. It was shown that the occurrence of SOC depends on details in the grain-level dissipation mechanism. With *spherical* grains, a stretched-exponential distribution was observed, implying a characteristic scale, and is inconsistent with SOC. However, with more elongated grains, the dynamics were dominated by sliding grains. These induced higher friction, and a power-law distribution of avalanche sizes was found. This provides the first experimental results of SOC behaviour in slowly driven granular systems. Theoretical models of rice piles are related to a

variety of different physical systems which share the same universality class, Paczuski and Boettcher (1996)

3.2.2.3 Computer Simulation Results

The study of sandpiles and related systems exhibiting SOC has to a great extent been based on simulations that use cellular automata models. Several factors which affect the behaviour exhibited by sandpile models have already been discussed. Unsurprisingly, these factors together with the sample size (no. of events or trials in the simulation) under various dynamics all have a direct bearing on the nature and precision of the results obtained, Manna (1990) (1991), Ruskin (1993)

As a final point, it is worth noting that both theoretical and simulation studies to date confine themselves to grains of a uniform size, whereas in a real pile the grain size is irregular leading to a virtually continuous avalanche of the finest grains when the sandpile approaches the critical point.

We now consider some specific examples of sandpile automata that we have implemented under various conditions and automata rules. These illustrate behaviour corresponding to a variety of applications. Systems sizes range from $L=256$, where L is the linear dimension of pile, to $L=1024$.

3.3 Studies of Sandpile Models

3.3.1 Simple Sandpile Height Models and SOC

We have looked in what follows at two versions of sandpiles namely (i) the simple height model with toppling rules as described in Section 3.2.1, (ii) the direct random model, where directed refers to the fact that toppling is in a preferred direction and sharing is random (as in (i)). This also uses the height dynamics.

For the direct sandpile height model, we have used the square lattice with steady height values of a site equal to 0, 1, 2, 3 and critical height $h_c = 4$ (Here we use height variable h instead of z). Thus for $h_c \geq 4$ the site topples. Simple features of simulation have been varied namely lattice size $= L^2$ and No. of trials (samples). The range of L was 32 to 1024 at which size storage was already a problem for

the larger number of trials, which range from 10000, to 50000 and 100000. These examples were implemented on both VAX and UNIX systems available in DCU. The dynamics of the directed model (iii) may be described similarly to those of the simple undirected model, Eqns (3.2.7-3.2.8) with an integer variable $h_{(i,j)}$ associated with each site. Again these are discrete and diffusive but are now supplemented by the preferred direction condition so that if any site $h_{(i,j)} \geq h_c$, it will topple only if the direction of toppling is allowed. The local height $h_{(i,j)}$ is then decreased. We have again built the sandpile on a square lattice where $h_{c(i,j)} = 2$, so that the two neighbouring forward sites $j \pm = j \pm [1 \pm (-1)^i] / 2$ are increased by 1

$$h_{(i,j)} \rightarrow h_{(i,j)} - h_{c(i,j)} \quad (3.3.1)$$

$$h_{(i+1, j \pm)} \rightarrow h_{(i+1, j \pm)} + 1 \quad (3.3.2)$$

i.e. when $i = \text{odd}$,

$$h_{(i+1, j)} \rightarrow h_{(i+1, j)} + 1 \quad (3.3.2a)$$

$$h_{(i+1, j-1)} \rightarrow h_{(i+1, j-1)} + 1 \quad (3.3.2b)$$

when $i = \text{even}$,

$$h_{(i+1, j+1)} \rightarrow h_{(i+1, j+1)} + 1 \quad (3.3.2c)$$

$$h_{(i+1, j)} \rightarrow h_{(i+1, j)} + 1 \quad (3.3.2d)$$

Starting with random initial conditions, a particle is added at one randomly chosen site at a given row of the lattice. If at that site the condition is satisfied, then two particles slide to the two nearest neighbours at the next row, where the toppling condition may be fulfilled again, leading to more topples and so on. We follow an avalanche until the system regains its stability, and then the next particle is added at the randomly chosen site. Sand grains are allowed to leave the system when the avalanche reaches the boundary.

3.3.2 Results and Conclusions

The form of the size and time distributions of avalanches is shown in Figs 3.3.1-3.3.2 for modest system size $L=512$, as an example. Similar results are obtained for different systems we discussed above. These show clearly that a scaling region exists, corresponding to the linear part of distribution of avalanche size, i.e. $\log D(s)$ vs $\log s$. We observe that as the lattice size increases, the linear part is

smoother and increases in length for larger N_0 of trials, permitting more precise estimation of the exponent, Eqns (3.2.8-3.2.9), before degenerating into chaotic or noisy behaviour for very large avalanche sizes. The largest avalanches observable are directly related to the number of particles in the sandpile so that a small sized sandpile necessarily limits the observation of large avalanches. Averaging over a large N_0 of trials or samples is clearly desirable in order to improve the statistics and we note that both N_0 of trials and lattice dimension L are modest in this work. The behaviour of the lifetime distribution vs $\log t$ is similar to that shown for size

We illustrate for $L=512$ and 10000 trials in Figs 3.3.1-2. Our estimates of the exponents τ and b' are given to be $\tau=1.81$, $b'=0.45$. Comparing these with those quoted by Bak et al (1989), $\tau=2.0$, $b'=0.43$, Manna (1990), $\tau=8/7$, the simple decay exponent $b'=19/15$, Ruskin (1993) $\tau=1.016$ to 1.093 , $b'=0.423$ to 0.457 , and $b'=1.012$ to 1.119 for a perturbation of size 1 for L variable, (perturbation also variable, Ruskin (1993)), it seems clear that we have good agreement with previous results with respect to the lifetime exponent. However, our value for τ is rather high, compared to more recent results, but agrees reasonably well with the initial theoretical sandpile models, Bak et al (1987), Dhar et al (1989) which made rather simplistic assumptions on the finite-size effect. This discrepancy may be due therefore to the size of the system which we have studied, compared to previously

More recently, Lubeck and Usadel (1997) have considered the directed BTW 2D sandpile model in a large scale, up to system size of $L=4096$. They also introduce a new method for statistically analysing the data to reduce the finite-size effects and obtain results, $\tau=2.293$ and $b'=1.48$, which are in agreement with the results obtained by renormalization group approach, Pietronero et al (1990)

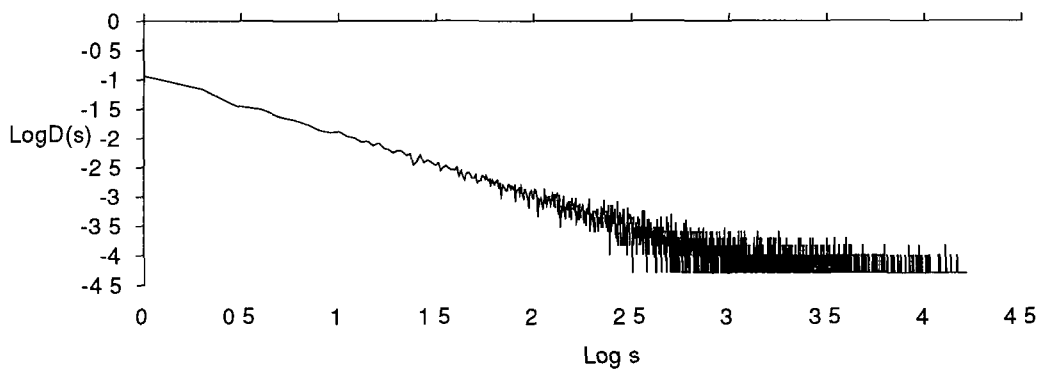


Fig 3 3 1 Distribution of avalanches size with $L=512$ and No of trials =10000

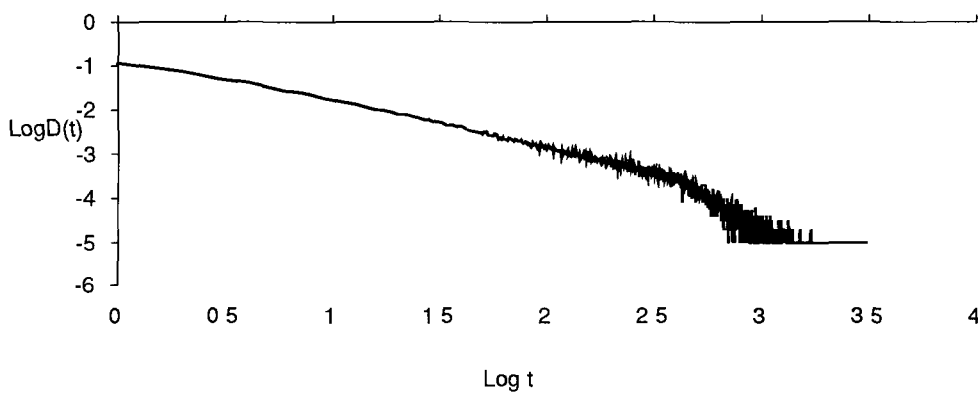


Fig3 3 2 Distribution of avalanches lifetime t with $L=512$ and No of trials=10000

3.3.3 The Directed Sandpile Model with Holes: Introduction for a Preliminary Note

We have also studied for a small system, the directed critical height model on a 2D square lattice in which a fraction of sites p are considered as holes. Thus the

system is additionally dissipative. The sand grains may also leave the system through these holes during the dynamic evolution. The distribution of defect sites or holes is random and can be considered as either *annealed* (increasing the system temperature, for example to reach an energetically more stable configuration in which the free energy is minimized) or *quenched*, (quickly reducing the temperature of a system, for example to trap a state favourable only at high temperatures). For the sandpile system, annealed defects arise when the probability p that a defect may occur at each lattice site is fixed only for a single event. The distribution of defects is generated randomly for each event, and is not memorised for the next event. Quenched defects arise when a distribution of defect sites is generated for each concentration p and held fixed during all events.

For the directed height model with holes, Figs 3.3.3-4 illustrate size and duration distributions for a typical $N_{\text{trials}}=10000$, where the first 10% of trials are left for the system to reach the steady state. It has been shown, Dhar et al (1989), Tadic et al (1992) that the existence of a preferred direction should lead to a new universality class, compared to the undirected model previously discussed. It is evident that our results differ from those obtained in the first model, (Section 3.3.2). No clear linear region is obtained, particularly in the size distribution and this supports the view that directed and undirected models do not follow similar scaling laws. In fact, the evidence for scaling is weak from our effort in the directed case, but this work considered small-sized simulations only (even compared to the undirected case) and consequently, the statistics are poor.

Tadic et al (1992) noted that power-law behaviour for size and time with exponents $\tau=0.43$ and $b'=0.30$. It is less clear, however, how hole concentration affects this behaviour. Our very small systems consider $L=128$, with concentration of defects (holes) given by $p=0$ and $p=0.05$ and $p=0.2$. Results obtained for the low concentration are similar to these for $p=0$ (no holes), but the systematic deviations in the numeric values compared to the limiting law of form (Eqns(3.3.4-5)) are due to the finite duration of the simulation imposed by the holes, i.e. distributions are truncated. Tadic et al (1992) argued that the self-organised critical state is lost in the presence of defects if the modified dynamic rules violate locally the height conservation.

As a preliminary look at dissipative systems, we considered the Tadic et al Model of introducing holes into the board. It is unlikely that small sandpiles under such restrictions can show the same wide range of fluctuations, since as noted for simple piles, (Section 3.2.2.2), large and small pile can behave very differently. Our limited study thus indicates that a crossover from SOC to non-SOC for a defective system is reached rapidly for small system size, but provides little qualification of this or comment on Eqn (3.2.10). An extended investigation, however, should include a wider range of p values.

For more complex defect cases, Tadic and Ramaswamy (1996) have studied in detail three models of driven sandpile type automata in the presence of quenched random defects. These models are termed the random site, random bond and random slope

models and when the dynamics are conservative, the concentration-dependent exponents are nonuniversal. In the case of nonconservative defects, the asymptotic state is subcritical.

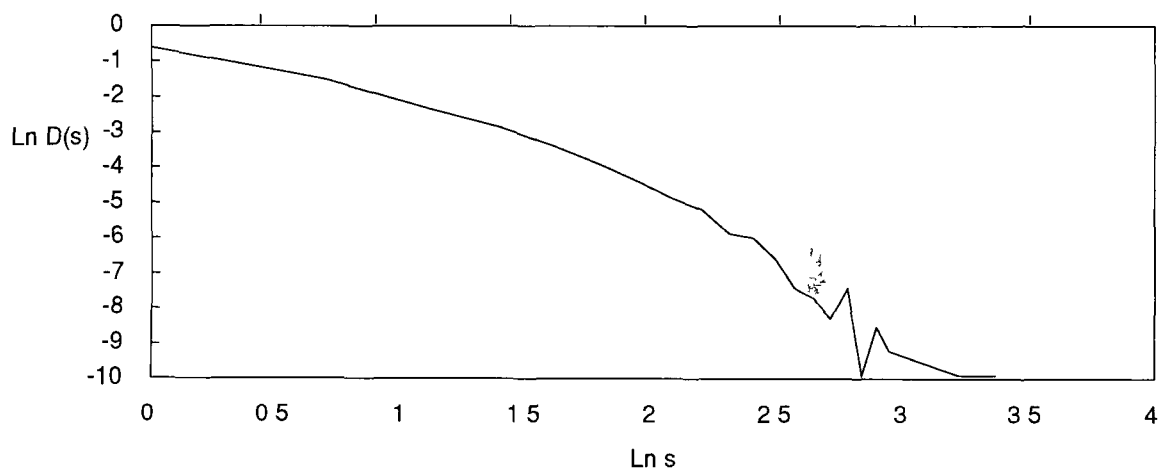


Fig 3.3.3 Distribution of avalanches size s for directed sandpile model with $L=128$, and No. of trials=10000

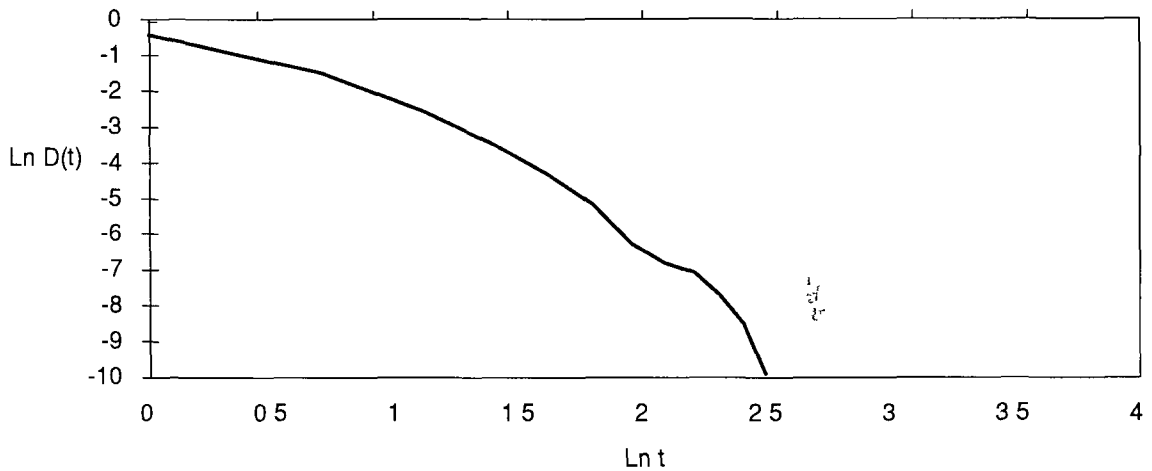


Fig3 3 4 Distribution of avalanches lifetime t for the directed sandpile model with $L=128$, No of trials=10000

3.4 Dissipative Sandpile Models

3.4.1 Nonconservative Sandpile Model

The original sandpile CA models are noise driven models in that the sand grains are added to randomly chosen sites in a pile, and either the *local dynamics* are conserved (i.e. no energy loss during the toppling) or the local dynamical law is conserved. The BTW relaxation rules conserve the dynamical variable z except at the boundary. Earlier studies have shown that conservative interaction rules are essential for obtaining SOC in the sandpile models, Manna et al (1990), and are also obeyed e.g. in the earthquake model, Hwa and Kardar (1989). Further investigation has shown that only those nonequilibrium systems with either a conservation law or a special continuous symmetry, demonstrate scale-invariance. Grinstein et al (1990). However, more work on deterministic models, e.g. of earthquakes, demonstrates the existence of SOC without a conserved quantity and is intriguing as it suggests a different mechanism for overall scale-invariant structures, Christensen and Olami (1993), Olami et al (1992), Janosi and Kertesz (1993). The nonconservative model also demonstrates SOC, in the sense that the probability for energy release during an earthquake is a power law. However, the model is found to be nonuniversal in the sense that exponents change continuously

as a function of the parameters of the models. Interest has also been directed to systems with uniform driving of the dynamics, Grassberger (1994). The evidence supports the view that scale-invariance holds for deterministic models of earthquakes, forest fires, and sandpiles, Middleton and Tao (1995), but not for others, e.g. a stochastic height sandpile model on the Bethe Lattice, Markosava (1995). It seems clear that the intrinsic features of *dissipative systems* and the real *origin* of SOC merits further exploration in view of these findings.

We have, therefore, considered some further examples of dissipative systems in more details. The dissipative sandpile models in what follows, exhibit no local conservation of energy with fixed perturbation. Sand is still randomly added to a site, generally resulting in avalanches in which the redistribution of sand grains is accompanied by energy loss according to local dynamical rules. Grains reaching toppling conditions at the boundary will ultimately fall out of the system.

3.4.2 Various Dissipative Models

3.4.2.1 BTW and Zhang Dissipative Models

Two simple types of dissipative models were initially proposed, one driven by random discrete BTW model and the other the continuous-energy Zhang model under local nonconservative conditions.

Of interest is whether the BTW model retains critical behaviour when introducing nonconservative dynamics in the interior of the system. The simple way to consider this is to change rule Eqn (3.2.6), for example, to

$$z_{(i,j)} \rightarrow z_{(i,j)} - 5 \tag{3.4.1}$$

with Eqn (3.2.7) remaining unchanged. This means one grain of sand is lost or dissipated for every topple. In the stationary state, the average rate of dissipation equals the average rate of flow into the system. Thus, $\langle s \rangle = 1/P_{z_c}$ where P_{z_c} is the probability of adding a grain to a site with z_c units, causing an avalanche. This probability approaches a constant value when $L \rightarrow \infty$, which means $\langle s \rangle$ will achieve a finite value. It is obvious that such a system cannot display SOC. The avalanche size distribution decays exponentially with a characteristic avalanche size, regardless of the system size, and avalanches seem to be localized.

With $\epsilon < 0.25$ is chosen in Eqns(3.2.11-3.2.12), the dynamics of the Zhang model are nonconservative. When δE is chosen in the range $[0, 1]$, the nonconservative relaxation rule again produces a characteristic avalanche size. This model is also noncritical in the presence of nonconservation, Diaz-Guilera (1994), Vespignani et al (1995)

3.4.2.2 CA and CML Dissipative Models

In a two-dimensional conservative sandpile CA model, all the space, time and state variables are integer (Eqns (3.2.2-3.2.3)). However, for the *dissipative height* sandpile model, this may not be the case since the local dynamics lead to changed values of local energy. Using both CA and coupled map lattice (CML) models, (Kaneko (1989)), for a nonconservation system with both discrete and continuous fixed dynamics respectively, a parameter α is introduced for the former which gives local energy loss during the toppling events, $0 \leq \alpha \leq 1$, with $\alpha=0$ equivalent to no loss. Therefore, in a two-dimensional model, Eqn (3.2.5) will be modified to be

$$h_{(i\pm 1, j\pm 1)} = h_{(i\pm 1, j\pm 1)} + (1-\alpha) \quad (3.4.2)$$

We choose the same value for α for all the neighbouring sites of (i, j) , and allow the neighbouring sites to topple simultaneously. This fixed discrete amount of energy loss accompanying grain toppling, results in avalanches which occur slowly compared to those for the nondissipative model, i.e. the lifetimes are longer. The higher the value of α , the more energy is lost during the evolution.

For the continuously driven dissipative model, i.e. the so-called CML model, we choose continuous state variables $F_n(i)$ in the lattice which evolve under a non-linear function map $f(x)$ to describe deterministically the loss of the local energy during a topple. In contrast to the dissipative CA model, the corresponding toppling rule in a two-dimensional CML model may be given by

$$h_{(i\pm 1, j\pm 1)} = h_{(i\pm 1, j\pm 1)} + F_n(i\pm 1, j\pm 1) \quad (3.4.3)$$

where we define $F_{n+1}(i) = f(F_n(i))$, ($F_0(i) = 1$). Since the local energy loss must be less than or equal to the whole local energy available, the corresponding values $F_n(i)$ must satisfy $0 \leq F_n(i) \leq 1$, and correspondingly $0 \leq f(x) \leq 1$

We have chosen to use two different function maps $f(x)$ representing different dissipation patterns which are either parabolic (non-periodic) or periodic respectively, i.e.

$$f(x)=1-ax^2 \quad (3.4.4)$$

$$f(x)=1-a\sin(x) \quad (3.4.5)$$

here a is a constant, $0 \leq a \leq 1$ and when $a=0$, $f(x) \equiv 1$, and $F_n(i) \equiv 1$, local conservation holds. The toppling and avalanche procedures in the CML models are similar to those of CA models, but the subsequent toppling energy distribution is influenced by the current toppling energy loss. The dynamics of this CML model resemble in some sense the continuous stick-slip earthquake model which has been discussed in Christensen et al (1992).

It is obvious that the dissipative pattern observed depends on the choice of function $f(x)$. Our choice reflects, to some extent, extreme conditions satisfying sand transport, (Fig. 3.4.1). Clearly, functions which correspond to more complex local dynamics can also be chosen. In what follows, we investigate whether local conservation is either a necessary and/or sufficient condition for a dissipative system to exhibit SOC in both CA and CML dissipative models for various values of α and different choices of $f(x)$ respectively.

3.4.3 Results for CA and CML models

Boundary conditions are taken to be open only here, consistent with those in the non-dissipative models. Periodic boundary conditions are considered in detail elsewhere, Middleton and Tao (1995). The main influence of the open boundary is to lead to continuous loss of the sand to its neighbouring sites.

3.4.3.1 Dissipative sandpile, CA model

We have implemented the discretely driven dissipative CA model, Eqns (3.4.2), with values of $\alpha = 0.03, 0.3, 0.5, 0.8$ respectively. Distributions of size, s , and lifetime, t , are shown in Figs. 3.4.2-3.4.3. We observe that distributions are qualitatively similar for the different values of α . The increasing dissipation in the CA model causes a decrease in the quantity of avalanches. Multiple toppling events do not occur any more due to the introduction of dissipation, and the

distribution displays no fixed power-law dependence. It seems clear that the dissipative CA model does not exhibit SOC unlike the nondissipative model. This agrees with results on the fundamental importance of the conservation law in demonstrating SOC, Manna et al (1990)

3.4.3.2 Dissipative sandpile; CML models

Simulation results for the dissipative CML models, with different choice of $f(x)$, (Equations (3.4.4) and (3.4.5)), are shown in Figs 3.4.4-3.4.7 respectively. Several different values of a have been chosen to examine the influence of $f(x)$ in these models.

Choosing $a=0.03, 0.3, 0.5, 0.8$, for the CML model with $f(x)$ given by Equation (3.4.4), we obtain very similar distribution results to those obtained previously, (Figs 3.4.6-3.4.7) above, where dissipation leads to rapid truncation with respect to both s and t . Avalanches take a long time to occur because individual toppling events happen slowly, and this is more obvious for a large dissipation. Again, there are no long-range correlations to indicate scale-invariance of the avalanches, i.e. no evidence to support the existence of SOC for any value of a chosen.

For very small energy dissipation, i.e. $0 < a < 0.1$ with $f(x)$ as above, we chose $a=0.0003, 0.003, 0.03, 0.05$ and 0.1 to examine the sensitivity of the threshold. However, size and time distributions are effectively the same so that even small interior energy loss in the CML model appears to cause the whole system to lose its original properties of SOC.

However, for the dissipative CML model with $f(x)$ of periodic form, Equation (3.4.5), we have observed some surprising and interesting simulation results, (Figs 3.4.4-3.4.5 for the size and time distributions respectively). It is clear that these quantities follow the power-law distributions which are characteristic of SOC. Exponents obtained are roughly, $\tau=2.25$ and $b'=1.25$. We illustrate for $a=0.1$, but similar behaviour has been observed for a chosen to be any value in the range $0 < a < 1$. The evidence supports the view that SOC does exist where the dissipative pattern of energy loss is represented by periodic and continuous local dynamics. However, the exponents are qualitatively different for the cases of local

nonconservation and conservation models

Recently, several authors have attempted explanations on the nature of SOC in these dissipative systems, Strocka et al (1995), Ahl (1995) From our numerical simulation results, it appears that, for a dissipative model, SOC depends, at least in part, on the nature of the local dynamics rather than the conservation law

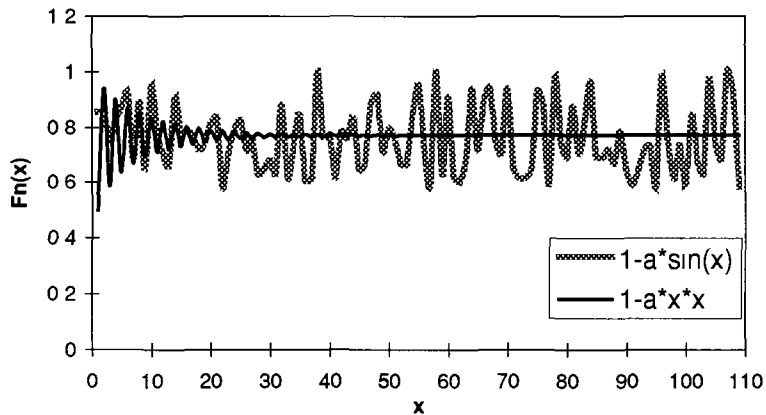


Fig 3 4 1 The continuous variables $F(x)$ of site x for two types of function $f(x)$ (non-periodic and periodic respectively) representing local energy dissipation Both chaotic (non-periodic) and periodic behaviour are often seen in many physical systems

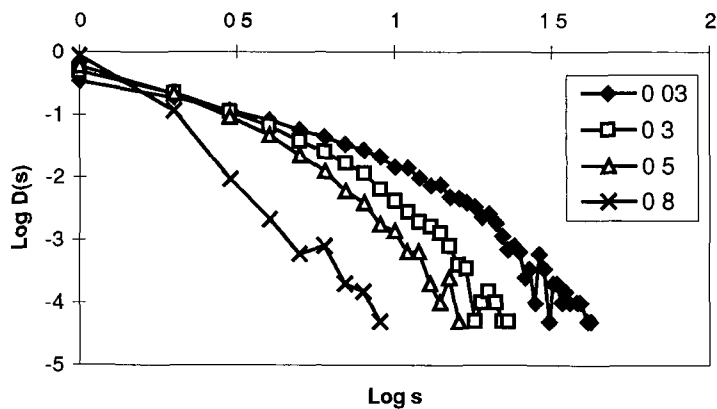


Fig 3 4 2 Distribution of avalanches with size s for the dissipative CA model

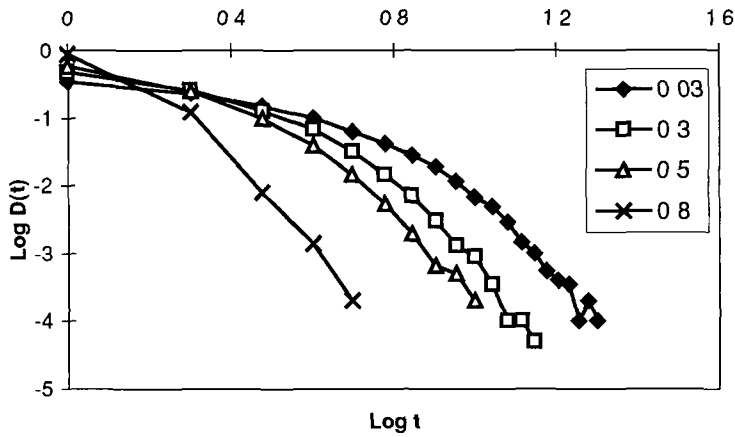


Fig 3 4 3 Distribution of avalanche lifetimes t for the dissipative CA model

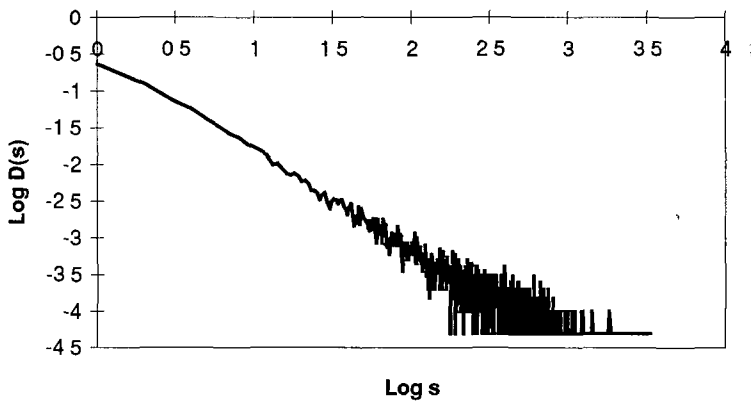


Fig 3 4 4 Distribution of avalanches size s for the dissipative CML model, with dissipation dynamic given by continuous function $f(x)=1-\sin(x)$

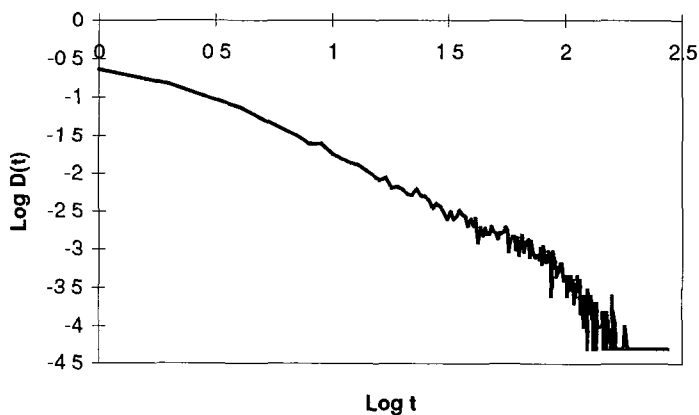


Fig 3 4 5 Distribution of avalanche lifetime t for the dissipative CML model with dissipation dynamic given by continuous function $f(x)=1-\sin(x)$

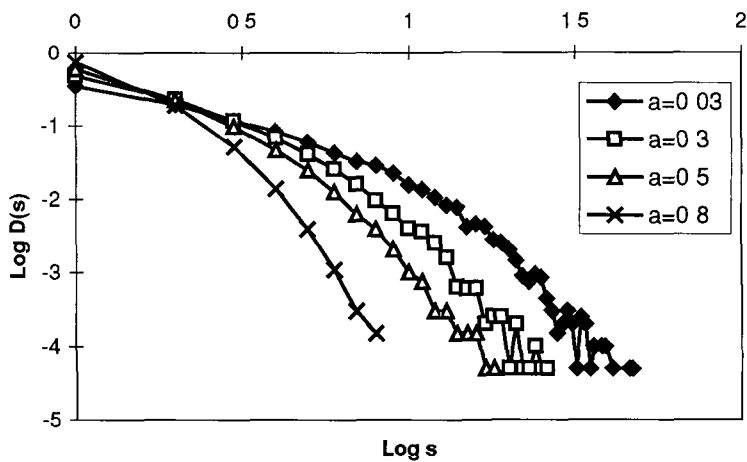


Fig 3 4 6 Distribution of avalanche size s for the dissipative CML model with dissipation dynamic given by continuous function $f(x)=1-ax^2$

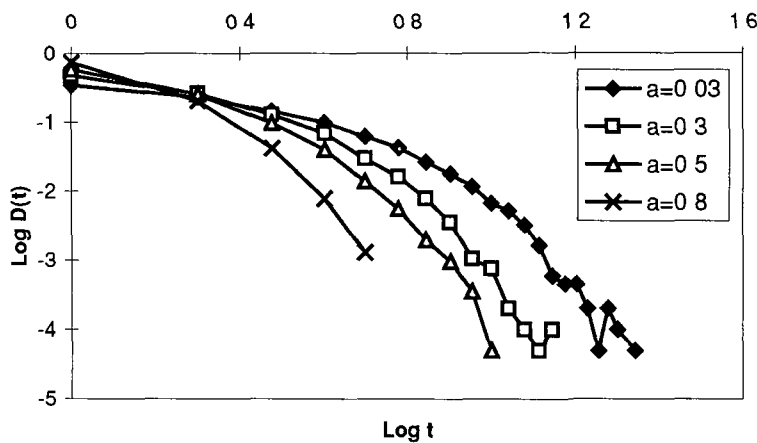


Fig 3 4 7 Distribution of avalanche lifetime t for the dissipative CML model with dissipation dynamic given by continuous function $f(x)=1-ax^2$

3.4.3.3 Conclusion

We have studied both discretely and continuously driven dissipative sandpile models, (CA and CML type respectively), under the height dynamic. From the simulation results obtained, we find no evidence for the existence of SOC when dissipation is introduced into the BTW, Zhang, and CA model. Thus, a necessary and sufficient condition for SOC appears to be that the conservation law should hold, in agreement with findings of former authors. However, SOC is apparently exhibited by some dissipative CML models, with results from our limited investigation supporting the view that local dynamics rather than local

conservation determine whether the phenomenon is observed. This conclusion is in agreement with that for a deterministic dissipative model, Middleton and Tao (1995), but not with findings for a stochastically driven dissipative model on the Bethe lattice, Markosava (1995). Exponents for the avalanche distributions for s and t are quantitatively different for the local conservation and nonconservation models.

3.5 SOC and Complex Systems

Most models for which we have discussed SOC are discrete in both space and time, they are cellular automata or some variants of CA. More realistic models might involve infinities of coupled differential equations, but for very many elements, it is unlikely that the discretization affects the asymptotic behaviour, w.r.t. time and space in which we are interested. Moreover, cellular automata seem particularly suited to systems with many metastable states, as in many of the complex systems that we considered.

Sandpile models clearly provide considerable and often contradictory insight into the phenomena of SOC. Bak and Chen (1991) have concluded that the theory of SOC can be described in terms of many composite systems naturally evolving to a critical state, in which a minor event starts a chain reaction that can affect any number of elements in the system. Although composite systems produce more *minor* events than catastrophes, chain reactions of *all sizes* are an integral part of the dynamics. According to this theory, the mechanism that leads to minor events is the same one that leads to major events. Furthermore, composite systems *never* reach equilibrium but instead evolve from one metastable state to the next. This theory clearly has attractions in terms of describing natural events, such as earthquakes. The simplicity of the models suggest that the phenomenon of SOC could be universal. Certainly possibilities have been scrutinised by many researchers in various fields so far, e.g. statistical mechanics, condensed matter physics, geophysics, biology, and economy. An interesting aspect is that the dynamics of SOC systems are intermittent, with avalanches of activity separating periods of relative quiescence.

Another important point is that avalanches are predictably displayed in long-term patterns, although it is impossible to predetermine when a system will reach

instability and how much adjustment is required to regain stability except on a short-term basis, Kagan and Knopoff (1987) Overall avalanches observed display a log-linear relationship for a real system, in agreement with that observed in earthquakes by Gutenberg and Richter (1956) These authors found a straight line with a slope (critical exponent) between -1.25 and -1.50 from earthquake model, depending on the fault under study

The presence of defects in 2D directed sandpile automata leads to some interesting effects For the case of random defects, some concentration-dependent scaling exponents have been obtained, It appears that varying the concentration of defects is a mechanism for continuously tuning the local rules of relaxation, which may finally lead to a phase transition between metastable states with different properties

In a slowly driven or evolving system, the physical time between lattice updates is very short when avalanches are propagating and very long when the system is being perturbed In the Zhang model, the transfer of energy depends on the energy of the lattice, whereas it is a fixed quantity for the BTW models When introducing nonconservative relaxation rules into the stochastically driven BTW and Zhang models, the distribution of avalanche sizes decays exponentially with a characteristic avalanche size The systems are subcritical However, the occurrence of criticality in some nonconservative models, e.g. continuous deterministically driven OFC model and CML models, is very intriguing since it suggests a different mechanism for the generation of the scale invariance (OFC model is an earthquake model, see Olami et al (1992)) Since moreover, the majority of natural phenomena are nonconservative, the SOC behavior of nonconservative systems is probably more important to understand than the corresponding behavior of conservative systems

3.6 In Summary

In this chapter, we consider the problems involved in simulation methods applied to physical and related systems with few constraints Examples of cellular automata modelled "sandpiles" and their applicability to real world systems have been described and the phenomenon of SOC discussed. Recent theoretical

developments are presented and assessed in terms of findings from experimental investigations. Results of our implementations of those models for both conservative and nonconservative systems are also given.

Chapter 4 Cellular Network Models

Our second computer simulation application deals with a class of non-equilibrium systems with underlying disordered patterns known as cellular networks. Materials with cellular structure appear in nature in a disparately wide range of fields, such as engineering, physics, geology, metallurgy, biology, ecology and so on, and their statistical behaviour can be investigated by monitoring the network evolution through time.

In what follows, we investigate the evolutionary behaviour and the statistical properties of a typical cellular network model, the 2D soap froth model, which provides valuable insight into the behaviour of complex disordered cellular systems. The computer methods of constructing 2D froth models have been introduced. We concentrate in particular here on details of the direct simulation method for various different system sizes with both ordered and disordered initial conditions. The different stages related to the concentration of defects or amount of disorder during froth evolution have also been analysed and results are discussed.

The original form of the programme for direct simulations, which we have used, is due to Weaire and Kermode (1983b) (1984), Kermode and Weaire (1990). Various adaptations and modifications which we have made are detailed briefly in this chapter and the full code is given in Appendix E (diskette) together with supplementary programmes for illustrations of the froth evolution etc. Further general points on comparative simulation techniques for this type of problem are discussed in Chapter 5.

4.1 Background and Introduction

4.1.1 Cellular Structures

4.1.1.1 Introduction

Many materials occurring in nature possess a cellular network, which means they have structures composed of either two or three-dimensional polygonal compact domains separated by well-defined sharp boundaries. For example, consider the pattern formed by a soap froth confined between two transparent plates. The

geometric structure of this system consists of a tiling of the plane by domains or cells of nearly polygonal shape. In the three-dimensional case, the domains assume polyhedral-like shapes which are almost homogeneous and are separated by thin boundaries. One of the oldest such patterns can be found in the Giant's Causeway in North Ireland, Bulkley (1693). Samuel Foley (1694) first calculated the distribution function for a two dimensional network of grains. A particular class of cellular structures, (which evolve either in time or as some external parameter is changed and for which an energy is associated with the boundaries), has become a subject of much interest over recent decades. Models of such patterns can be found in a wide range of fields, e.g. soap froths, foams, magnetic bubbles in garnets, polycrystalline metals, alloys, and branches of physics such as hydrodynamics, Glazier and Weaire (1992).

The applications of cellular network models have covered a wide range of areas. For instance, foams are beautiful examples of heterogeneous materials, with properties closely related to their structural characteristics.³ The structures of foams are varied: liquid foams, such as those made of the soap bubbles familiar to all, solid foams such as in cellular materials and so on. The use of foams ranges from transport of granular media in pipes to fire suppression and explosion attenuation. Thus the geometry of soap bubble arrangements in confined environments is an emerging research subject, where several intriguing phase transitions have been recently observed, such as those with bamboo-like or spiral structures. The problem of foam stability is more specific to liquid foams, however, and is connected with the important issue of emulsion stability, Exerowa et al (1992), Aveyard (1995). We concentrate here on the studies of dry froth in which the liquid fraction is ignored, (i.e. no Plateau borders), in order to demonstrate a direct approach to computer simulation of such systems. Computational implications for extending these simulations to wet froths are briefly noted in final chapter.

Weaire and Rivier (1984) first introduced the type of cellular network problem described above, and this has motivated further developments on many aspects of cellular systems. A more recent review, Stavans (1993), has put emphasis on the scaling exponents characterising the time dependence of the average scale of cellular structures in evolution. Some specialised reviews also deal with important aspects of particular systems, e.g. the geometric properties of biological tissues,

Dormer (1988), and the chemical application of solid foams and liquid foams, Goldfarb et al (1988)

In contrast to the cellular system models, discussed in last chapter, any small perturbation in cellular network models will have an influence on all network elements, i.e. local adjustment will be related not only to nearest-neighbours, but also to second nearest-neighbours

4.1.1.2 History

The soap froth as an ideal model of a cellular network has attracted considerable attention in that it provides valuable insight into the behaviour of several complex disordered systems. Many efforts have been made to connect the soap froth model to other models in biology, metallurgy, ecology and so on. As long ago as (1925) (1928) (1931), Lewis studied froth and living cells in an experiment on cucumber. He recorded ordered and disordered patterns and gave an empirical relation between the number of sides of a cell and its area. Some years later, Thompson (1942) noted the analogy between froth bubbles and cells of biological organisms. In particular, he quoted the similarity between grain growth in molluscan shells and a model of a crystal growing in albumin. Bragg and Nye (1947) first proposed that froth could be used to model grain growth in metals, but had not deduced that the individual bubbles may be considered similar to atoms in whole crystal grains. Later, Smith (1952) (1954) discovered that the soap froth represented the closest approach in an experimental system to ideal grain growth in a metal. From this observation, his analysis shown that each separately oriented grain was analogous to one bubble in the froth and that grain boundaries in a metal corresponded to soap films. Population biologists have further considered the influence of cellular patterns during evolution. For example, ecologists deal not only with behaviour within a single habitat but also with the interaction between an ensemble of them, as for instance in the territorial competition in fish and other species, Hasegawa and Tanemura (1976)

4.1.2 Applications: Soap Froth Model

4.1.2.1 Basic Geometrical Relations and Topological Process

The dynamics in a cellular structure are driven by surface tension or surface energy forces. The structure consists of a network of boundaries on a surface, which has the property that three boundaries meet at every intersection or vertex for the two-dimensional case. A two-dimensional cellular structure embedded on the Euclidean plane consists of a tiling of non-intersecting polygonal cells or faces, whose boundaries are formed by curved edges impinging on vertex points. According to Euler's theorem, in general form, the relationship between the number of faces F , edges E and vertices V of a polygonal domain can be expressed as

$$F - E + V = \chi \quad (4.1.1)$$

where χ is the Euler characteristic. Then $\chi = 0$ for a network on the surface of a torus (or for a planar network subject to periodic boundary conditions) and $\chi = 2$ for a network on the surface of sphere in which case the network is topologically equivalent to a convex polyhedron, (the original application of the result). Then $\chi = 1$ corresponds to a finite network on the infinite plane. The fundamental nature of Euler's theorem for topology comes about because the invariant it represents specifies the topological type of the surface on which the network is drawn. The network is built of polygonal domains whose boundaries join at vertices with coordination number equal to three in cellular structures. Applying this theorem to large networks, we have that the average number of sides per polygonal domain is equal to six.

During the evolution of a cellular structure, there are changes in the local connectivity of the edge network. These changes can be broken down into elementary processes or transformations, which obey the topological constraints. There are two basic types of topological rearrangements which have been observed in soap froths, foams and metallurgical grain aggregates, namely, T1 and T2 processes, which preserve topological properties by effecting changes in the number of sides of the cells involved in the transformation. The T1 and T2 processes are shown in Figure 4.1.1 (a), (b) and (c), where for the T1 case two cells lose one side each and two others gain one. For the T2 process, a cell with more than three sides can vanish through a series of T1 processes, to make it

three-sided, for example, in (b), the three-sided cell disappears with each neighbour losing a side, in (c), the four-sided cell disappears with the number of sides of two neighbours remaining constant while that of the other two decreases by one. Similarly, for the five-sided cell, the number of sides of two neighbours is left constant, two other neighbours lose one side each and the fifth neighbour gains a side. And so on for six, seven and higher order cells.

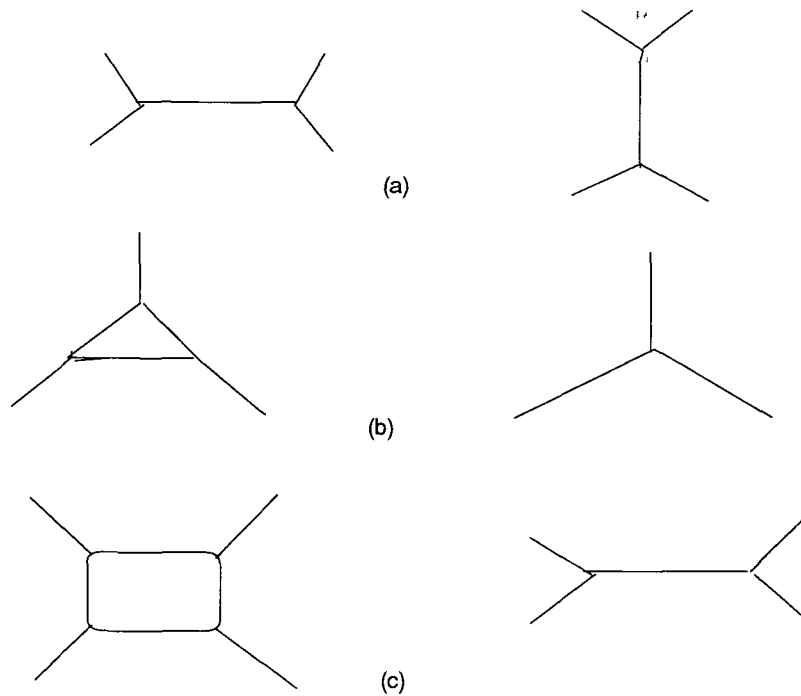


Figure 4.1.1 Elementary Topological Processes
 (a) Side Swapping or T1 process
 (b) Disappearance of a three-sided bubble or T2(3) process
 (c) Disappearance of a four-sided bubble or T2(4) process

It is noted that four-sided cells have two possible decay configurations in contrast to three-sided cells whose decay state is unique. Since the classic work of Smith (1952) on soap froth, it has been conventional wisdom to think that T2 processes of four-cells do not occur. According to Smith, the vanishing of four-sided bubbles is mediated by T1 processes in which bubbles become three-sided first and then decay directly by shrinking. This claim has not been vindicated, however, by experiments on froth or in other cellular structures, where direct vanishing of four- and five-sided cells is observed, Glazier et al (1987). Theoretical support for the experimental results has been provided by Fradkov et

al (1993) The authors pointed out that the decay configuration which a fourfold or fivefold vertex will adopt, from all those possible in a particular situation, is determined by system-dependent characteristics such as the physical size of the boundaries with respect to the system thickness They argue that this may endow the evolution with a stochastic character

4.1.2.2 Von Neumann's Law and Scaling State

In cellular network systems, a balance of forces imposes restrictions on the angles between boundaries at each vertex Generally speaking, in a real case, it proves impossible to satisfy these restrictions unless boundaries are curved Evolution is driven by mechanisms that relax this curvature and thus minimise boundary length The simple and elegant theoretical basic to describe the dynamics of curvature-driven cellular network structure is due to Von Neumann (1952) and was supported by the original soap froth experiments of Smith (1952)

Von Neumann showed that the rate of change of area with time of an individual cell and its number of sides n are related by the expression

$$dA/dt = k(n-6) \quad (4.1.2)$$

Here A is the area of an n -sided cell and k a constant which depends both on the solubility of the gas which diffuses through the soap film and the thickness of the latter However, a possible variant of Von Neumann's law was recently proposed by de Icaza-Herrera and Castano (1995), which took into account the effect of cell's area as well, given as

$$dA/dt = kA(n-6) \quad (4.1.3)$$

We compare these equations of froth coarsening from different initial configurations in due course

Clearly, Eqn (4.1.2) means that only a cell with less than six sides shrinks, while that with more than six sides grows A cell with six sides neither grows nor shrinks, although it may change its shape, as diffusion proceeds, until such time as it is involved in a topological change, when it no longer has six sides This is shown in Fig 4.1.2 and is particularly important in relation to *transient behaviour* since we can regard diffusion as occurring during the topological transformation processes according to equation (4.1.2)

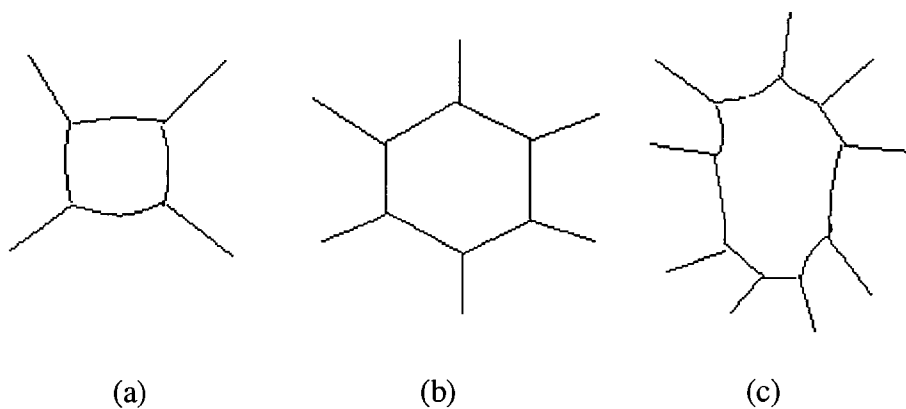


Fig 4 1 2 Typical shapes of cells as function of their number of sides n in an equilibrated system (a) cell with $n < 6$ have boundaries bulging outwards
 (b) cell with $n = 6$ have straight boundaries
 (c) cell with $n > 6$ have boundaries bulging inwards

The only pattern that is stable under Von Neumann's law is the perfect hexagonal network. Even the existence of only a single defect pair will result in the collapse and eventual disappearance of all the cells in the network. As the average length scale grows continuously with time, we are interested in the dynamic properties of the system, measured by statistics such as the distribution of the number of the cell sides, $f(n)$, and the second moment of $f(n)$, μ_2 , which would be expected to be constant, if the froth attains dynamic equilibrium, i.e. reaches a *scaling state*.

4.1.2.3 Lewis and Aboav-Weaire Laws

The correlation functions of interest are those between area, (or diameter), and number of sides, usually known as Lewis Law, and correlations between the number of sides of neighbouring bubbles, (the Aboav-Weaire law).

Lewis (1928) observed the following linear relationship between the average area of an n -sided bubble $\langle A_n \rangle$ and n

$$\langle A_n \rangle = k(n - \alpha) \quad (4.1.4)$$

where k and α are constants dependent, respectively, on the average area of all bubbles and on the bubble pattern. This relation is valid for a large class of cellular structures provided n is large enough.

Aboav (1974) found that the topological correlation effect among different cells is then described by

$$m(n) = (6 - a) + (6a + \mu_2)/n \quad (4.1.5)$$

where a is a constant ($a=1/2$), and $m(n)$ is the average number of sides of the neighbours of an n -sided bubble. This is known as Aboav's Law and for the special case of $a=1$, is usually called the Aboav-Weaire law.

4.1.2.4 Simple Soap Froth Model

The soap froth is the simplest and most familiar structure which has the characteristic of surface-energy-minimisation, i.e. each cell is of some constant predetermined area (in two-dimensions) and the system is in equilibrium when the total length of all cell edges is a minimum with respect to any small distortion. It represents the closest analogy to an experimental system with ideal growth. A soap froth has all boundaries equivalent, with its evolution driven by a transfer of gas between neighbouring bubbles and governed by Von Neumann's law. This constraint can be satisfied only if the boundaries are curved. We focus on an ideal dry froth, where the balance of forces gives all internal angles of the network equal to 120° and the mean number of sides $\langle n \rangle = 6$. Evolution is through T1 processes (neighbour switching) and T2 processes (cell vanishing), (Fig. 4.1.1)

From Eqn (4.1.2), we obtain the average area of a bubble $\langle A \rangle$ to be proportional to the time, t , i.e. asymptotic linear scaling of the froth, $\langle A \rangle \sim t^\alpha$. Also, it can be predicted that in a scaling state, the average length scale, $\langle d \rangle$, has the form $\langle d \rangle \sim t^\beta$, where β is the growth exponent. The pattern of the froth is also characterised by a single length scale, the mean cell radius $\langle r \rangle$, ($\langle d \rangle = 2\langle r \rangle$). The average size of the cell is a function of time, in the sense that it gets smaller or larger as time goes on.

Further a random structure can be characterised in terms of the distribution functions of its properties, namely the probability that a given bubble has a given area relative to the mean area, $\langle A \rangle$, of the pattern and the topological distribution function $f(n)$, the probability that a bubble in the pattern has n sides. Thus, moments are given by

$$\mu_k = \sum (n-6)^k f(n) \quad (4.1.6)$$

By definition from equation (4.1.6), $\mu_0 = 0$, $\mu_1 = 0$. The dispersion and skewness of the distribution is measured as usual by the second and third moments. In the evolution of a froth, the value of the second moment μ_2 is a fundamental quantity

4.2 Current Studies of Froths

4.2.1 Experimental Studies and Results

The first experiments on coarsening of soap froth were carried out by Smith (1952), based on some photographs taken during the evolution of a froth, initially non-uniform which was observed to evolve from a few thousand tiny bubbles to a few hundreds. While Smith found that soap froth mimics grain growth in metals, the former does not include the complexities of grain boundaries with orientation-dependent energies. Smith's analysis suggested that long-term asymptotic behaviour was just a change of scale, with no change of the size distribution. He also found that dynamic scaling properties can be characterised after initial transience by system statistics such as the second moment, $\mu_2 = 1.5$ and the average area of a bubble $\langle A \rangle$ dependent on an exponent, as indicated previously, with $\alpha = 1$. There was a tendency towards a fixed, time-independent distribution of number of sides and relative sides. He concluded that only three-sided bubbles could disappear directly, however, as noted earlier, whereas four- and five-sided bubbles could not, but evolve through T1 processes to become three-sided first, then vanish directly via a T2 process.

Smith's conclusions were challenged by an analysis published by Aboav (1980), based on a *different* set of photographs of Smith, using an alternative experimental method, where the initial bubbles were formed with roughly uniform size. Evolution was again followed from thousands of cells to hundreds of cells. From the statistical data, Aboav found that no stable limiting distribution of sizes existed and the second moment $\mu_2 \sim \langle d \rangle$, (roughly from 0.64-2.86), increased with average linear intercept $\langle d \rangle$, where $\langle d \rangle \sim \langle A \rangle^{1/2}$, i.e. $\alpha = 2$.

Much later, Glazier et al (1987) carried out a set of experiments and found that T2 processes *could* include direct disappearance of four- and five-sided bubbles without any prior side-shedding. Several types of initial condition both ordered and disorder were considered. In the ordered case, large ordered domains of six-sided bubbles are separated by dislocations formed by pairs of five- and seven-sided bubbles. As t increases, five-sided bubbles shrink while seven-sided ones grow. As the five-sided bubbles disappear, they affect the number of sides of the neighbouring hexagonal bubble and the spatial extent of the ordered regions.

steadily decrease. Once all the ordered domains disappear, evolution proceeds with disordered configurations. A relaxation region is thus found followed by power-law behaviour. Glazier et al (1987) found that, irrespective of the nature of the initial conditions, froth evolution behaved asymptotically as $\langle A \rangle \sim t^\alpha$ with $\alpha = 0.59 \pm 0.11$. The difference with the expected value $\alpha = 1$ was traced later, to the fact that the experiments were performed with a fixed amount of fluid.

Stavans and Glazier (1989) studied the long-term scaling regime in terms of the distribution $f(n)$ and its dispersion in both ordered and disordered froths. Within experimental error, $f(n)$ remains unchanged during the evolution after transient states have died out. A more precise measurement of $f(n)$ is also given, comparing results from a number of systems, they observed that $f(5)$ is higher than $f(6)$. They also provided evidence for the validity of the Aboav-Weaire law, with the second moment $\mu_2 = 1.4$, and obtained excellent agreement with the measured dependence of $m(n)$ on n .

4.2.2 Theoretical Results

Several theoretical analytical methods have been used to describe the evolution of cellular networks from various aspects.

(I) Mean-Field Theory

Flyvbjerg and Jeppesen (1991) derived a time-independent equation for the normalised distribution by introducing a generating function and solving analytically the partial differential equation obtained. Furthermore, Flyvbjerg (1992) has obtained a master equation, which is very similar to that of Fradkov et al (1988), but without assuming a maximum entropy distribution of the area. A numerical solution was obtained for the distribution of the number of sides without any free parameters.

Stavans et al (1991) pursued from the onset a two-track approach separating the calculation of areas from that of purely topological properties. They wrote dynamical equations for the variables without including T1 processes as a first step. The form of the equations neglected the appearance of two-sided cells. They found a line of fixed points instead of a unique fixed point as one would naively expect. Results here support the asymptotic time-independent behaviour of froth. Recently Segel et al (1993) extended the approach of Stavans et al to the

calculation of area-related properties. Their results are in agreement with experiment for all values of n and Lewis's law is valid for large values of n .

(II) Maximum Entropy Method

Eeenakker (1986) used a hybrid approach to describe the evolution of a froth. He derived a dynamic equation for the area distribution function. He argued that scaling behaviour is not exhibited in the solution. Instead, some cyclic behaviour is obtained, whereas disordered configurations collapse into ordered ones, consisting mostly of six-sided cells. Then evolve to disordered again. No such behaviour has been seen in any experiment so far.

De Almeida and Iglesias (1988) have studied maximum entropy to calculate the topological functions. Their predictions for side distribution $f(n)$ is in agreement with those obtained from froth experiments, corresponding to the second moment, $\mu_2 = 1.5$. However, the area distributions do not match experimental data for any value considered.

(III) Topological Model

Levitan (1994) first proposed a topological model to implement the rearrangement of the froth by random T2 processes. He considered the froth in terms of the areas of the bubbles and constructed an approximate topological realisation of the froth structure by labelling sites of the bubble lattice to create an adjacency matrix of nearest-neighbour connectivity. His model was used to solve von Neumann's equations on a geometrically realistic network of bubbles up to the point when the first bubble disappears. Since a T2 process is selected randomly, the neighbouring bubbles change their topological classes corresponding to the adjacency matrix changes. This model has also been unsuccessfully applied to the analysis of a single defect in a hexagonal network, Section 4.3.2. Recently, Levitan and Domany (1995) (1996) have proposed subsequent, revised versions of this topological model to correct the former results. Some extra assumptions have been taken to apply to the original model. One such, takes into account the effects of the areas of the topological classes of the neighbouring bubbles on the results of a T2 process. Lengths of the sides of 4-sided and 5-sided bubbles are calculated to obtain specified rectangles and pentagons of bubbles. The obvious advantage of these topological models is that they can deal with the macroscopic evolution of a froth with a very large system size. They have also been used to observe the

behaviour of the remaining bubbles, (so-called survivors) in some detail, Levitan and Domany (1997) A system size of over 40,000 bubbles has been studied so far However, results and conclusions obtained by those topological models seem in poor agreement with those by experiment and simulation methods Some details are given in the following section

(IV) Logistic Map Theory

Rivier (1985) first suggested describing the froth network using a logistic map, which means a space-filling pattern consisting of a central cell surrounded by concentric layers of cells For detailed definitions and proofs, see Rivier and Aste (1996), Aste et al (1996) Applying this dynamic map to the froth structures, Aste and Rivier (1997) studied the topological properties of physical froths, which are cellular networks with homogeneous shape and sizes They have found that in 2D, the logistic map has one parameter, given as a function of the average topological properties of the cells in the layers The curvature of the space tiled by the froth can also be obtained from their calculations

From this shell structure map, a clear illustration is also provided of diversity between cellular networks and simple cellular systems While both consist of simple cells, the difference in the evolution laws is intrinsic Connectivity relations between cells in the network are widespread and pervasive as opposed to local Any cell can be influenced by the disturbance in the network even it is far away from the central cell and the network adjustment take place instantly Whereas only the nearest neighbour sites of the cell can be affected in a *simple* cellular system in the first step, i.e. the connectivity is local However, cellular automata rules govern transitions between these simple elements As we described earlier in Section 2.4 the local adjustment occurs simultaneously, while the whole system is adjusted in subsequent time steps

4.2.3 Computer Simulation Algorithms and Early Results

Investigating a 2-D froth gives us the opportunity to observe the details of the structure since it is easier to visualise and model than a 3-D one Generally speaking, four methods to date have been used to simulate froths These are (i) direct simulation (ii) the Monte Carlo method (iii) the vertex model (iv) the Potts

model (variant of MC) We discuss these alternative approaches briefly in what follows, concentrating on (i) for specific studies described later in the Chapter

4.2.3.1 Direct Simulation

Weaire and Kermode (1983b) (1984), Kermode and Weaire(1990) proposed a 2D-FROTH program to investigate the equilibrium properties This program creates a finite sample of the froth network model with periodic boundary conditions and equilibrates it by an iterative procedure The pattern reaches equilibrium by a repeated cycle of local adjustments The soap froth is a strictly chaotic system, so the detailed evolution of the pattern may depend on the *sequence* in which adjustments are made The program distinguishes between topological and diffusive adjustments

Most studies so far assume that the cellular network is incompressible, and in the case of a froth, attempts to compress it simply minimise the surface energy of the soap film at all times The radius of curvature of each side is

$$r = c(P_1 - P_2)^{-1} \quad (4.2.1)$$

where P_1 and P_2 are the pressures in the two adjacent cells and c is a constant related to the surface tension T by

$$c = 2T \quad (4.2.2)$$

These conditions are satisfied for each cell area

Assuming that the rate of diffusion R of gas across each side is proportional to the length l of that side and to the pressure difference across it

$$R = kl(P_1 - P_2) \quad (4.2.3)$$

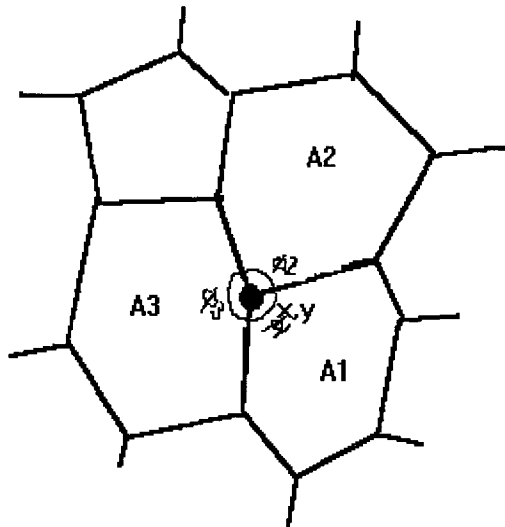
where k is a constant According to Equn (4.1.2), only the cells whose number of sides $n \neq 6$ contribute to froth evolution The cells with fewer than six sides will shrink and those with more than six sides will grow

The local variables chosen to relax at each step, are the position of a vertex and the pressures of the three surrounding cells Although two arcs with the same curvature can be drawn to connect two vertices, it is assumed that it is always the smaller arc that occurs in the network, (also supported by the experimental evidence)

Equations expressing the dependence of the vertex angles and their neighbouring cells areas are given by

$$\begin{bmatrix} \frac{\partial A_1}{\partial p_1} & \frac{\partial A_1}{\partial p_2} & \frac{\partial A_1}{\partial p_3} & \frac{\partial A_1}{\partial x} & \frac{\partial A_1}{\partial y} \\ \frac{\partial A_2}{\partial p_1} & \frac{\partial A_2}{\partial p_2} & \frac{\partial A_2}{\partial p_3} & \frac{\partial A_2}{\partial x} & \frac{\partial A_2}{\partial y} \\ \frac{\partial A_3}{\partial p_1} & \frac{\partial A_3}{\partial p_2} & \frac{\partial A_3}{\partial p_3} & \frac{\partial A_3}{\partial x} & \frac{\partial A_3}{\partial y} \\ \frac{\partial \phi_1}{\partial p_1} & \frac{\partial \phi_1}{\partial p_2} & \frac{\partial \phi_1}{\partial p_3} & \frac{\partial \phi_1}{\partial x} & \frac{\partial \phi_1}{\partial y} \\ \frac{\partial \phi_2}{\partial p_1} & \frac{\partial \phi_2}{\partial p_2} & \frac{\partial \phi_2}{\partial p_3} & \frac{\partial \phi_2}{\partial x} & \frac{\partial \phi_2}{\partial y} \end{bmatrix} \begin{bmatrix} \Delta p_1 \\ \Delta p_2 \\ \Delta p_3 \\ \Delta x \\ \Delta y \end{bmatrix} = \begin{bmatrix} \Delta A_1 \\ \Delta A_2 \\ \Delta A_3 \\ \Delta \phi_1 \\ \Delta \phi_2 \end{bmatrix} \quad (4.2.4)$$

where p_1, p_2, p_3 are pressures and x, y are vertex co-ordinates



so Eqns (4.2.4) as a function of the five variables are approximated by a linear form, and numerical differentiation is used to determine the coefficients. The angles and areas change as the froth equilibrates (i.e. angles optimum at 120°), and area adjustments involve vertices of other cells also.

Since the topological changes (T1 and T2) are the essential mechanism of froth evolution, direct simulation implements these topological rearrangements in a direct way. This means that after each local *relaxation* of a vertex, the first step is to test the possibility of a T1 process then specify the adjustment by solving the equations. If the proposed displacement is \mathbf{D} , and \mathbf{R}_i are vectors linking the vertex

in equation to its nearest-neighbours, then a T1 process takes place if the following is satisfied

$$D \cdot R_i > R_i \cdot R_j \quad (4.2.5)$$

The T2 process only occurs in two cases. Firstly, and most frequently, is in the diffusion procedure where changes of area are calculated. A T2 process will take place if the target area is zero or negative. Secondly, wherever it is convenient for a cell to disappear, then the target area is designed to have a small positive value. The existence of very small cells can cause some problems in the program, so any cell with area less than 0.1% of unit area, is forced to disappear (convergence).

As noted above, the diffusion process involves a transfer of gas across boundary. The net rate of diffusion for a cell is given by Eqn (4.1.2) and governs the cell area. The total area remains the same and the average number of cell sides is six, see Section (4.1.2.1).

The 2D FROTH program structure is as follows

```

PROGRAM FROTH

CALL SETUP      // Create Voronoi network
CALL INPUT      // Input parameters
CALL STAT       //Initialise
//Start evolution loop //
DO 10 I=1,IJSTEP // Increment step number
  ISTEP=ISTEP+1
  CALL DIFFUS   //Diffuse network
  CALL EQUIL    //Equilibrates the network
  CALL STAT     //Performs statistical calculations
10 CONTINUE
CALL OUTPUT
CALL STAT
CALL EXITFR     //Exit the program
END

```

Early results showed that for small system size equal to 100 cells, the simulated froth did not reach a scaling state, and μ_2 increased (roughly) in a linear fashion with time. For several samples of 500 cells, with differing initial structures, Weaire and Le1 (1990) obtained the asymptotic value of $\mu_2 = 1.42 \pm 0.05$. Simulations

starting from ordered configurations showed an early increase of μ_2 followed by a decrease and eventual achievement of a steady state value. Initial configurations characterised by different degrees of disorder were allowed to evolve and in all cases scaling was achieved. Herdtle and Aref (1991) using a similar method to Weaire and Kermode, however, obtained $\mu_2 = 1.2$ for a system of size 1024 cells. The difference lies mainly in the way the structure is relaxed towards equilibrium, which Kermode and Weaire (1990) specified as a sequence of local adjustments of pressures and vertices, whereas Aref and Herdtle considered all these variables to be adjusted simultaneously in each iteration.

4.2.3.2 Monte Carlo Method

The Monte Carlo method depends on representing the solution of a problem as a parameter of a hypothetical population, and using a random sequence of numbers to construct a sample of the population, from which statistical estimates of the parameter can be obtained. Wejchert et al (1986) discussed the Monte Carlo simulation of the evolution of a two-dimensional soap froth, based on discretization of the problem. These authors used a triangular lattice which has six nearest neighbours in two-dimensional space (i.e. has a hexagonal dual). Two neighbouring lattice points with different assigned integers are automatically separated by a cell boundary. A clustered group of lattice points labelled with an integer k , represents a particular bubble k .

This method incorporates explicitly the rapid equilibration of boundaries present in soap froths. All cells involved are of uniform same size and shape. This equilibration was also performed under the constraint of *constant bubble area*, which was built into the interaction Hamiltonian

$$H = 1/2N \sum_{i,j \text{ neighbours}} \delta_{\sigma(i,j)\sigma(i',j')} - 1 + \lambda/N \sum_{\text{cell } k} (a_k - \hat{a}_k)^2 \quad (4.2.6)$$

where k indexes the bubbles and each bubble present in the network at any time has a different integer label, \hat{a}_k is determined *target area* for the k th bubble according to Von Neumann's law, and λ is a constant. This Hamiltonian relaxes to the surface energy case, (which refers to the creation of pressure differences that result in gas diffusion), with the constraint that each bubble has a fixed target area.

\hat{a}_k The target areas were updated according to von Neumann's law, eqn(4.1.2), reproduced here for convenience

$$d\hat{a}_k/dt = k(n_k - 6) \quad (4.2.7)$$

Starting from a disordered Voronoi distribution of cells, the results of Wejchert et al are in agreement with the computational results by direct simulation and are compatible with experimental values of Smith (1952). An asymptotic regime was found for which the grain growth exponent in the soap froth simulation is $\beta=0.49 \pm 0.03$. After an initial transition period, the second moment reached an average steady state value of $\mu_2 = 1.6 \pm 0.1$. This kind of disparity between the μ_2 values appears to reflect dependence on initial structure, system size etc.

4.2.3.3 Topological Analysis (Vertex Model)

Kawasaki et al (1989)(1990) constructed vertex models in which the topological properties of the boundary of a froth are retained. In this case, when bubbles meet, the vertices are treated as pseudo-particles, and are subjected to forces determined by the positions of the neighbouring vertices. The connections between the vertices are assumed to be straight and deviations from 120° angles are used to determine an effective curvature. The vertices move to minimise bond length according to equations of motion of the form

$$\sum_j D_{ij} (v_i + v_j/2) = -\sigma \sum_j (r_i - r_j) / |r_i - r_j| \quad (4.2.8)$$

where r_i is the position of the i th vertex, v_i is its velocity, $\sigma > 0$ is a surface tension, and D_{ij} a tensorial friction coefficient associated with boundary motion. The sum is over all vertices j linked to vertex i by a bond. The enormous reduction in variables makes this method computationally very efficient so that very large systems can be simulated. However, the morphology of the configurations so generated is somewhat different from that of many real systems due to the very nature of the model. The extreme simplicity of the model is difficult to relate to the real physics of a froth structure. Kawasaki (1990) and co-workers found that scaling behaviour was obtained after short transient period with $\beta = 0.5$, but did not obey von Neumann's law, and their scaling state distributions generally differ remarkably from experimental results. This may be due to the assumption that all boundaries are straight lines regardless of the effect of interfacial curvature.

4.2.3.4 The Potts model

The Potts model is a generalisation of the Ising model in which spins on a lattice have q possible equivalent states. The simulation of the Potts model takes a quasi-microscopic view of froth evolution. The surface energy of the Potts model on a lattice is proportional to the total length of grain boundary in the system. The Hamiltonian describes the energy that results from various interactions. Each grain is defined as the region of a lattice in which vertices have a given value of spin (i,j) and the Hamiltonian is simply the surface energy due to spins that do not interact

$$H = -\sum_{i,j \text{ neighbors } i,j'} \delta_{\sigma(i),\sigma(j')} - I \quad (4.2.9)$$

In a zero temperature simulation, a site is selected at random and assigned a new spin if the change reduces the energy. This may be extended to a standard finite temperature Monte Carlo simulation (see e.g. Binder (1986)). The lattice has a surface energy that depends on boundary orientation. We characterise the anisotropy of the lattice by the ratio of the highest to the lowest surface energy per unit length.

There are two basic differences between the Potts model and the real experimental soap froth. The diffusion time of gas across a soap film is much slower than the equilibration time of the film along its length, while in the Potts model and most metals the two times are the same. Thus, soap froths are closer in shape to true equilibrium surfaces than are grain boundaries in the Potts model and metals. Furthermore, the Potts model has lattice *anisotropy* while the soap froth is entirely isotropic.

Glazier (1990) has presented a comparison between a next-nearest-neighbour $q=\infty$ Potts model on a square lattice and the experimental evolution of a two-dimensional soap froth. Starting from identical initial conditions and comparing the pattern evolution, dynamics, distribution functions and correlations of the two, the basic agreement between them is excellent. The Potts model is able to reproduce reasonable distribution functions, reach a scaling state with $\beta = 0.5$ and $\mu_2 = 1.5 + 0.3$ and achieves nearly perfect agreement on the correlation functions for the Aboav-Weaire law. There are, however, a few systematic deviations which may be due to the influence of subtle anisotropy and equilibration effects. In the

Potts model, highly anisotropic lattices, (where e.g. the relative distances to neighbours are in the ratio 1:2:4), produce frozen patterns and the scaling states of moderately anisotropic lattices (e.g. with ratio 1:1.5:1) have distribution functions which are flatter and broader than those of the soap froth, e.g. $\mu_2 = 2.4$ rather than the 1.5. Also, the disordering process takes more time than in the soap froth and the grain boundaries do not have uniform curvature.

Glazier et al (1989) with a Potts model simulation have observed that the area for cells with few sides is larger than that predicted by Lewis's hypothesis. Many-sided cells are smaller than predicted as well, and the distributions of normalised area are constant. The correlation seems to be independent of the degree of equilibration of the froth and would appear to depend on local rather than long range equilibration. For example, a very large number of cells with few sides can rapidly change sides by T1 processes without having to wait for cells to disappear.

4.3 2D Froth Models- Implementations via Direct Simulation Methods

4.3.1 2D Froth with Voronoi Network

4.3.1.1 Voronoi Network

Voronoi construction has been used to form the initial condition of a disordered network, Boots (1982). The Voronoi network is that network formed by convex cells whose boundaries are determined by all the perpendicular bisectors of all the lines joining a set of n -tuples, Grunham and Shephard (1987). Since it automatically creates a controlled amount of disorder, the Voronoi network was used for most initial configurations in the early investigation of froth evolution, Weaire and Kermode, (1983)(1984), Weaire and Lei (1990). In order to compute the network, we can use its dual, the Delauney tessellation. This is the division of space into a set of triangles whose apices belong to the set of initial points, where, for each triangle, no other point exists inside the circumscribed circle of that triangle. The Delauney tessellation is shown in Fig. 4.3.1.

A Voronoi network can be constructed by random generation of a set of initial points, i.e. the simplest case is where the bubbles form a tiling of the plane produced from a number of seed points scattered over the domain. These bubbles

arise by associating with each seed the set of points in the plane that are closer to it than to any other seed. Each vertex in such a tiling is trivalent except for degeneracies due to symmetry. The angles in the Voronoi pattern are not in general 120° , but these angles can be obtained by allowing the Voronoi tiling to relax elastically. If we impose constraints on the distribution of initial seeds, then we obtain special patterns, for example, two seeds subject to the condition that these are a certain minimum distance apart leads to the so-called hard-disk or hard-core Voronoi setup, Weaire and Rivier (1984). It has been noted that Voronoi patterns with a hard core tend to have lower values of the second moment than those with no constraint, Herdte and Aref (1992). The hard-core one can be used to set up a more regular network but still with some random structure.

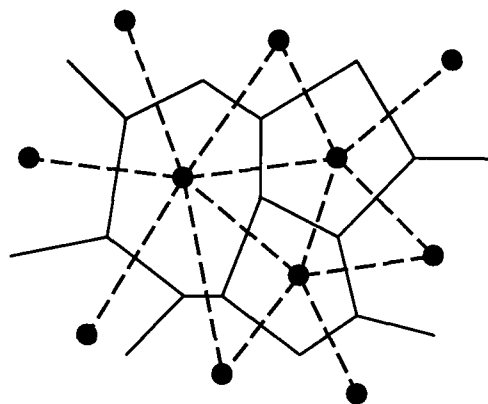


Fig 4.3.1 a section of Dual of the Voronoi network

4.3.1.2 Voronoi Froth Models- Large Scale Systems

We have constructed Voronoi networks for froth systems with several hundred bubbles by *direct simulation* methods, and have also extended the simulations to larger systems which would be more realistic for the investigation of true randomised froth structures. System sizes range up to several thousands of bubbles. In particular, we report on the scaling properties for a hard-disk Voronoi network for a system of 3000 cells, (Fig 4.3.2)

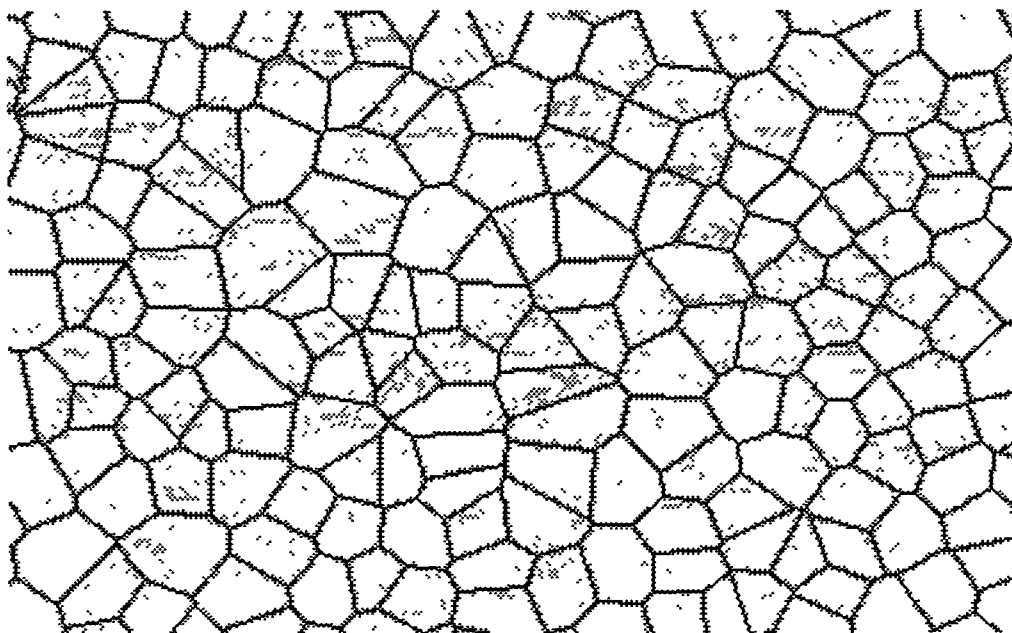


Fig 4 3 2 2D froth with a hard-disk Voronoi Network

4.3.2 Defective 2D Froth Models: The Simple Case

4.3.2 1 Ordered and Disordered Froth

Some difficulties exist in the literature as to what is meant by *ordered* initial conditions. Different underlying structures (monodisperse and polydisperse) have been specified, which correspond apparently to the same initial value of μ_2 . Since this comes from a summation over the non-hexagonal side distribution, Equn (4 1 5), there are several possible configurations for a froth with the same μ_2 , i.e. for the same distribution $f(n)$. This is irrespective of whether the area distribution is uniform or non-uniform, or whether the defects are randomly distributed or clustered. Equally, μ_2 may be the same despite different $f(n)$ reflecting very different froth structure. It seems clear that μ_2 alone is insufficient to quantify the degree of disorder and that more specific details of the initial structure are required. This is hardly surprising, given the elusive nature of the concept, and has been implicitly recognised by a number of authors.

The simplest local *topological dislocation* is defined as a pentagon-heptagon construction in an otherwise hexagonal structure, Weaire and Rivier (1984), where this construct satisfies Euler's law, (Equn (4 1 1) and Fig 4 3 3). Alternatively, the dislocation may be formed by *forcing* a T1 or T2 process, leading to a paired pentagonal-heptagonal dislocation, (Fig 4 3.4 (a) and (b)).

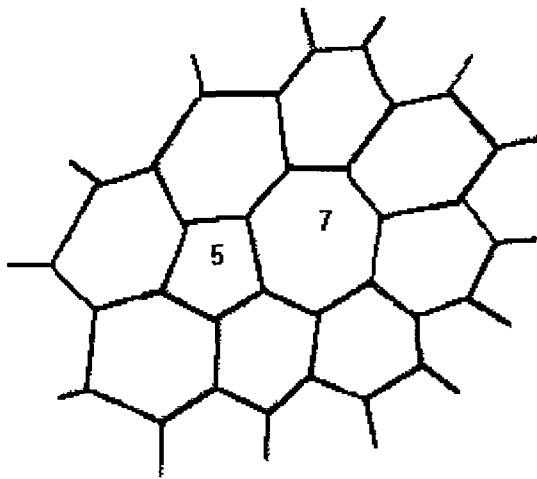


Fig 4 3 3 A topological dislocation with a pentagonal-heptagonal cell pair

Defining an *ordered* initial froth to be a uniform hexagonal, (monodisperse), network, then a *highly ordered* froth consists of such a network with one or a few “seeded” defects present in what is essentially still a regular structure. A *disordered* froth is non-ordered and is taken to be a non-uniform (polydisperse) network with random localised topological dislocations. A *highly disordered* froth is thus clearly non-uniform hexagonal in structure and can have a large number of these dislocations. Voronoi networks are in some ways typical of disordered structure.

Froth *reversibility* was discussed by Weaire and Le1 (1990), and Herdtle and Aref (1992). In mathematical terms reversing froth evolution involves writing $-k$ instead of k in Von Neumann’s law Equn (4 1 2). Distinction between so-called *ordered* and *disordered* froths can be made on the basis of this property. In an *ordered* froth, the dislocation can be made to disappear through a series of T1 processes, resulting in a final structure which is uniform hexagonal (monodisperse, $\mu_2 = 0$). In a *disordered* froth, however, some topological dislocations *always* exist although their location will change after one or more T1 processes. The froth thus remains a polydisperse network with a minimum value of μ_2 ($\mu_2 > 0$). The irreversibility of a polydisperse froth is implicitly considered in previous work of Weaire and Le1 (1990), and Herdtle and Aref (1992).

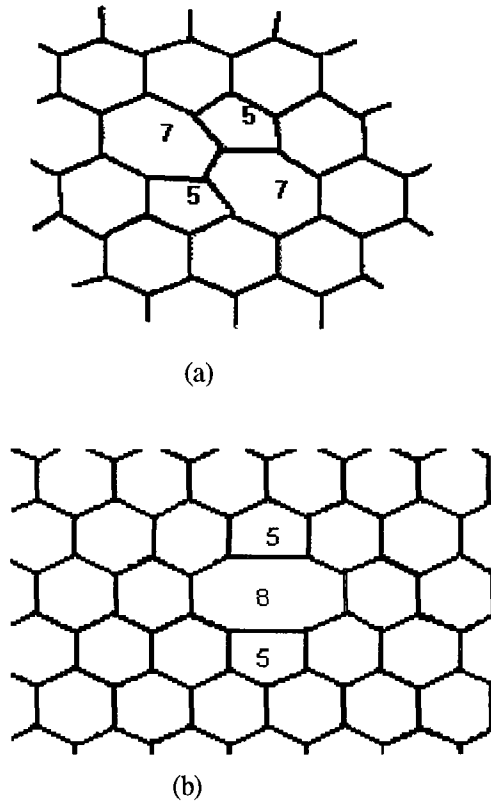


Fig 4 3 4 (a) (b) A topological dislocation
 (a) with pentagonal-heptagonal cell pairs formed by a T1 process,
 (b) with a pentagonal-octagonal cell formed by a T2 process

From these definitions of *order* and *disorder*, it seems clear that Smith (1952) described a highly disordered system whereas Aboav (1980) investigated one which was highly ordered in that its underpinning was the hexagonal form. Both ordered and disordered initial conditions were considered in Glazier et al (1990) whereas Weaire and Le1 (1990) discussed disordered systems only. Investigations of froth behaviour when a single defect is present in a highly ordered system are due to Levitan (1994), Ruskin and Feng (1995). We consider details of froth evolution for a range of different initial conditions in what follows.

4.3.2.2 *Single Defect 2D Froth Model*

The question of initial conditions was raised in earlier work cited above. It is known that a system with only hexagonal patterns is in full equilibrium with regard to diffusion, i.e. a *perfect ordered* froth. However, it is of interest to examine quantitatively the introduction of disorder into such a system. We consider initially the single defect case.

The initially transient behaviour of a relatively ordered froth has been interpreted in terms of the growth of individual topological *defects*. The study of this growth was first taken up by Levitan (1994), who considered the insertion of a single such defect into a froth of hexagonal cells. He used an approximation which is attractive in that it offers the potential to simulate larger, closer-to-asymptotic systems, but results obtained were in disagreement with previous tentative conclusions, (Weaire in Blackman and Taguena (1989)). We have re-examined this problem by direct simulations which are more extensive than those previously undertaken.

Levitan's method first forces a T1 topological process, to take place in a group of cells and follows this with a T2 process, for which the probabilities of a triangle, square and pentagon being formed are the same. In fact, the first T1 process gives rise to two five-sided cells and two seven-sided cells in the network, (Fig 4.3.4(a)). Levitan used a mean field theory to show that the topological distribution associated with a single defect approaches a fixed asymptotic form, with a high peak $f(6) \approx 0.6$. This implies that μ_2 attains a *different* and *stable* value in conflict with previous predictions.

We have implemented a 2D dry froth with a single topological defect, based on a perfect hexagonal network to ensure correspondence with Levitan's original construction. The defect is based on a symmetrical arrangement of two pairs of pentagonal and heptagonal cells with minor discrepancies in the areas of the component cells and with all hexagonal cells surrounding the defect having the same area, (Fig 4.3.4(a)). Additionally, we consider another type of topological defect, where the distortion is achieved by suppressing an edge in the original network giving an eight-sided cell with two symmetrical five-sided cells amongst its nearest neighbours (Fig 4.3.4(b)). We have also used another ordered construction to create a third kind of defect, in which the areas of the defect and its neighbouring cells have been adjusted, (detailed Figs are shown in Appendix C). Periodic boundary conditions are used but, for convenience, the defective cell is centrally placed in the network, since the system is size limited, so that we can monitor the evolution for as long as possible. Calculations are not pursued beyond the stage where the defect impacts on the boundary.

4.3.3 Multiple Defects in an Ordered / Disordered Froth

A froth with *multiple* defects is an extension of the single defect example where now increased amounts of disorder are considered to be introduced into the initial hexagonal network. We also consider initial structures for the froth network which are both ordered and disordered (p89) *before* insertion of the defects.

Direct simulation is again used to investigate froth evolution for different system sizes and initial set-ups in order to obtain information directly on each time step during the whole evolution. Defects which are sparse in the froth as a whole evolve naturally before impacting on each other after a long period of time. We consider systems of size up to 1600 cells and initial structures which range from *highly ordered to highly disordered*.

4.3.3.1 Multiple Defects in an Ordered Froth

From our definition, an *ordered* froth is based on the hexagonal network, where for any value of n , all cells have roughly the same initial area. For a *highly ordered* hexagonal network, we have introduced a number of defects, d , as a pair of pentagon-heptagon dislocations,

- (i) $d=4$ in a system of size 400 cells ($\mu_2=0.05$),
- (ii) $d=7$ in a system of size 900 cells, ($\mu_2 \approx 0.03$),

For a hexagonal network with *low order*, we have introduced,

- (iii) $d=30$ in a system of 400 cells, ($\mu_2 = 0.3$),
- (iv) $d=60$ in a system of 900 cells ($\mu_2 \approx 0.27$)

4.3.3.2 Multiple Defects in a Disordered Froth

In a *disordered froth* normally obtained from the Voronoi network, the area of an n -sided cell may vary considerably and μ_2 provides an indicator of the degree and nature of disorder arising from increased dispersion in $f(n)$. For a *highly disordered* froth, we have considered the evolution of

- (v) a system of 900 cells with initial $\mu_2 \approx 1.2$,
- (vi) a system of 1600 cells with initial $\mu_2 = 1.6$, ($f(4)=0.12$, $f(5)=0.25$, $f(6)=0.28$, $f(7)=0.09$, $f(9)=0.02$, $f(10)=0.01$)

For a froth with *less disorder*, formed by reverse diffusion, corresponding to low μ_2 in a polydisperse network, we have considered

(vii) a system of 900 cells with initial $\mu_2 \approx 0.22$ (minimum),

(viii) a system of 1600 cells with initial $\mu_2 \approx 0.28$, ($f(5) \approx 0.13$, $f(6) \approx 0.74$, $f(7) \approx 0.12$, $f(8) \approx 0.01$)

SUBROUTINE SETUP

//This subroutine sets up a 2D hexagonal lattice with a number of defects. The dimensions are given by NX*NY, the number of vertices in the x and y directions respectively.

```

DO 20 I=1,NX
  IT=MOD(I,2)
  DO 10 J=1,NY
    N=I+(J-1)*NX
    NT=MOD(I+J,2)
    X(N)=FLOAT(I-1)*RT32+RT34
    IF (NT.EQ.0) THEN
      Y(N)=FLOAT(J-1)*1.5+1.0
      NN(N,1)=I+MOD(J,NY)*NX
      NN(N,2)=MOD(I-2+NX,NX)+1+(J-1)*NX
      NN(N,3)=MOD(I,NX)+1+(J-1)*NX
      NC(N,1)=(MOD(I-2+NX,NX)+2-IT+MOD(J-2+NY,NY)*NX)/2
      NC(N,2)=(N+IT)/2
      NC(N,3)=(MOD(I-3+NX,NX)+1+IT+(J-1)*NX)/2
    ELSE
      Y(N)=FLOAT(J-1)*1.5+0.5
      NN(N,1)=MOD(I-2+NX,NX)+1+(J-1)*NX
      NN(N,2)=I+MOD(J-2+NY,NY)*NX
      NN(N,3)=MOD(I,NX)+1+(J-1)*NX
      NC(N,1)=(I+IT+MOD(J-2+NY,NY)*NX)/2
      NC(N,2)=(MOD(I-2+NX,NX)+2-IT+(J-1)*NX)/2
      NC(N,3)=(MOD(I-3+NX,NX)+1+IT+MOD(J-2+NY,NY)*NX)/2
    ENDIF
  10 CONTINUE
20 CONTINUE
  NTOT=NX*NY
  NT2=NTOT/2
  DO 50 K=1,NTOT-1

```

```

DO 51 J=1,3
IF (NN(K,J) .GE. N1 .AND. NN(K,J) .LE N2) THEN
  NN(K,J) =NN(K,J) -1
ELSEIF (NN(K,J) GT N2) THEN
  NN(K,J) =NN(K,J) -2
ELSEIF (NN(K,J) .EQ. N2 .AND. K.LT (N2-1)) THEN
  NN(K,J) =NN(K,J) -1
ELSEIF (NN(K,J) EQ N2 AND K GE. (N2-1)) THEN
  NN(K,J) =NN(K,J) -2
ENDIF
IF (NC(K,J) .GE. N3) THEN
  NC(K,J) =NC(K,J) -1
ENDIF
51 CONTINUE
50 CONTINUE
NTV=NTOT-I1
I2=I1/2
NTC=NT2-I2
DO 30 K=1,NTOT
  IVLIST(K)=K
30 CONTINUE
RT32=RT32*3.0
DO 40 K=1,NT2
  ICLIST(K)=K
  NCELL(K)=6
  VOL(K)=RT32
  P(K)=0 0
40 CONTINUE
NCELL(435)=7
NCELL(466)=7
NCELL(436)=5
NCELL(465)=5
RS1=(SQRT(10.0)-2 )/2.
VOL(435)=RT32+RT34
VOL(436)=5*RT34
VOL(465)=RT32-RT34
VOL(466)=RT32+RT34
X(931)=X(931)+0.5*RT34
Y(931)=Y(931)+5./8.
X(932)=X(932)-0.5*RT34
Y(932)=Y(932)-5./8.

```

```
ENDIF
RETURN
END
```

27

We give detailed results for some of these models in the next Section as examples. An example is also shown on the diskette in Appendix E.

4.4 Results and Discussion

4.4.1 Voronoi Disordered Froth

4.4.1.1 Additional Notes on Direct Simulation Implementation- Performance

For direct simulation, it is possible to specify the precise geometrical description of the structure and its evolution. We note that Kermode and Weaire (1990) used the routines F04ARF and F04ATF in the NAG library to solve the matrix equation, but these are not available in the NAG library version available on the VAX cluster in DCU. We have, therefore, modified the programme by using instead the Gauss method. The external library CALCOM is also unavailable, so that for the current preliminary studies we have omitted the 2D-Froth graph plotting routine and substituted our own, written in C. A copy of this program is given on diskette together with 2D-Froth program in Appendix E.

For the largest system considered size 3000 cells with initial disordered Voronoi network set-up, the volume of information to be stored is considerable and run times are of the order of several hours for each stage of the simulation due to the large number of complicated network checks and continuously iterated calculations. A 3000-cell system appears to be the practical limit for the computing power of the hardware configuration that we have used for this sequential approach. For 1000 and 3000 cell systems, the first runs required more than 5 and 12 hours respectively, and succeeding runs about 2 and 7 hours on the VAX cluster available in DCU. We concentrate on specific distributions of interest in what follows.

27

The time steps are small in our simulation so that it is easy to observe detailed topological distributions and related behaviour exactly for each step. Here the number of time steps relates to the number of diffusion and equilibration

processes which have taken place, with the evolution time, T , measured in units of $\langle A_0 \rangle / k$, where $\langle A_0 \rangle$ is the initial average area over all cells, and k is the constant in Von Neumann's Law, and may be arbitrarily chosen, (Kermode and Weaire (1990))

4.4.1.2 Results of Froth Simulation

We examine the distributions of number of sides and area, and the respective correlations. For the systems of 1000 and 3000 cells, we obtain the values of the second moment, $\mu_2 = 1.5$ and $\mu_2 = 1.63$ respectively, where the later one is high compared to values quoted by previous authors with the exception of Wejchert et al (1986). This in part may be ascribed to the much larger network, so that more cells are involved in a knock-on effect from a given topological change and partly to a choice of different scale factors and hence the handling of small cells as noted earlier, (Section 4.2.3.2). Nevertheless, clear equilibrium behaviour is established. In Fig. 4.4.1-2, the distribution functions $f(n)$ and the second moment, μ_2 , for a system of 3000 cells are shown. Eqn (4.1.2) suggests that the rate of area change is the same for all n -sided cells, irrespective of the nature of neighbouring cells. In a real system, the large cells are more likely to touch the boundary of a finite area than the small cells, so that we have a systematic bias against the inclusion of very large cells in our distribution function. Also, we know that rate of growth of a cell is dependent on its shape, i.e. is only affected by the number of sides of the original cell configuration. Therefore, it is unnecessary to calculate all the side lengths and sum the diffusion across each side in order to determine the rate of growth for a cell.

We have also looked at the correlations between area or diameter, $\langle A_n \rangle$, (or d), and number of sides, n , (Lewis's Law), and correlations between n and $m(n)$, the number of sides of neighbouring bubbles, (Aboav-Weaire law). Results are shown in Figs 4.4.3-4. For the former, we expect a linear relation between the cell area and the number of sides, where $\langle A_n \rangle$ and n are recorded at various stages during the evolution of the soap froth. Agreement is obtained with Lewis Law, also with the Aboav-Weaire Law, but a is not normally quoted values of 1 or 1.2, ($a \approx 0.7$)

Also deviations from Lewis Law appear to be more marked for the smaller system, i.e. system size of 1000, although departure from linearity is small

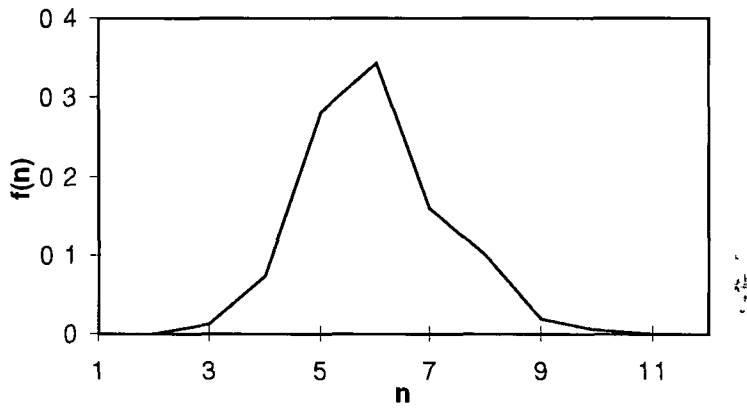


Fig 4 4 1 side distribution $f(n)$ vs side No n in a system of size 3000

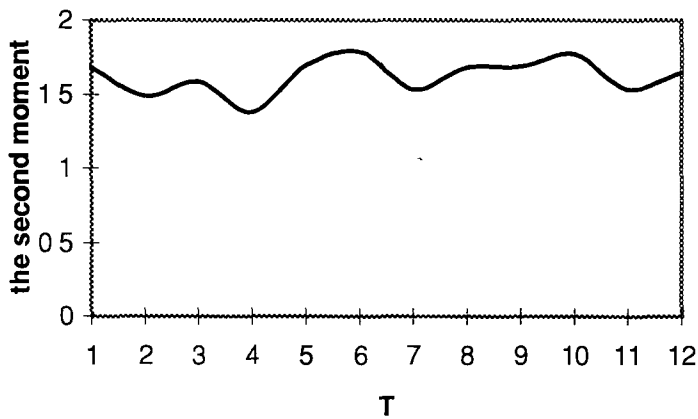


Fig 4 4 2 the second moment, μ_2 vs T

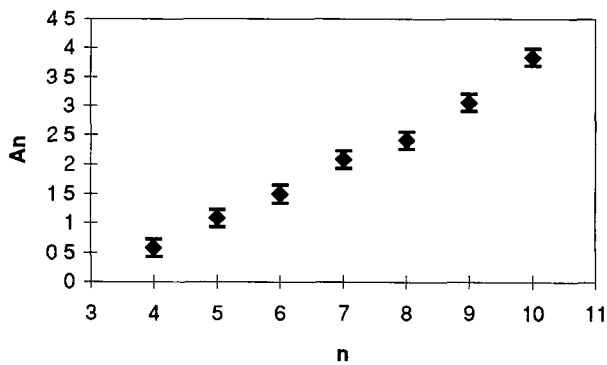


Fig 4.4 3 Lewis Law for a system of size 3000

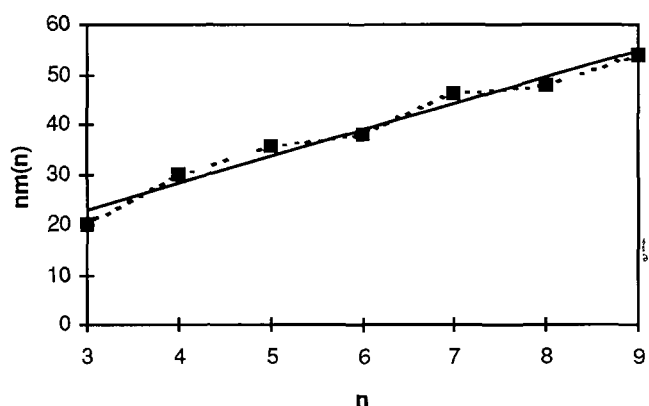


Fig 4 4 4 Aboav-Weaire Law for a system of size 3000

Precise geometrical description of the structure and evolution of the froth are presented in an example given in Appendix D for a system of size 900. We have extended such calculations to hundreds or even thousands of cells, and obtained results from the simulations which show that scaling laws during the evolution of a froth are in reasonable agreement with experiment, and previous simulation studies.

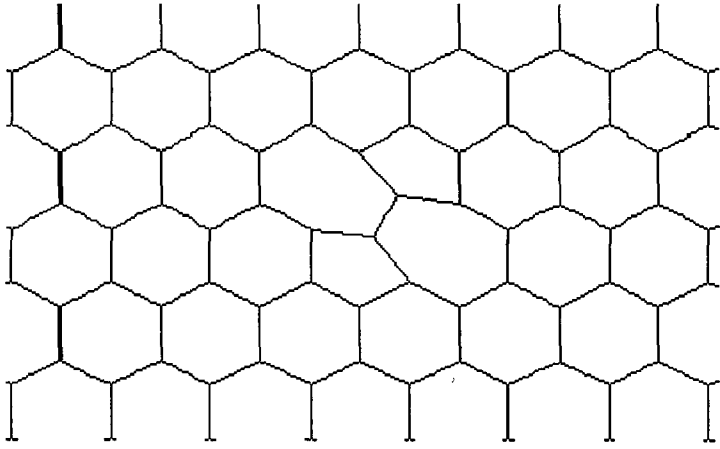
4.4.2 Froth with a Single Defect

We have implemented the froth with a single defect, (Fig 4 3 3 and Appendix C), for systems of size 100, 400 and 900 cells respectively. We give details of the results for a system of size 400 cells as an example. Similar results are found for all system sizes used.

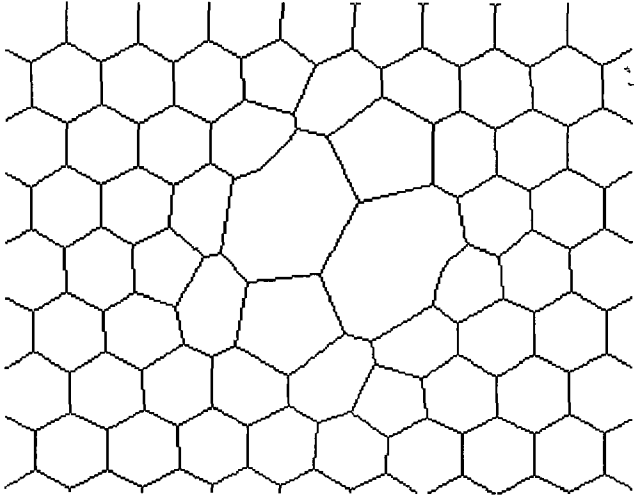
If we define an approximately circular “front” of disturbance surrounding the large defective cell and including cells which have undergone a single topological change, the circular “front” will include these (plus other cells which impinge on the circle in part, but which have not yet undergone change). Levitan (1994) similarly defines a “cluster”, which refers to the “front” used in our simulations plus a boundary of hexagonal cells. The slight modification we have used does not affect the behaviour of μ_2 , or the size distribution but enables us to consider separately μ_2 in the front.

Figs 4 4.5 show the evolution within the front at specific time steps for different initial defect types, corresponding to Fig 4 3 4(a). We can see that the number of

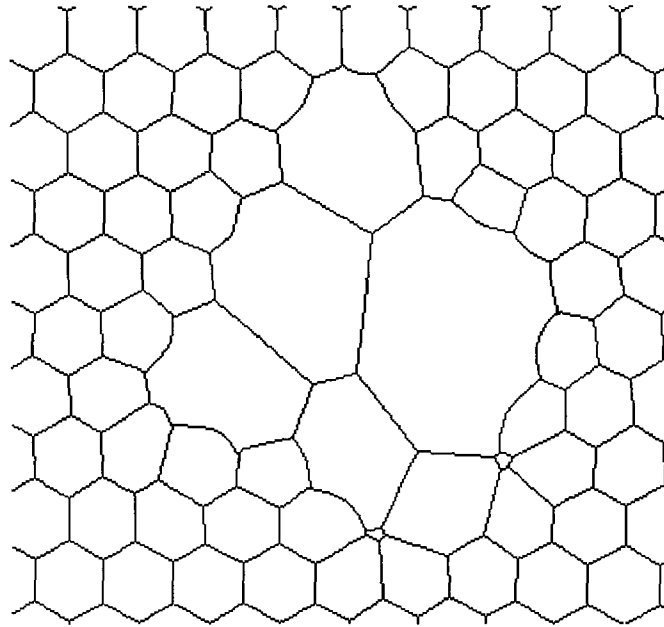
area of the disturbance. For the defect formed by edge suppression, starting from the ordered non-Voronoi network set-up (see Fig. 4.3.4(b)) and ordered Voronoi network (see Appendix C), we have observed very similar behaviour in the froth evolution. We give detailed results for the initial structure shown in Figs. 4.3.3 (a) and (b) as follows.



(a)



(b)

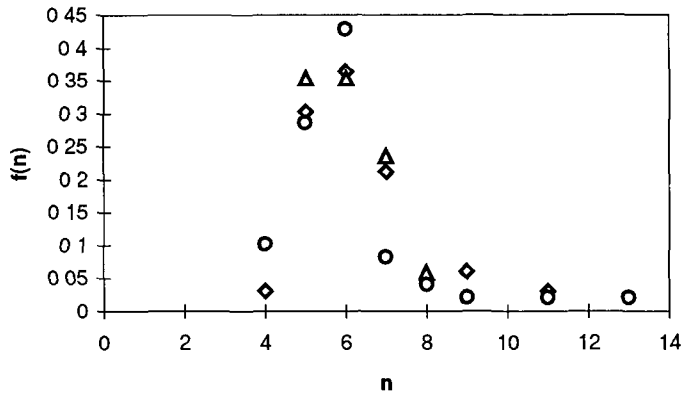


(c)

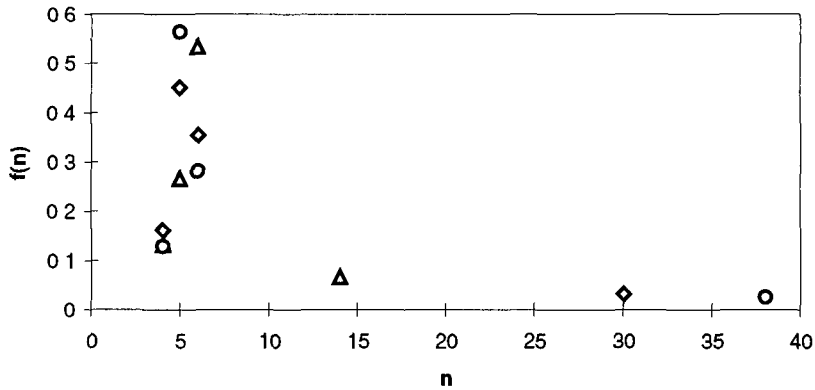
Fig 4 4 5 (a) (b) (c) Evolution of a froth with a single defect in a hexagonal network with time steps of 0, 40 and 100 respectively

The topological distribution $f(n)$ *inside the front*, is shown in Figs 4 4 6 (a) and (b), at specific time steps for the different defect topologies (Figs 4 3 3 (a) and (b) respectively) We find that there tends to be a peak at $n=5$ in the front as evolution time increases, as opposed to the overall network of a normal froth which has a peak with $n=5$ and $n=6$, Herdtle and Aref (1992) However, the distribution $f(n)$ is now, of course markedly right-skewed These features are not extraordinary as movement of the front results in continual incrementation of the number of sides of the large defective cell

From our results, the second moment, μ_2 continues to change with time without reaching a fixed limit Figs 4 4 7(a) and (b) show how the second moment, μ_2 , in the overall network changes vs time, T The range of T includes about 200 diffusion and equilibration processes in our simulation Topological and diffusive adjustments are made sequentially within each time step and considerable details of the evolution may be observed



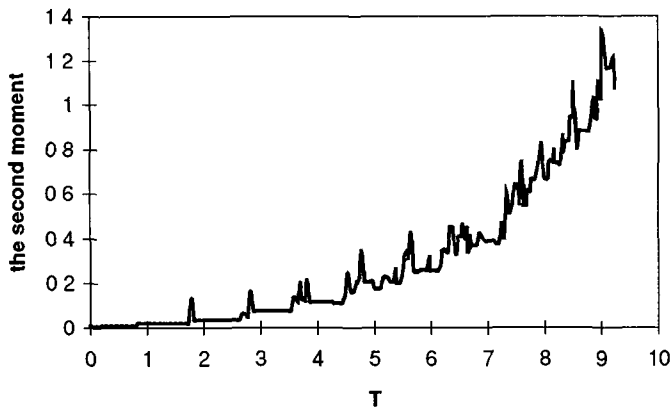
(a)



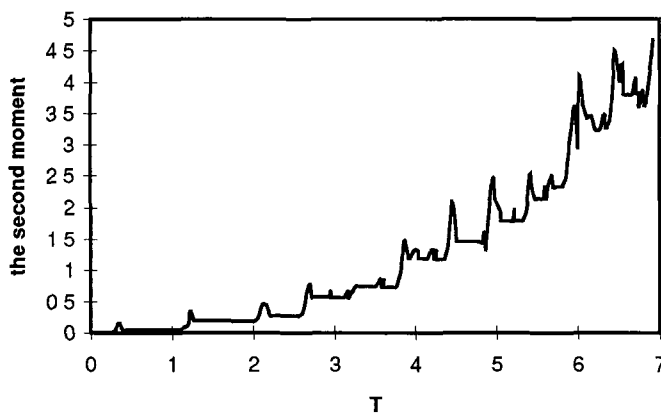
(b)

Fig 4 4 6(a) (b) Topological distribution $f(n)$ in the *front* with time step of 60(Δ), 120(\diamond), and 160(o) Initial set-up Fig 4 3 3 (a) (b) respectively

Fluctuations in the value of μ_2 around the underlying trend can be explained directly in terms of the T1 and T2 processes, with a high μ_2 corresponding to the defect surrounded by a number of three- or four-sided cells, and a sudden decrease in μ_2 associated with the disappearance of one of these cells. During growth in area of the defect, μ_2 keeps a relatively stable value until the next T1 occurs. Clearly, as more cells are involved in the evolution and the number of sides of the defect increases, the value of μ_2 *overall* changes more rapidly and is dominated by the contribution of the defective cell. Over the whole range of T , $\mu_2 \sim T^\beta$ appears to describe the observed behaviour, with $\beta > 1$. However, few changes take place initially, relative to the evolution as a whole, and for the upper range of T , μ_2 vs T is roughly linear, although it is not clear that a true asymptote is attained.



(a)



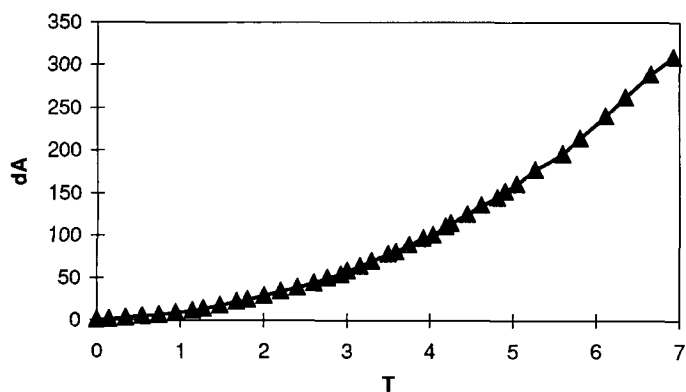
(b)

Fig 4 4 7(a) (b) μ_2 in the overall network vs time T for a froth of 400 cells Initial set-up Fig 4 3 3 (a) (b) respectively

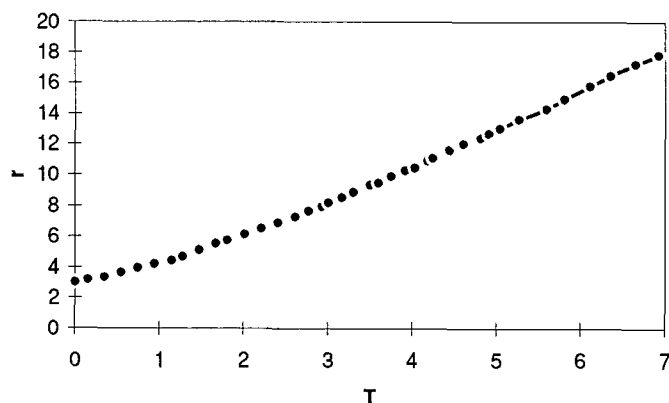
For a simple theoretical model of a large defect with N sides surrounded by N small cells, newly converted side lengths of the small cells will be characteristic of the whole network, $l \propto N^{-1/5} \sim A(d)^{-0.5}$, with $A(d)$ the area of the defect. Then, in the asymptotic limit, Von Neumann's law becomes $dA(d)/dt = kA(d)^{-0.5}$, $l \propto A(d)^{-0.5} \sim T^{-2}$. Similarly, *in the front*, the topological distribution will be dominated by the defect, so that $\mu_2(d) \sim N^2$ with $N \sim T$, $l \propto \mu_2(d) \sim T^2$.

Furthermore, the defect gradually involves more and more cells in the overall network, so that asymptotically the exponents for the front and the overall network should be the same. From our simulations, we find *for the defect* that $A(d)$ increases with T at the expense of other cells distorted by topological changes. If we define the increased area $\Delta A(d) = A(d) - A(d)_0$, where $A(d)_0$ is the

original area of the defect, for the defect formed by edge suppression, e.g. Figs 4.3.3(b), we obtain roughly $\Delta A(d) \sim T^2$ after the initial period of evolution, with the radius of the rough perturbation circle, $r \sim T$ approximately, Figs 4.4.8 (a) and (b) illustrate for the set-up of Fig 4.3.3 (b). Furthermore, we find that $\mu_2(d)$ changes roughly *linearly* with the average intercept, $\langle d \rangle$, where $\langle d \rangle$ equals the square root of the average cell area in the front, Fig 4.4.9



(a)



(b)

Figs 4.4.8 (a) (b) Increase in defective area $\Delta A(d)$ vs time, T , for a froth of 400 cells. Initial structure Fig 4.3.3 (a) and (b) respectively

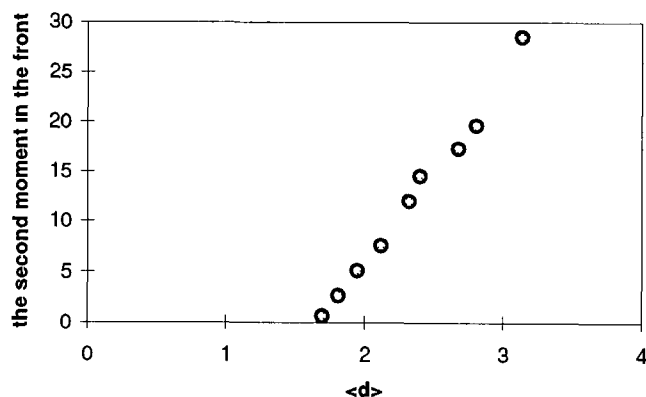


Fig 4.4.9 $\mu_2(d)$ in the *front* vs average intercept, $\langle d \rangle$

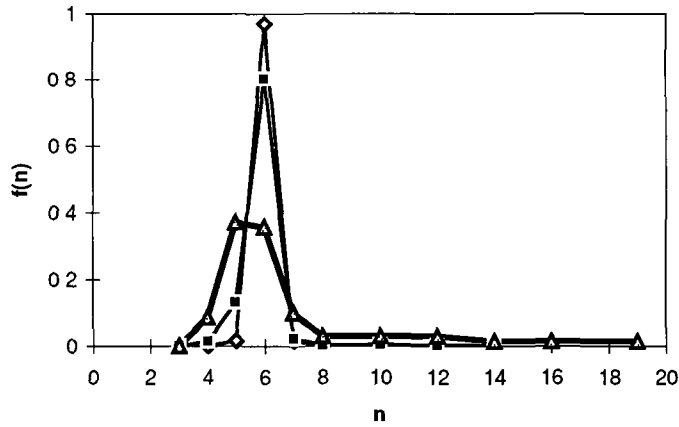
It seems clear that the behaviour of a froth with a single defect in a uniform hexagonal network does *not* lead to a normal scaling state as found for the non-defective froth by numerical simulation and as predicted by theory. We find that $f(n)$ in the front tends to develop a long tail extending to large values of n and with a peak at $n=5$. This is in agreement with Aboav (1980), who also quotes $\alpha = 2$ for the area growth exponent. However, the suggestion that μ_2 *overall* varies linearly with time (comment by Weaire and Kermode (1983a) on Aboav's work), is not wholly supported by our findings and is in conflict with the predictions of the simple model. It is only with hindsight that it has been suspected that Aboav was dealing with a transient system with defects, characterised by different values of the growth exponents. Our own results are probably not in the asymptotic region since the maximum number of sides achieved by any defect is $N=44$ at the late stage. Nevertheless, they are supported by recent work of Jiang et al (1995). In summary, we find that there is some similarity between the behaviour of our system and that of Levitan (1994), but we do *not* agree with a *fixed* form for $f(n)$ as obtained by Levitan. The value of μ_2 , whether for the front or for the overall network, does not reach a steady-state after initial fluctuations at this system size, unlike normal froth evolution.

4.4.3 Monodisperse and Polydisperse

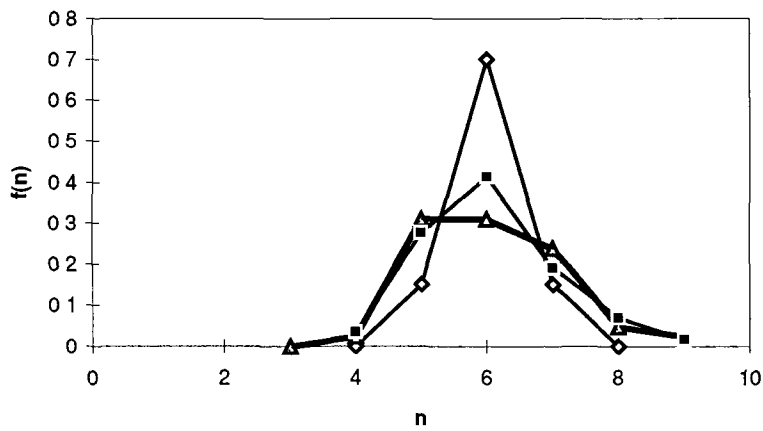
4.4.3.1 Results and Discussion

Similar behaviour is observed for initial conditions noted in section 4.2.3, for example (i) and (ii), and also for example (iii) and (iv), results are thus discussed in detail for (ii) and (iv) only.

For the *ordered* froth, (defined p89), the side distribution, $f(n)$, is illustrated in Figs 4.4.10 (a) and (b) for specific time steps. Since a single time step consists of the number of diffusion and equilibrium processes which have occurred, the evolution time, t , is measured in units of $\langle A_0 \rangle / k$, as previously with k a constant defined in Eqn. (4.1.2). The second moment, μ_2 , vs time and the average area, $\langle A \rangle$ vs time are shown in Figs 4.4.11-12. Agreement with the Aboav-Weaire law is shown in Fig 4.4.13, where a is approximately constant ($a \approx 1.05$).

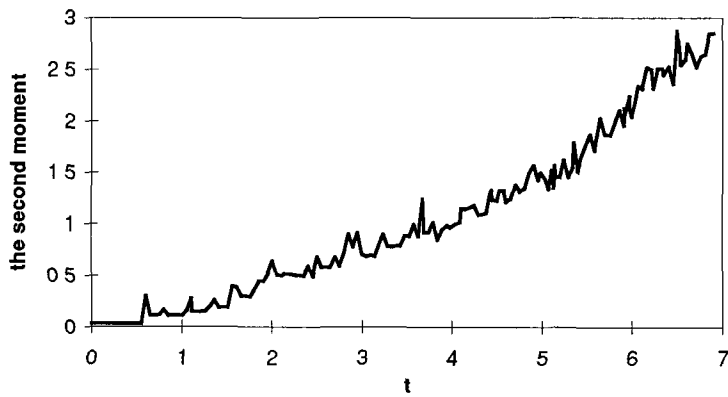


(a)

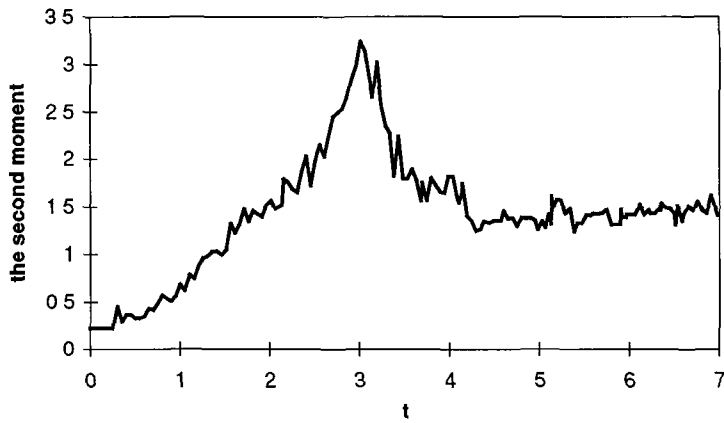


(b)

Fig 4 4 10(a) (b) The side distribution, $f(n)$ at time steps of 0, 120, 260 for a highly (iv) and a low ordered froth (iv), the heavier dark line represents $f(n)$ in the quasi-scaling scaling state



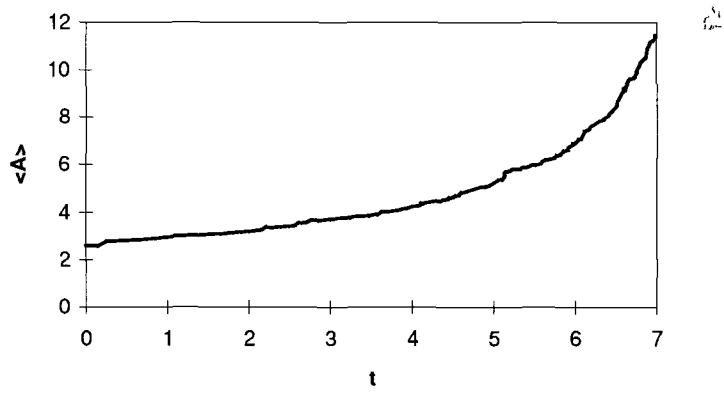
(a)



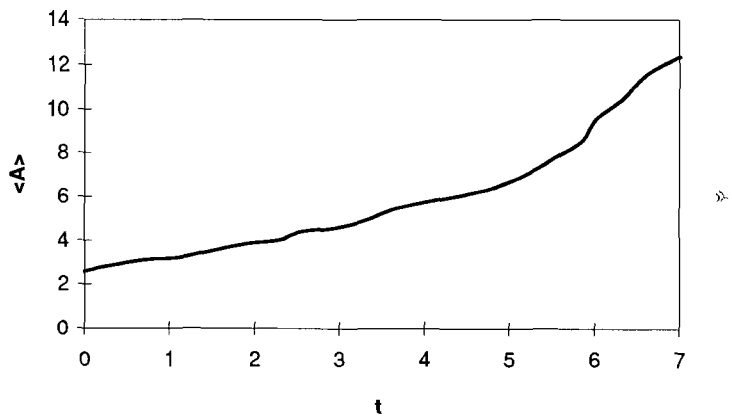
(b)

Figs 4 4 11 μ_2 vs time in an ordered froth with initial set-ups

(a) (ii), (b) (iv) respectively



(a)



(b)

Figs 4 4 12 The average area of all cells, $\langle A \rangle$ vs time

with initial set-ups (a) (ii), (b) (iv) respectively

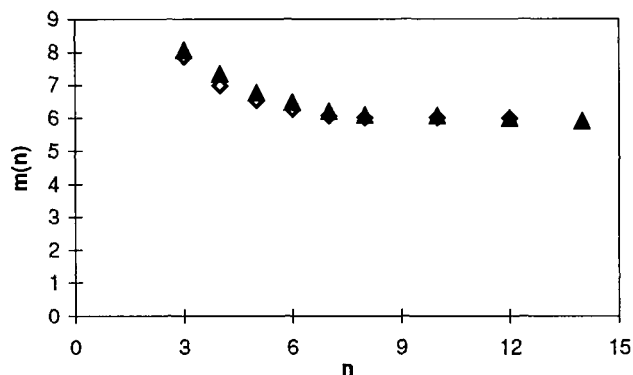


Fig 4 4 13 Aboav-Weaire Law in a low (▲) and highly (◊) ordered froth
 If considering the alternative illustration, i.e. $nm(n)$ vs n (as shown
 in Fig 4 4 4), the line corresponds to constant $a \approx 1.05$

For a *highly ordered* froth, we observe that the side distribution $f(n)$ is markedly right-skewed with the long tail reflecting the presence of many-sided cells, (Fig 4 4 10(a)). The second moment grows indefinitely with time, $\mu_2 \sim t$, as a result, (Fig 4 4 11(a)). Therefore, if the system size is large enough, we expect that μ_2 will continue to increase as larger many-sided cells are formed. Our findings for μ_2 vs t and also for the average area of all cells $\langle A \rangle \sim t^\alpha$, $\alpha = 2$ are in agreement with those of a single defect as discussed in Section 4 4 2.

The scaling state is reached when both $f(n)$ and μ_2 attain time-invariant values and obviously does not apply for a *highly ordered* froth, where neither $f(n)$ nor μ_2 tend to a fixed form. However, if we truncate $f(n)$ at $n = n^*$, ($n^* < 12$), we find that the side distribution $f(n^*)$ is effectively fixed after the initial period of evolution, (see e.g. Fig 4 4 10(a), $f(4) \approx 0.08$, $f(5) \approx 0.37$, $f(6) \approx 0.35$, $f(7) \approx 0.09$). Such a froth may be said to be in a *quasi-scaling state*, although clearly μ_2 for *all* n continues to increase. This suggests, additionally, that a more appropriate measure of the froth structure might well be the third or fourth moment of the distribution, $f(n)$.

The emergence of a quasi-scaling state in the *highly ordered* froth, however, does not tend to wholly support the view that Aboav's results describe a transient stage, but requires focus on the later time-evolution, which is not provided. In fact, ten percent of the initial 5000 cells remained for the value of μ_2 given in this work, Aboav (1980). An alternative explanation, that the long-term evolutionary behaviour of a highly ordered froth reaches partial equilibrium at best, obtains

some support from the results presented here and is examined further in the next Section

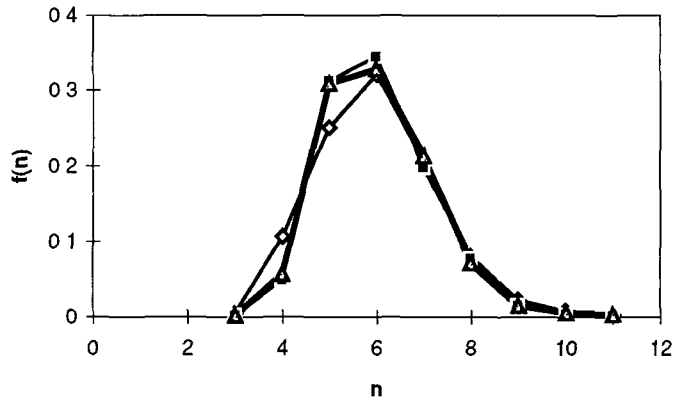
In contrast, for the *low ordered* froth, (initial conditions as in (iv), Section 4.3.3.1, i.e. seeding the hexagonal structure with defects), (Fig. 4.4.10(b)), the side distribution $f(n)$ does tend to a fixed form, e.g. $f(5) \approx 0.31$, $f(6) \approx 0.30$, $f(7) \approx 0.26$, and the second moment μ_2 vs t exhibits one notable peak before finally reaching a stable value of $\mu_2 \approx 1.5$ after initial fluctuations (Fig. 4.4.11(b)). The average area of the cells now behaves as $\langle A \rangle \sim t^\alpha$, where $1 < \alpha < 2$. These scaling properties are consistent with those obtained by experiment (Stavans and Glazier (1989)). We also find that there may be two peaks before μ_2 reaches a stable value e.g. in (vi) with *clustered* defects. Furthermore, the Aboav/Aboav-Weaire law is obeyed in a *high/low ordered* froth respectively in Fig. 4.4.13, with $a \approx 1.05$.

It appears, then, that normal as opposed to quasi-scaling in an ordered froth depends on the initial side distribution $f(n)$, i.e. the number of defects, d , or concentration d_N , ($=d/N_0$, N_0 =the initial system size), with a corresponding threshold or critical value $\mu_2(d')$ partially determining the degree of disorder. Froths with initial defects of various types (see Section 4.3 for example), either randomly seeded or clustered, may correspond to the same μ_2 , but exhibit different *evolutionary behaviour* before a final state. For example, one or more peaks may be observed for μ_2 vs t in the low ordered froth depending respectively on whether defects are seeded randomly or clustered. Nevertheless, if the system size is *large*, the ordered froth will tend to either a quasi-scaling or scaling state, regardless of the initial conditions. Otherwise, transient behaviour only may be observed (see next Section). Moreover, our results suggest that while $\mu_2(d')$ is low, (e.g. around 0.2 for a system up to a thousand cells), this value increases for large system size indicating that the proportion or density of defects in the overall froth determine the threshold value.

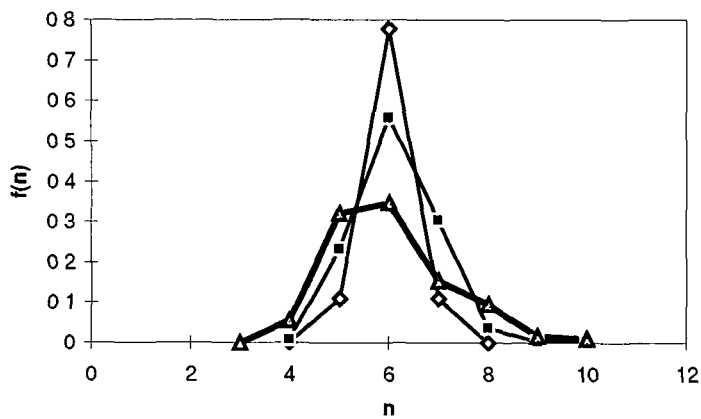
For the disordered froth (starting from the non-hexagonal structure as defined p.89) with initial conditions of (v) to (viii), we give detailed results for examples (vi) and (viii), since behaviour is apparently similar under similar initial conditions.

Figs. 4.4.14(a) (b) illustrate the topological distribution, $f(n)$, at time steps of 0, 120, 260, corresponding to the initial, middle and final evolution stage for the

disordered Voronoi structure Figs 4.4.15-16 show how the second moment μ_2 and average area $\langle A \rangle$ change with time for examples (v1) and (v111) respectively. For the correlation laws, e.g. the Aboav (Aboav-Weaire) law, we found that the constant a does not have the value of 1 or 1.2 as for the normal case, but has a different value of $a \approx 0.6-0.7$ roughly, shown in Fig. 4.4.17

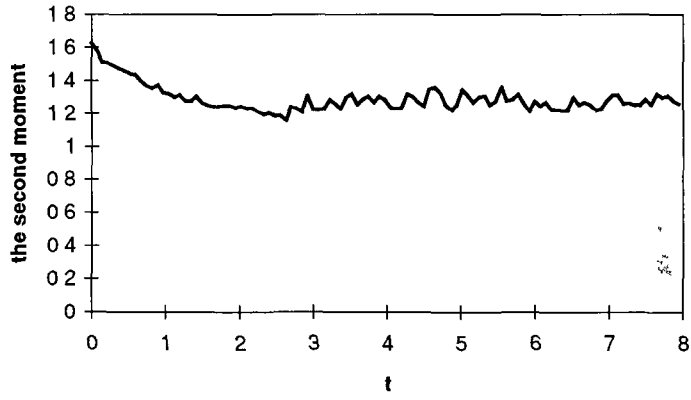


(a)

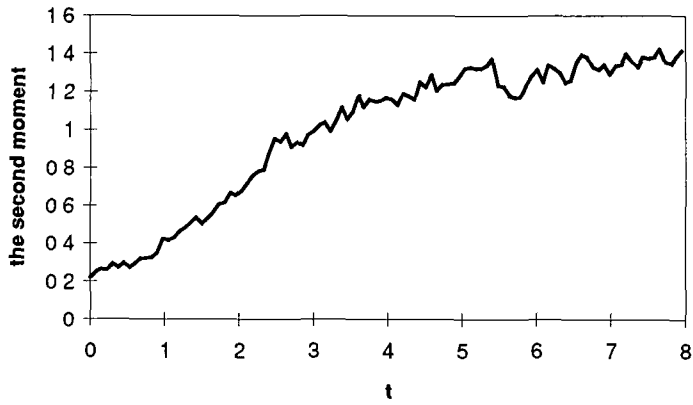


(b)

Figs 4.4.14 The side distribution, $f(n)$ at time steps of 0, 120, 260 for (v1) a high disordered and (v111) a less disordered froth, the heavier dark line represents $f(n)$ in the scaling state

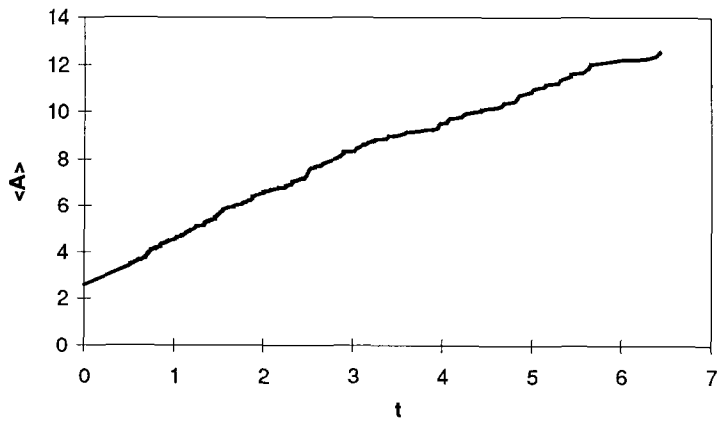


(a)

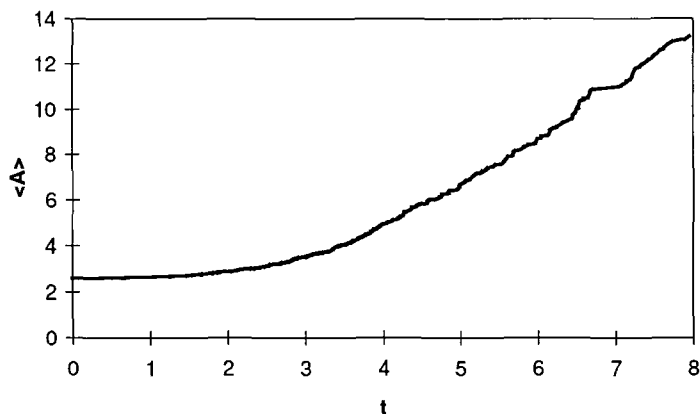


(b)

Figs 4.4.15 μ_2 vs time in a high and low disordered froth with initial set-ups (a) (vi), (b) (viii) respectively



(a)



(b)

Figs 4.4.16 The average area of all cells, $\langle A \rangle$ vs time, with initial set-ups (a) (vi), (b) (viii) respectively

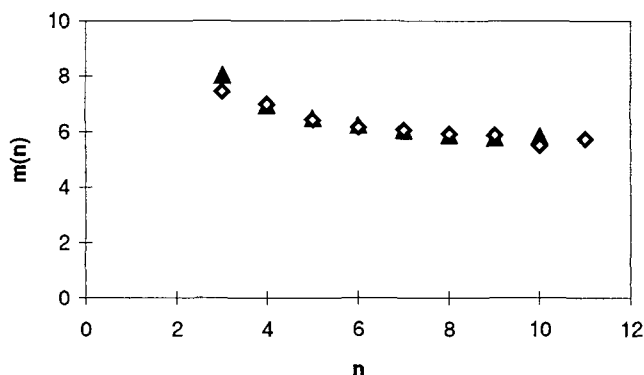


Fig 4.4.17 Aboav-Weaire law in a high (▲) and low (◇) disordered froth. If considering the alternative illustration, i.e. $m(n)$ vs n (as shown in Fig 4.4.4), the line corresponds to constant $a \approx 0.6-0.7$

For *high* or *low disordered* froths, (Figs 4.4.18-20), the side distribution $f(n)$ always tends to a fixed form, (e.g. $f(5) \approx 0.32$, $f(6) \approx 0.35$, $f(7) \approx 0.18$), with a stable value of $\mu_2 \approx 1.4$. Thus the disordered froth in the scaling state relates the average area of all cells with t through $\langle A \rangle \sim t^\alpha$, with $\alpha=1$. Neither the Aboav or Aboav-Weaire law has constant a as previously (p.73) according to our simulation results and in agreement with previous work for *disordered* froth evolution, e.g. Smith (1952), Weaire and Lei (1990), Herdtle and Aref (1992). However, “ordered” initial condition ($\mu_2 < 0.4$) obtained by reverse diffusion in the previous work of Weaire and Lei (1990), Herdtle and Aref (1992), in fact, is a less *disordered*

structure by our definition. The semantic distinction here, can be confusing, but relates to whether the original structure can be defined as ordered (in the sense of p 89) or disordered. A good definition remains elusive!

Consequently, our results support the existence of a universal scaling state, irrespective of system size, for a *disordered* froth, based on a Voronoi construction. We find that μ_2 vs t has either a *lower* peak value, ($\mu_2 < 2.0$), than that observed for an *ordered* froth (Fig 4.4.15(b)) or increases monotonically (Fig 4.4.19(b)). While there appears to be agreement as to the location of the μ_2 peak during *ordered* and *disordered* froth evolution, it seems likely that it is merely a coincident surface phenomena since the peak values are different. (For example, we obtain a high peak, (such as $\mu_2 > 3.0$) for the *ordered* froth, (under condition (iv)), whereas for the *disordered* froth we observe either a small peak ($\mu_2 < 2.0$) or none). This agrees with former work, Stavans and Glazier (1989), and Weaire and Lei (1990), where μ_2 was found to rise rapidly to a maximum ($\mu_2 \approx 2.65$ and $\mu_2 \approx 1.9$ respectively), then dropped to the constant value $\mu_2 \approx 1.4$. Furthermore, the phenomenon of more than one peak for μ_2 vs time (see Glazier et al (1990)), appears to be a peculiarity of the *ordered* froth and we find no evidence for multiple peaks for any *disordered* system we have simulated.

4.4.3.2 Conclusions on Single/Multiple Defect(s)

For a froth with a single defect, our results for the behaviour of the *front* are in agreement with the original experimental work of Aboav (1980), and indicate that a different scaling relation applies in an *ordered froth*, (i.e. a *quasi-scaling* state at best). Regardless of the defect type and initial configuration, for a single defect, $d=1$, there are some grounds for supporting the suggested system behaviour put forward by Levitan (1994), but the overall results are in conflict with his predictions for the quantities characterising the long-term evolution. For a froth with multiple defects, $d>1$, we have reconciled apparent discrepancies in the scaling properties describing the froth evolution. In particular, our findings support the view that again a quasi-scaling state at best is achieved in a *highly ordered* froth, where the side distribution, $f(n^*)$ ($n^* < 12$) tends to have a fixed form whereas $f(n)$ for *all* n has long tail corresponding to the unlimited growth of μ_2 . These

remarks must be qualified of course by noting that only finite systems to moderate size can be simulated directly. A universal scaling state is, however, attained for both the *disordered* and *low ordered* froth, where $f(n)$ has a fixed form corresponding to a system-invariant asymptotic value of $\mu_2 \approx 1.4$. Additionally, we offer an alternative explanation on the early result of Aboav(1980) indicating that the ordered froth may progress beyond transience or, alternatively, exhibits a prolonged transient region. This is further discussed in what follows. We also find that the Aboav (or Aboav-Weaire) law has different values of constant a in the ordered and disordered froth.

4.4.4 A Note on Stages of Evolution in a 2-D Froth

From the above, it appears that the evolutionary process of 2D froth consists of two regions involving several distinct stages, which are characterised by the froth structure. In particular, *transient* behaviour which reflects initial levels of froth disorder can be varied both in its nature and duration. The final stage of froth evolution is associated with a few remaining bubbles, which change relatively slowly, unlike the many, frequent changes originally associated with transience. Thus, late configurations do not affect achievement of scaling, but influence the rate at which it is attained.

The studies of ordered 2-D froths with single/multiple *defects* provide some examples for length of transition period, which appears to be related to *concentration* of defects, and highly ordered systems with few defects exhibit an anomalous approach to the scaling state. The question of the way in which these factors influence the length of the transient and other stages is discussed here.

In many areas of statistical physics, the evolutionary time $T \rightarrow \infty$ as $N \rightarrow \infty$, but scales are not interchangeable, since two distinct regions are involved, (a) $1 \ll T \ll T(N)$, and (b) $T \gg T(N)$, where for some $T > T(N)$, finite size-effects operate. This is demonstrated also in zero-temperature simulations of Potts models, Derrida et al (1996), which may be relevant to recent bubble growth experiments, Tam et al (1997). Consequently, any discussion of froth evolution must include behaviour in both regions (a) and (b).

The key factor in transience, as *originally* described, appeared to be that the early evolution in region (a) involved a large number of bubbles in topological changes, producing considerable variation in the form of $f(n)$ and value of μ_2 . Actual time taken is thus dependent on system and simulation characteristics are difficult to quantify precisely. Clearly, as the number of bubbles decreases, the sizes of the remainder tend to increase so that the number of bubbles remaining, (or "survivors" - expressed as a percentage of the initial number), is then crucial as an indicator of the potential for further change and in the determination of $T(N)$. For a large system where scaling is achievable, transient effects would normally be expected to occur for a relatively large number of survivors, i.e. $T \ll T(N)$. However, defects are known to affect the nature of transient behaviour. It seems clear, therefore, that duration of any stage in the froth evolution depends on the concentration of defects and their distribution, (whether clustered or random). Some illustrative evidence can be provided in support of this view as follows.

For a random Voronoi structure used as a sample of disordered froth, early numerical studies for very small system size ($N=100$) recorded initially rapidly changing behaviour, even though scaling could not be observed, Weaire and Kermode (1983b). This is due to the fact that the transient effects are rapidly overtaken by the finite size of the system. In subsequent studies on larger systems of several hundreds of bubbles, the nature of the early evolution was variable but a unique final state was achieved with a fixed form size distribution, corresponding to a stable value of μ_2 , irrespective of the amount of disorder in the initial froth structure, Weaire and Lei (1990), i.e. the scaling state was observed, (region (a) as usual). However, this result does not hold for special cases of disorder, e.g. the occurrence of a single defect in an otherwise ordered froth, where the scaling state is not observed at all for moderate system size. (See section 4.4.2 earlier).

In an ordered froth, the behaviour varies considerably with the number of defects introduced. The anomalous case for a single initial topological dislocation reduces evolution of the froth to that of a single large bubble or single compound bubble cluster, which proceeds to grow until the froth is consumed. Thus μ_2 for the whole system grows indefinitely with time, (region (b)). The nature of the initial topological dislocation is reflected in the configuration achieved by the froth in the

final stages of evolution, (examples are given in Ruskin and Feng (1995)) However, the side distributions $f(n)$ are similar except for the presence of several large bubbles, (forming a compound cluster in the dislocation caused by a T1 process), which have the effect of reducing the extreme skew in $f(n)$ Furthermore, for few defects, an intermediate stage in region (a) is observed, which neither reflects the many, rapid changes associated with transience nor the final fixed value of scaling This "quasi-scaling" or slow approach to true scaling, has been noted for moderate system size, ($N=400$), and is characterised by a relatively stable "local pattern", with fixed side distribution $f(n^*)$ and $\mu_2(n^*)$ for $n^* < 12$, see Section 4.3.3, Fig. 4.4.18 shows $\mu_2(n^*)$ vs survivor percentage for one defect

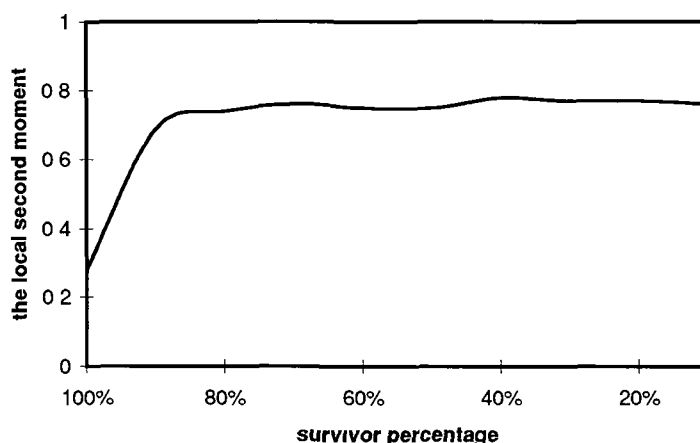


Fig. 4.4.18 The local second moment, $\mu_2(n^*)$ vs survivor percentage for one defect

For increased disorder, the number of defects ($d \geq 2$), or concentration of defects, d_N , ($=d/N_0$, N_0 =the initial system size), determine transient characteristics, (region (a)) For a large, initially ordered, system with d or d_N small, (and defects clustered), the situation is essentially similar to that of the one defect case, although more large bubbles in the compound cluster imply further limitation on the skew in $f(n)$ For randomly seeded defects, the growth of μ_2 continues unchecked until such time as the growth of one defect impinges on another, when it slows down An intermediate stage is again observed with stable $\mu_2(n^*)$, (≈ 0.76 , e.g. for $N_0 = 900$ with $d=4$), attained early in the evolution, despite μ_2 increasing For a system which is sufficiently large, the evolution will still achieve equilibrium, (region (a)) for d_N small Thus μ_2 would be expected to reach its peak

value and start to decrease at a rate which depends on the system characteristics. To some extent, this argument is supported by results obtained for a system of $N_0=40,000$ bubbles with $d=500$ defects ($d_N=0.0125$), Levitan and Domany (1996). A protracted intermediate period again appears to be a feature of the low concentration of defects since the authors found that, from 40,000 to 1000 bubbles, ($0.025N_0$), the second moment, μ_2 , continued to grow, whereas from around 600 bubbles to 200 bubbles remaining, ($0.015N_0$ to $0.005N_0$), μ_2 decreased and a stable value was obtained. Here, all the evolutionary period, prior to obtaining a fixed value for μ_2 is described as *transient*, even though it is clear that the percentage of bubbles remaining to take part in topological changes, is very small, so that finite size effects might be expected to operate here, ($T \rightarrow T(N)$). It seems likely that the increase in overall μ_2 therefore predominantly reflects a large number of changes for relatively few large bubbles. It is arguable whether the transient period should thus be defined as time taken to reach the point at which μ_2 shows no further increase, (apart from local fluctuations) or, strictly, as the time taken for μ_2 to reach a fixed final value. Either definition allows for early stage anomalies such as those found for the final case considered below, but fails to provide much information on changes in the internal froth structure.

For the case of the ordered froth with a high density of defects, the transience is clearly confined to the early stages of the evolution, (in region (a)), and is much more variable in form than found for low d_N , with behaviour dependent on different initial conditions. For example, μ_2 vs time may have one, two or more peaks. While rate of approach to scaling is affected, therefore, achievement of the scaling state is not. Examples of the effect of varying amounts of disorder on behaviour and length of transience have been crudely quantified, but μ_2 alone is not a particularly satisfactory criterion here. A more reasonable quantity is clearly the concentration of defects, d_N . The evidence suggests that the critical concentration of randomly seeded defects, below which scaling is not observed for finite froth systems, is around 1% of the initial number of bubbles, (based on a survey of current results). In this sense, $T(N)$ can be roughly defined as that time it takes the froth to evolve to the point where only $0.01N_0$ bubbles remain. For very

few survivors and an effectively infinitely large system, the evolution of the froth becomes that of the large bubbles, ((region (b) and no scaling)

Fig 4 4 19 illustrates changes in the second moment μ_2 vs time, t for different defect concentrations, $d_N = 0.05, 0.2$ and 0.4 in a system size of 2500 (This is modest compared to Levitan and Domany (1996) 40,000 bubbles) For $d_N < 0.05$, it is clear that the speed of μ_2 increase will be more slower, i.e. it takes even longer to observe the scaling stage. In contrast, for $d_N > 0.4$, the transient period is much shorter. A similar effect to that shown in Fig 4 4 19 is also observed for nucleation when raindrops form out of supersaturated vapour and different laws apply depending on whether a number of drops grow simultaneously or one drop consumes all the vapour, McGraw and Laaksonen (1996)

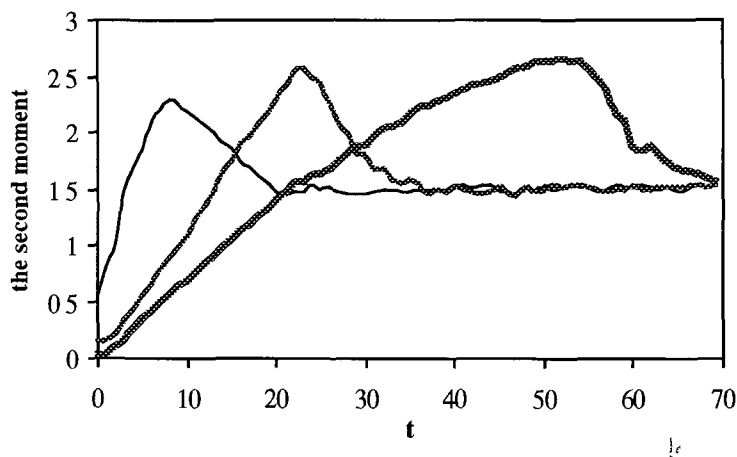


Fig 4 4 19 the second moment, μ_2 , of the whole system vs time, t , for defect concentrations $d_N = 0.05, 0.2$ (mid-dark line) and 0.4 (dark-line) respectively. For $d_N < 0.05$, μ_2 tends to have a short right-skew, e.g. a long transient period, for $d_N > 0.4$, μ_2 has a long right-skew.

In summary, for a disordered 2D froth, transient and scaling stages in the evolution are easily identifiable, with μ_2 rapidly achieving stability. For an ordered froth, stages in the evolution are less clear and are highly dependent on the defect concentration, d_N . For d_N large, early evolutionary behaviour is variable, but the situation is essentially as for the disordered froth. For very small d_N , the period to scaling is protracted and, based on μ_2 alone, appears to correspond to long transience. However, this quantity is less informative about topological changes.

taking place in the system than $\mu_2(n^*)$. This suggests that the period of many, rapid changes is relatively short and that the majority of the system stabilises fairly rapidly. The final constant value of μ_2 will be obtained only if the initial system is very large. This suggests a critical concentration of defects for finite systems, below which scaling is not observed. The concentration of defects also appears to determine the length of the transient period.

Chapter 5 MC Simulations and other Considerations

5.1 System Simulation with MC: Introduction

There are clearly practical limitations in extending simulations on cellular networks such as 2D froths by direct methods given the sequential nature of many of the original algorithms and limited hardware. The available options thus include parallelization or vectorization of the algorithms and alternative simulation methods, which deal with system statistics as aggregates rather than as detailed topological alternatives. One other option would be changes of hardware but this of course calls for massive investment. The performance of distributed systems may offer alternatives to super computers.

With respect to the development of parallel algorithms, this would seem to offer a better option, although for some of these complex systems, notably the froth networks, such development offers a whole new project in itself. Heermann and Burkitt (1991) Neither is parallelization always appropriate for systems of complex type and also of course generates its own problem, for example load balancing algorithms, Hegarty et al (1996) Nevertheless, in subsequent section of this chapter we discuss some of the implications for a parallel approach. The third options of simulations which deal with the statistics of a hypothetical population which in some sense mirrors the real one, is considered first in what follows.

In particular, if we continue with the example of 2D froth, we note that direct simulation of the evolution of several thousand cells on the system used on VAX in DCU takes of the order of two days (system size = 3000 cells). It appears, therefore, that this approach is limited for systems consisting of large numbers of cells. It is also not clear that the direct method will be sufficiently flexible to modify easily for other related cellular systems, e.g. grain growth, in particular where an increase in scale influences both the effects observed and the time taken for them to stabilise. In what follows, we therefore consider alternative simulations of Monte Carlo type for these systems.

5.1.1 Simple Systems

The Monte Carlo (MC) approach (introduced Section 2.5) has been used successfully on a number of problems on surface behaviour for simple cellular systems, e.g. cellular automata (CA) models, spin systems, and percolation models, Hammersley and Handscomb (1964), Binder (1986), Stauffer (1991), (and also Jain (1992)) Long-term large-scale effects for those systems can be investigated in terms of a large number of discrete rather than continuous samples. The generation of random numbers is used to determine whether or not an event relating to, for example, an atom or energy change takes place. The system is then allowed under certain criteria to move to a new configuration.

5.1.2 MC for Froths: General Points

Wejchert et al (1986) provided an alternative simulation method for studies of froth evolution. Based on discretization of the froth, each *bubble* is assumed to consist of a cluster of hexagonal *cells*, (samples), of the same size and shape. Early MC studies were used to investigate the effect of the area constraint, λ , on time taken to achieve froth equilibrium.

Given that froth coarsening involves the loss by a T2 process of n-sided bubbles with n less than six, then disappearance initially involves gradual bubble area shrinkage. The mechanism of this MC simulation is thus to model basic hexagonal cells flipping in bubbles which have no. of sides n less than six in every MC trial, where each bubble consists of an aggregation of these basic cells. As a cell flip is "allowed", so the bubble's area shrinks till it eventually disappears. The MC approach can thus also be used to investigate the influence on froth evolution of bubble area, area difference, neighbouring cells and so on.

The total energy of a 2D froth is given by $E = 2\sigma \sum l_i$, where σ is surface tension, (or surface energy), which creates pressure differences. These result in gas diffusion and the summation is over all bubble walls, of length, l_i , i.e. the boundary lengths of all bubbles. To minimise the surface energy of the cells in the network, the total energy Eqn (4.2.6) reproduced here for convenience, is given by

$$H = \sum_{(i,j)} \sum_{(i',j')} \delta \sigma_{(i,j)\sigma_{(i',j')}} - 1 + (\lambda/N) \sum_{\text{bubble } k} (A_{\text{act}} - A_{\text{tar}})^2 \quad (5.1.1)$$

where cell (i',j') is the nearest neighbour of cell (i,j) , so $\delta \sigma_{(i,j)\sigma_{(i',j')}}$ is the length of bubble side, (i.e. length, l_i), where $\sigma_{(i,j)\sigma_{(i',j')}}$ is surface tension between cell (i,j) and (i',j') . So, $\delta \sigma_{(i,j)\sigma_{(i',j')}} = 0$ if cell (i,j) and its neighbour cell (i',j') belong to the same bubble, but otherwise $= 1$. The total No. of bubbles = N , A_{act} and A_{tar} are actual area and target area of bubble k , with A_{act} determined by Equn (4.1.2), and λ , a constant that specifies the strength of the area constraint.

5.1.3 Implementation for 2D Froth

Conventional MC simulation using the Metropolis method involves steps which for a soap froth, may be represented for one MC trial by

- (i) Start with a Voronoi network of bubbles consisting of hexagons from which a cell is randomly chosen
- (ii) Randomly select a new cell from one of its six nearest-neighbours
- (iii) Calculate change in surface energy ΔE , Equn(5.1.1)
- (iv) For $\Delta E \leq 0$, accept new configuration (Typically ΔE depends on control parameters, $\delta \sigma_{(i,j)\sigma_{(i',j')}}$)
- (v) For $\Delta E > 0$, retain the old configuration

We illustrate cell flipping for *one MC trial* in Fig 5.1.1, where the following sequence applies. If a randomly chosen cell (i, j) of a bubble k_1 is in the boundary of an n_1 -sided bubble k_1 and an n_2 -sided bubble k_2 , then randomly select one of six nearest neighbours of cell (i,j) . If the new cell, either cell $(i+1,j)$ or $(i,j+1)$, shown in Fig 5.1.1, satisfies the condition of $\Delta E \leq 0$, (step(iv)), the cell (i,j) will flip from bubble k_1 to its neighbour k_2 , irrespective of whether bubble side No. n_1 is less than, equal to, or greater than n_2 . Then the area difference between bubble k_1 and k_2 , ΔA , will update due to the actual area, A_{act} of bubble k_1 and k_2 having changed, while the target area, A_{tar} of bubble k_1 and k_2 will stay the same.

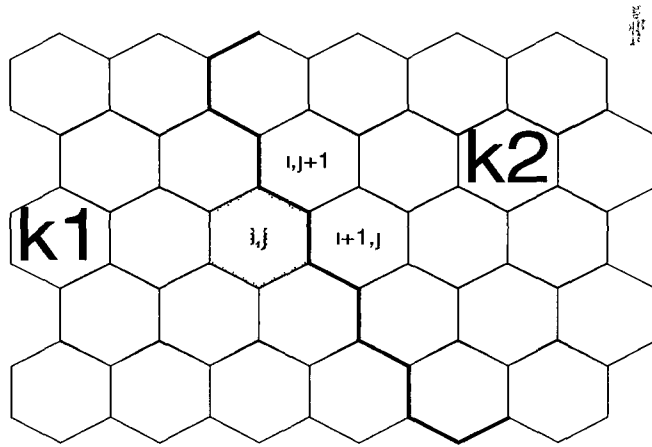


Fig 5 1 1 An example of Cell flipping in MC simulation

A more complex example is to consider a cell at the boundaries of three bubbles, or more, see Fig 5 1 2 and 5 1 3. If cell (i,j) occurs at the boundaries of three bubbles k_1 , k_2 and k_3 , (with notation similar to the two bubble case), then, if any one of the nearest-neighbour cells $((i+1,j)$, $(i,j+1)$, or $(i-1,j+1))$ satisfies the cell flipping condition, $\Delta E \leq 0$, then cell (i,j) in bubble k_1 may flip to either bubble k_2 or k_3 across the boundary. The choice of nearest-neighbour again is *random*. Area difference, ΔA will update to give, $\Delta A_{k_1} = \Delta A_{k_1} + 1$, and $\Delta A_k = \Delta A_k - 1$ ($k =$ either k_2 or k_3), and again, the target area of bubbles, k_1 , k_2 , and k_3 , ($A_{tar}(k_1, k_2, k_3)$) remain the same.

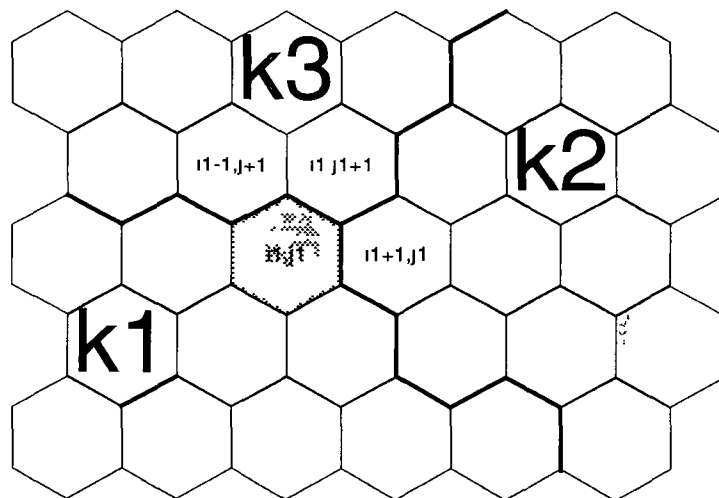


Fig 5 1 2 Cell flipping between three bubbles

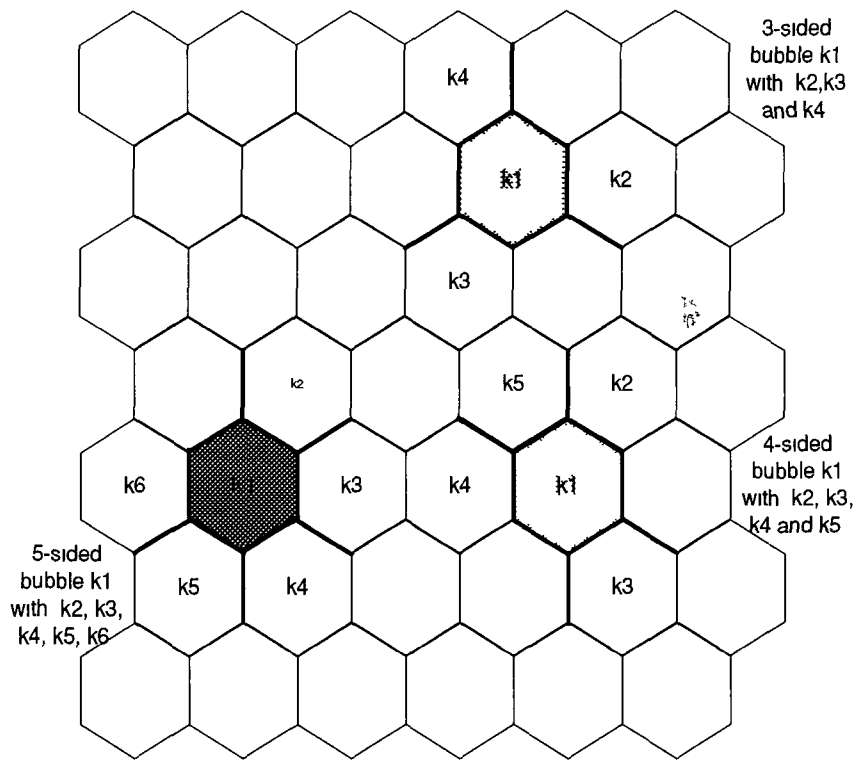


Fig 5 1 3 Cell flipping between four or five bubbles

For a T2 process, simulated by MC, energy changes, ΔE , (cell by cell reduction or flipping), will be negative for small bubble cells. However, ΔE depends on the nearest-neighbour of a given cell chosen, the parameter λ and so on. We also need to know the characteristics of recipient bubble, n , $\langle A \rangle$, ΔA . The evolution time is measured by Monte Carlo Step (MCS), which refers to the repetition of one MC trial until all cells have been considered.

5. In initial simulations, we choose the area difference, due to bubble diffusion between actual and target area, ΔA , to be 5% of the average area of a 5-sided or 7-sided bubble, i.e. $\Delta A = -(n-6) \cdot 5\% \cdot \langle A_0 \rangle$, where $\Delta A = A_{act} - A_{tar}$, $\langle A_0 \rangle$ is the initial average area of bubble in the system. Thus, $\Delta A = 0$ for a six-sided bubble, $\Delta A > 0$ for a n -sided (less than six) bubble, and $\Delta A < 0$ for a n -sided (greater than six) bubble. Froth equilibrium is achieved for the total average area difference less than the given maximum difference.

5.1.4 Froth Coarsening

5.1.4.1 Notes by MC

As a further series of points on the MC simulation, we note the following

- (i) CPU time is affected by λ , but also by value of control parameter, (temperature equivalent, $T=0$ always for step (i) to (v) in a single trial)
Also affected most importantly by ΔA ,
- (ii) No of sides, n , of a nearest-neighbour bubble will change with a bubble disappearance (Euler's law) Thus, A_{tar} , ΔA for nearest-neighbours of a disappearing bubble must be updated instantaneously before next MC trial

In what follows, we consider the importance of the choices of λ , ΔA , $\langle A \rangle$ for an efficient and realistic MC simulation following Wejchert et al (1996)

From the procedure described it seems clear that achievement of a "scaling-state" should depend on the environment of a disappearing bubble, (i.e. large or small neighbour), and therefore on percentage reduction in target area, A_{tar} , ΔA as might be expected, (e.g. 2% average area will cause less cell flipping in one MCS, whereas large neighbours make cell flipping more likely, since energy difference, ΔE , condition more likely to be satisfied) and so on

However, the final disappearance of a "bubble" may be slow since the last cell can take a long time to flip. When a cell is the only cell in a 3-sided bubble, it must flip to nearest-neighbours, possibly taking many MC trials because it is a stochastic procession. This final disappearance also implies a reduction in the No of sides n of bubbles k_2 , k_3 , and k_4 . Both A_{act} and A_{tar} for k_2 , k_3 and k_4 will update instantaneously, and hence area difference, ΔA will change to $\Delta A'$, where $\Delta A' = -(n-6) \cdot 5\% \cdot \langle A \rangle$, given our choice of area difference above. This applies equally for a 4-sided or a 5-sided bubble. So, for any n -sided ($n < 6$) bubble, when the last cell in the bubble flips to one of its nearest-neighbours, bubble disappearance will occur accompanied by the reduction of the number of sides in nearest-neighbour

bubbles This leads to the typical fluctuations in μ_2 in froth coarsening, which we have noted earlier, Section 4.2

The main structure by MC method is given as follows, (for further details see Appendix E)

```
// Froth Program by MC Method//
CALL input // input data
CALL setup // Initial Configuration (Voronoi network)
CALL Equil // Equilibrium
do 10 i=1,n
CALL Diffus // diffusion
CALL Equil // Equilibrium implemented by MC trials
i=i+1
CALL OUTPUT
10 continue
CALL OUTPUT
END

SUBROUTINE Cflip //MC trial
itime= itime +1 //time step
Ocell=ga(i,j) // a cell (i,j)
ie1=ie1+1 // calculate the first term of
initial energy of a cell
Newk=int(ran(1)*6)+1 //random choose one of the six
neighbours of cell(i,j)
ie2=lambda(dv1*2+dv2*2)//calculate the second term
of initial energy
fe1=fe1+1 // supposed a cell is flipped,
calculate its first term of energy
fe2=lambda(dv3*2+dv4*2) //calculate its second term
of energy
oldenergy=ie1+ie2 //the sum of energy before flipping
newenergy=fe1+fe2 //the sum of energy after flipping

if (newenergy.le. oldenergy)then
//energy difference greater than 0,)
make= true. // accept the new configuration
else // Continue MC trial if temperature>0
```

```

        if(temp.gt.0)then
        if(exp(-(newenergy-oldenergy)/temp) gt ran(1))then
        make= true
        endif
        endif
    endif
END

```

5.1.4.2 Performance under Different Choices for $\langle A \rangle$ and λ

From the mechanism described in the last Section, it seems that whether a cell (i,j) flips or not may be dependent on the initial environment. We have implemented froth evolution with two different Voronoi networks for a 2D froth of size 1600 bubbles with 400* 400 cells. Here we measure the evolution time in terms of a Monte Carlo Step (MCS), which is defined as previously, (Section 5.1.3), i.e. the repetition of the sequence for one MC trial until all cells in the system have been considered.

In Fig. 5.1.4-5, we show variation of CPU time on MCS with the effect of refining λ and choice of area difference, ΔA . In Fig. 5.1.4, we show the effect of varying the choice of area difference ΔA (2% and 5% respectively) on the second moment, μ_2 vs time (measured in MCS's). In Fig. 5.1.5, the effect on CPU time (again in MCS's) vs λ is shown where the interest is in refining λ to produce greater response for reasonable time taken. For any value of λ much beyond 0.4, however, CPU time escalates rapidly, in agreement with the similar result obtained by Wejchert et al. (1986). The CPU time is clearly longer due to slow energy change for large values of parameter λ , Eqn. (5.1.1). Fixing the area difference as 2% of mean area $\langle A \rangle$ (Section 4.1.3) leads to a smooth evolution of μ_2 vs time. This is not surprising since μ_2 is sensitive to bubble disappearance at the lower percentage, thus it is less difficult to get flipping, and changes are less drastic. Results for quantities of interest are in good agreement with those obtained by previous simulation methods.

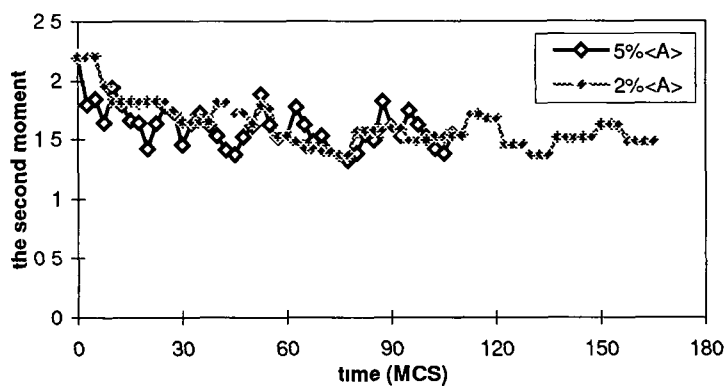


Fig 5 1 4 the second moment changes vs time (MCS)

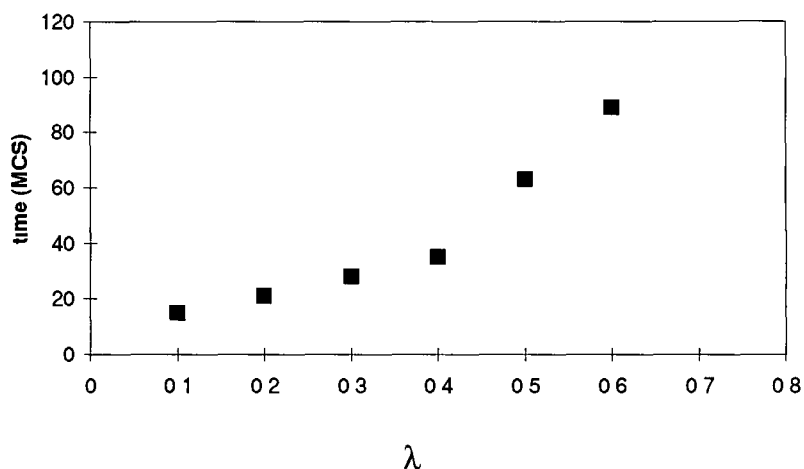


Fig 5 1 5 Time (MCS) taken vs λ

5 1.4.3 Performance of Bubble Area

The initial bubble area A also appears to influence bubble disappearance. Consider, e.g. a three-sided bubble with different n -sided nearest-neighbours, ($n=4, 5, 6, 7$). For a small value of λ , it is clear that the energy difference for all n -sided bubbles satisfies the condition $\Delta E \leq 0$, while for large λ , ΔE will vary with different number of bubble sides, e.g. for $n=6, 7$, $\Delta E < 0$, for $n < 6$, $\Delta E > 0$. The actual value of E depends, of course, on the Eqn (5.1.1)

In particular, we are interested here in the influence of bubble area on bubble disappearance. We consider the influence of initial area distribution for two types of Voronoi network, (i) no hard disk version, where the initial area distribution is non-uniform, or polydisperse, with $\mu_2 = 1.87$ (ii) hard-disk modification, where

the initial area distribution is not the same as (i), but still polydisperse, with $\mu_2 = 1.09$, (iii) hard-disk, where the initial area distribution is different, roughly uniform, or monodisperse, with $\mu_2 = 0.97$, closer to (ii)

For different Voronoi setups considered, the evolutionary behaviour for both polydisperse froths, initial conditions (i) and (ii), is similar, and indicates a rapid decrease in the No of bubbles with time, which is more marked for the froth with higher initial disorder or less uniformity of bubble area. However, for roughly uniform area, initial condition (iii), the decrease in the No of bubbles with time is much slower, although long-term behaviour is again similar to the previous cases ((i) and (ii)). We show the change in the No of bubbles disappearing with time in Fig 5.1.6

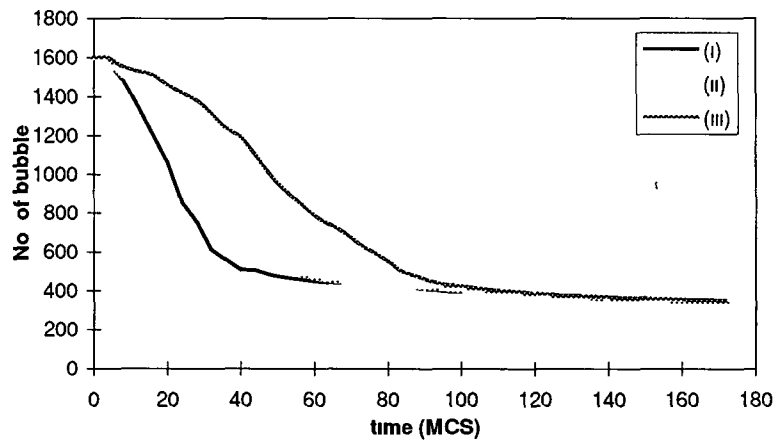


Fig 5.1.6 No of bubbles vs time

In previous experimental work, Glazier et al (1987) also note that the apparent rate of shrinkage of bubbles with few sides is smaller than that predicted by a pure linear fit. If Von Neumann's law holds in unmodified form, the evolutionary behaviour of froth with initial conditions, as for (ii) and (iii), i.e. roughly the same side distribution, but totally different area distributions, should be the same. However, we find that there are differences at the early *transient* stage, implying that initial bubble areas influence the rate or nature of froth evolution. This might be taken to suggest that a modified form of Von Neumann's law by Icaza-Herrera and Castano (1995), which accounts for area distribution, should apply to the early evolution. A possible form has been conjectured to be:

$$dA/dt = kA^{\alpha(n-6)} \quad (5.1.2)$$

where k and α ($0 \leq \alpha \leq 1$) are constants, $\alpha=0$ when Von Neumann's law holds in unmodified form, and $\alpha=1$ for a normal froth, Icaza-Herrera and Castano (1995). From Eqn (4.4.1), for the uniform area case, $dA/dt \sim (n-6)$ applies. A modified law for different area distributions also gains some support, however, from e.g. Herdtle and Aref (1992), who demonstrated some anomalous evolution results for bubble disappearance. Such anomalies appear, however, to relate to the early stage of evolution and Von Neumann's law is appropriate for the evolution as a whole. In contrast to direct simulation, the MC method is able to model large system size for less CPU time, (even though here only give an example of system size of 1600 bubbles). Moreover, the direct simulation program is much more complex and less flexible than MC methods. MC has been used to study other network pattern problem, e.g. grain growth, Anderson et al (1989). However, the disadvantage by MC is also obvious, e.g. the detailed information of evolution procedure obtained by the direct method is not available to anything like the same extent although MC results are fully acceptable on an *average* basis.

5.1.4.4 Summary

In summary, considerable effect on the froth evolution is obtained by varying the control parameters of a MC simulation of 2D froth. In particular, the construction appears to emphasise the importance of the environment on the flipping of a component cell of an n -sided bubble ($n < 6$) and hence on that bubble's disappearance. In *particular*, we consider the importance of the *environment* on the flipping of a component cell for a bubble with $n < 6$ and hence on that bubble's eventual disappearance. It is obvious that a large target area, A_{tar} and area difference, ΔA , in this context implies that the scaling state is achieved more rapidly during froth coarsening. Additionally, a modified Von Neumann's law best appears to offer an alternative explanation of the influence on early transient effect of area.

5.1.5 Technical Implications of Froth

5.1.5.1 Theoretical Implication

A realistic froth must include 3D and a few attempts to address the 3D case have been made so far. Clearly, such a cellular network is both more challenging and complicated and thus, is very difficult to describe using a direct model as in 2D. Of the approaches tried for a froth to date, Frost et al (1988) used a discrete description of the structural elements themselves, while Nagai et al (1990), considered only vertex points joined by straight lines as in the topological model, (Section 4.2.3.3). Other aspects of the problem have been considered, e.g. by Weaire and Glazier (1993) who give a relation between volume and number of faces in coarsening cellular patterns, and by Weaire and Phelan (1994) who have obtained a more efficient space-filling structure of 3-D froth which challenges Kelvin's original structure. More recently a logistic map formulation has been considered by Aste and Rivier (1996). For a recent review, see Weaire and Phelan (1996).

It is instructive to consider some of the reasons why a three-dimensional cellular network is so much harder to simulate than its two-dimensional counterpart, despite the fact that we can theoretically define very many dimensions in computational terms. The factor of computer time is crucial for simulation in 3D, because although the fraction of the volume affected by edge effects is much larger than in 2D, the time taken for equilibration to take place makes the simulation of large systems prohibitive. The memory storage and computation time required for such simulations is huge, limiting severely the size of system that can be simulated, and therefore making it difficult to obtain reliable information about scaling states which apply in the asymptotic limit.

In addition to these common technical difficulties the simulation of our specific cellular network, namely the realistic 3D froth present some additional problems, which are intrinsic to the nature of the problem. These include the fact that distribution functions which are fundamental to the statistics are more difficult to obtain since not all the structural details can be accessed simultaneously and with

ease Furthermore, the *theory* of the 3D froth faces an even more serious obstacle in that the basic equations for 2D froths, (e.g. Von Neumann's law, Euler's rule), *both* fail in three dimensions. Polygonal cells in 2D are separated by circular arcs with constant mean curvature that meet at equal angles of 120° . In contrast, polyhedral cells in 3D are separated by minimal surfaces with uniform mean curvature, three faces meet at equal dihedral angles along each cell edge, and four edges meet at each cell vertex at equal tetrahedral angles of $\cos^{-1}(-1/3) = 109.47^\circ$. In fact, the average number of faces, $\langle f \rangle$ of bubbles in a three dimensional froth can vary considerably, though most experiments yield a value near $f=14$. Instead the relation given by Nagai et al (1990) is

$$\langle n \rangle = 6 - 12 / \langle f \rangle \quad (5.1.3)$$

This implies that *two* parameters (i.e. n and f) are needed to characterise a cell in a three dimensional cellular structure as opposed to one ($=n$) in 2D. In the case of $n=5$, $f=12$, corresponds to the pentagonal dodecahedron, which is an important structure.

The elementary topological transformations also occur in rather different ways compared with 2D. A T1 process whereby the vertices common to an edge coalesce creating a new side, and a T2 process by which cells disappear directly by shrinking are shown in Fig. 5.1.7(a) (b). It is still not known however, how many different types of T2 processes there are because the average surface curvature of a bubble with tetrahedral angles 109.5° is not determined solely by its number of sides.

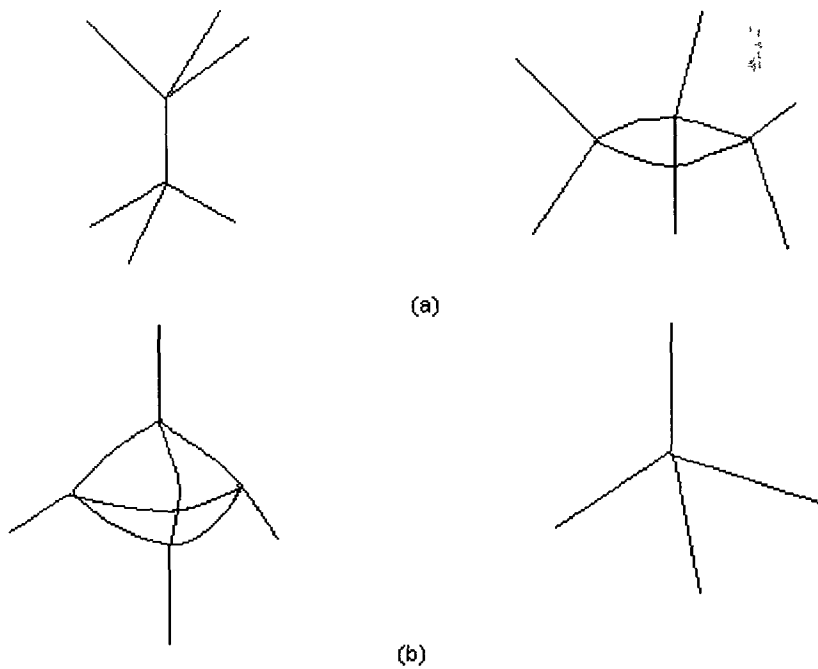


Fig 5 1 7 Elementary topological transformations in 3D

(a) T1 process or switching, (b) T2 process

The minimum information needed to determine the growth rate is also not known Rivier(1982) has suggested “patching up” with the relation

$$dA_f/dt = k (\langle f \rangle - f) \quad (5 1 4)$$

where f is the number of faces of the bubble or grain, A_f its volume, and $\langle f \rangle$ is the mean for all grains. This equation is reminiscent in form to Von Neumann’s law, but there are subtle differences between them. Equn(5 1 4) describes the evolution of an ensemble of cells instead of that of an individual cell. Furthermore it cannot be integrated to obtain the dependence of A_f on time. The topological network models in 3D, such as Equn(5 1 4), would appear to be no more difficult to handle than those in 2D, but there are ten or more types of disappearing bubbles. Recently, Rivier(1985) derived a three-dimensional version of the Aboav-Weaire law

$$mf(n) = c + 1/n [f(5-c) + (c-11)] \quad (5 1 5)$$

where $m_f(n)$ is the average number of sides of the neighbouring faces of an n -sided face belonging to an f -faceted cell, and c is a constant. Computational verification of this result is still lacking.

Durian et al (1990) performed a systematic experimental study of coarsening in three-dimensional foams. By monitoring the optical transmission of shaving cream foam over time, they found that the average bubble size in the bulk increases as a power law t^β with $\beta = 0.47 \pm 0.05$. Observations of foam's surface by optical microscopy showed that the dynamic processes consist of structural rearrangements of bubbles which differ from T1 processes in both nature and timescale. These rearrangement events are possibly due to the high liquid content of the foams used in the experiment. In fact, the examination of the microscope pictures shows nearly spherical bubbles. The origin, scaling behaviour and effects of these rearrangements upon the coarsening were not studied.

Computationally the question of computing capability and power available is closely linked to these difficulties of pinning down the underlying mechanisms and structures. Some successes have been recorded. For example, the Potts model can be extended to three dimensions provided that sufficient computer time is available. Anderson et al (1989) have run simulations on a $100 \times 100 \times 100$ lattice. For lattices with different anisotropy, these authors made a variety of distribution function measurements, obtaining $\langle f \rangle = 12.9$. The agreement with experimental values for metal grains is good, with the residual discrepancy compatible with anisotropy effects.

Glazier (1993) indicated that the coarsening behaviour of the 3D Potts model depends on grain topology, and concluded that a similar but weaker law holds for ensembles of bubbles in 3D. An expression corresponding to that found by Durian et al (1990) for shaving foam (section 5.1.4), was given by Glazier to be

$$V^{-1/3} dV/dt = k(f-f_0) \quad (5.1.6)$$

where k is a diffusion constant, f is the number of faces of a grain, f_0 is a constant, and V is the volume of a grain having f faces. Equ(5.1.6) shows that the average canonical growth rate of a grain depends linearly on its number of faces and is dependent on its volume, which is analogous to the modified Von Neumann's law

of Icaza-Herrera and Castano, which we have given in Equn(4 1 2) However, those equations only hold, of course, *on average* The growth rate of any *individual* grains need *not* depend on its number of faces, for example, some 16-faced grains grow, while others shrink Sire (1993) has also addressed the reason why only an average growth law holds in 3D Glazier has postulated a corrected average value for $\langle f \rangle$ based on this work with $f_0=15.8$, and subsequently found to obey an expression

$$f_0 = \langle f \rangle (1 + \mu_2 / \langle f \rangle^2) \quad (5 1 7)$$

(Weaire and Glazier (1993)), with $\langle f \rangle$ the average no of faces Further Potts model simulation results gave $\langle f \rangle = 13.7$ and $f_0 = 15.8 \pm 0.4$, in agreement with the result of Glazier (1993) The evidence then supports the view that the averaged growth rate in the Potts model is a linear function of the number of faces Equn (5 1 7) will apply to any other coarsening system, which has similar connections between growth rate v and f The accumulating evidence therefore continued to favour the use of statistical of simulation methods to further explore 3D froth features

5.1.5.2 Technical Implications for Froth by MC Method

The optimal structure for a monodisperse foam has been a subject of interest for centuries The question is what spacing filling arrangement of cells of equal volume has minimum surface area Kelvin (1887) proposed a truncated octahedron as a likely candidate for the optimal arrangement Weaire (1994) suggested two cathedral structures as a natural choice for intermediate values of liquid content These occur in the chemistry of tetrahedrally-bonded materials and there is a close analogy between tetrahedral structures and the froth or foam problem. In a recent breakthrough, Weaire and Phelan (1994) have given a counter-example to that of Kelvin which has a significantly lower surface energy The method used the surface Evolver software, (developed by Brakke (1992) (1995)), to minimise surface area, subject to the constraint of fixed cell volumes, for successively finer tessellations of the original cell faces In this way, the curvature of the surface can be progressively approximated with increasing accuracy It is found that the final Weaire-Phelan

structure, consisting of six fourteen-sided polyhedra and two irregular pentagonal dodecahedra, has surface energy which is approximately 0.3% less than that of Kelvin's solution

Weaire and Glazier (1994) also developed a simple construction based on the Kelvin and the Williams partitions that generates periodic or quasiperiodic 3D partitions. It has been used to distinguish the minimal-area structure under conditions of equal volume and equal pressure.

Given that the precise relationship between the topology and the rate of growth of a bubble for the 3D froth is not well-understood, most algorithms developed so far have concentrated on the whole structure level rather than the level of an individual bubble. However, MC simulation appeared to offer reasonable possibilities of extension to the 3D case since dealing with an ensemble of cells is an intrinsic mechanism of the approach.

Paralleling the 2D froth method, we considered the discretization of bubble volume by a cluster of samples (units). Given that the number of a given bubble's faces and that of its neighbours are more complex than for 2D, we consider initially a simple basic structure i.e. the cubic cell, so that aggregates of cubes would form the network bubbles. Implementation of cell flipping in cubic structure is a generalisation of the 2D case, but allocation of a flipped cell to nearest-neighbour bubbles is much more complicated. Clearly, a bubble's disappearance again depends on whether all constituent cells have flipped to one or more nearest-neighbour bubbles.

Since the energy of the 3D system is related to the bubble's surface energy, i.e. the length of boundaries or of all bubbles' face, a cell-flipping will affect either one or the other. The energy would be expected to have an equation which crudely parallels that for 2D, given e.g. by

$$H = (1/2N) \sum_{(i,j,k)} \sum_{(i',j',k')} \delta_{(i,j,k)(i',j',k')} - 1 + (\lambda/N) \sum_{\text{bubble } k} (V_{\text{act}} - V_{\text{tar}})^2 \quad (5.1.8)$$

Here, the analogy to the basic unit of the hexagonal cell in the 2D case is now a cubic cell, (i',j',k') is one of the nearest-neighbours of cell (i,j,k) and summation is over all faces. The maximum no. of choices for bubble assignment in cell-flipping is

now 7, as opposed to 5 in 2D; clearly a single MCS will include more complex MC trials.

For a 3D Voronoi network configuration, Equn (5.1.6) could be used as the approximate equivalent of Von Neumann's law in the 2D case. Assuming the volume difference due to bubble diffusion between actual volume and target volume, ΔV , to be 5% of the average volume of all bubbles, and the average No. of faces, $\langle f \rangle$ equal to 14, we can implement a cell flipping by MC method on 3D froth. Similar to 2-D froth, assumed for a 14-faced bubble, $\Delta V = 0$, for an n-faced bubble, ($n < 14$), $\Delta V > 0$, for $n > 14$, $\Delta V < 0$. Choosing the same volume difference for all the non-14-faced bubbles will obviously, however, introduce a bias in the 3D froth evolution.

5.2 Other Techniques

Both cellular automata and molecular dynamics techniques have also been used to study some cellular network models, in particular, grain growth and solid foam.

5.2.1 CA for Grain Growth

Grain growth, as an example of a cellular structure, is of great interest since it is one of the most important features in the control of microstructure. The energy of grain boundaries at equilibrium and topological requirements are two important factors in modelling grain growth, Atkinson (1988). Theoretical, experimental and simulation models have all been used to investigate system properties and in particular, the MC method has been successfully used to solve this problem. Based on the transition probability, MC methods have been applied to simulate processes of recrystallization, normal grain growth and abnormal grain growth, (Srolovitz et al. (1984), Anderson et al. (1989)). For a recent review, see Weaire and McMurry (1996).

Similarly to the froth, grain growth is one of the natural structure-evolving processes. Since the grain boundary network has similar patterns and characteristics to those of biological cells and ecological territories, cellular automata (CA) would seem to be applicable to their study. Hesselbarth and Gobel (1991) first applied a

CA model in primary recrystallization simulations and Liu et al (1996) further developed a formal CA model with further assumptions for the grain growth problem.

Using Von Neumann's definition of neighbourhood for a CA model, Wolfram (1984), Liu et al (1996) have given the transition process as

$$x(i,j,t) = F[x(i,j,t), x(i,j+1,t), x(i+1,j,t), x(i-1,j,t), x(i,j-1,t)] \quad (5.2.1)$$

where $x(i,j,t)$ represents the states of (i,j) cell at time t . The function F is the transition rule, which can be defined in a various way. The dynamics of CA are governed by local rules, (as we have described in Section 2.3), so that the locality of the dynamical rules allows efficient and flexible treatment of complex geometries. Thus, whether the final state of the system after a given period of time is homogeneous, chaotic or complex, depends on the definition of the transition rule. The Game of Life is a well-known example exhibiting variety and complexity in the development of CA even for simple rules, Vichniac (1986), but much more complexity is possible.

Liu et al (1996), for example, have modified the transition rule Eqn(5.2.1) to implement grain boundary migration due to curvature effect. A grain boundary is associated with a positive surface energy and migrates in some way to lower energy, e.g. two cells with different states are separated by a minimum unit length of grain boundary. The results of Liu et al (1996) on grain size distribution and growth kinetics are in agreement with those obtained from theory, experiment and MC simulation.

In general, the basic difference between the Monte Carlo (MC) method and CA lays in the transition between states of a cell in the system. In the MC method, the state transition is realised by randomly taking a number in the state of $N=1$ to Q , then putting it in the cell which is ready to change, calculating the energy difference, ΔE , between the old and new configuration and giving the probability of transition. For $\Delta E \leq 0$, a new configuration is accepted, with the probability $P=1$, for $\Delta E > 0$, with $P = \exp(-\Delta E/kT)$. Usually, the probability, P , is different from cell to cell in the MC simulation model. In contrast, for a CA model, the new state of a

cell comes from its neighbour cells, so for every cell, there is constant energy barrier, which must be overcome in a state transition with the same probability

5.2.2 Molecular Dynamics on Wet Foam

Durian (1995) discussed wet foam by focusing on entire bubbles rather than vertices, and proposed a simulation model, which has been constructed for the molecular dynamics approach (Section 2.5). In terms of structure and dynamics at the bubble scale, the model has been shown to reproduce the hall mark behaviour. This approach also allows reliable study of formations and flows at length scales greater than the average bubble size. However, the weakness of this method is that it can only be used in wet foam, not dry foams since no degrees of freedom are introduced for the bubbles shapes. Gardner et al (1997) also used molecular dynamics to analyse the scaling behaviour of 3D solid foam.

5.3 Computer Simulation Implementation

5.3.1 Simulation Approaches

Evolutionary dynamical systems have attracted considerable attention in recent years. Many efforts have been made to investigate their properties. Computational modelling techniques have provided new and valuable insight into the studies of these complex systems, both in terms of testing microscopic theories as well as practical methods for modelling processes as a whole. Although some current programs are less sophisticated than those of commercial software, a wide variety of techniques and computational environments have been used. Our aim has been to investigate several simulation approaches as a means of examining the dynamical behaviour in complex systems.

Traditional modelling and simulation has tended to concentrate on mathematical representations of complex physical and other systems with strong reliance on both numerical modelling and discrete methods. For more complex systems, there are two strategies available. One is to improve theory at higher levels which usually means improving on an approximate form and another is to simulate the behaviour of main elements. Theory thus tries to resolve computational difficulty by reducing

detailed information to a few degrees of freedom. For example, the objective of statistical mechanics is to observe not only the underlying state itself, but also the probability of the system being in any particular state

It appears that indirect simulations, e.g. MD, MC are less information rich than direct simulation (e.g. froth example). It is obvious that direct simulation can specifically provide us with more detailed information during the evolution on hundreds or, better, thousands of cells. However, it is far from ideal to try to obtain a scaling index from simulations limited by time and scale, so that improvements in the algorithms and their efficiency are clearly needed for fixed hardware provision. In contrast, the MC approach appears to offer the better general method for proceeding on a variety of associated questions e.g. grain growth and other similar networks

5.3.2 Languages Requirement

Currently, the most popular languages for computational scientists are Fortran 77, (Fortran 90), C and C++. Fortran, through the most popular for many years, however, does not allow the programmer to structure programs so that they reflect the logical order of idea involved in addressing a problem, and it is often complicated to delineate new contributions and modifications to existing large scientific Fortran codes. Due to inflexibility, Fortran appears to be losing ground, although Fortran 77 is much easier to use than C and C++, which is growing in popularity. From a computer science point of view, there is little difference between C and Fortran, except that C has marginally better facilities for structuring programs than the original Fortran 77. Far more differences exist between the various styles of parallel programming, where these differences are already having a big impact on software development for computational science and makes increased familiarity inevitable.

Frequently, because of the longer development time of the language, Fortran compilers are more robust and efficient for scientific applications in particular for supercomputers, although special version of C may perform as well or better on some massively parallel machines. Graphics and visualization are almost entirely done in C/C++ although FORTRAN implementations are possible. It is also

possible to use Fortran subprograms in C/C++ codes. For scientific programmes, we can take advantages of both languages, e.g. keeping the numerical Fortran routines for difficult number crunching and designing the software package with an object oriented language. In recent years, some of the more popular commercial numerical routine libraries have also been released in C version.

Computer languages keep evolving rapidly, and it is possible to discern a trend toward formal languages. A wide array of routines accomplishes a range of tasks from elementary to very complicated. For most users, programming will be limited to the connection of such routines by using graphical or verbal syntax. More recently, visualization packages in physical and other scientific applications have enjoyed a tremendous surge of interest. For instance, Surface Evolver has now become the standard software for computing the geometry of foams, Kraynik and Reunelt (1996).

5.3.3 Algorithms Limitation

It is known that the application of algorithms to the behaviour of very large systems would not have been possible, without highly optimised programs that reduce the memory requirements and the execution time. Even with the current, relatively advanced technology and sophisticated algorithms, most simulations are limited to a relatively small range of scales. They are prone to various types of error, and require a long time to implement. Choosing simplified mathematical models is an accepted option to understand and solve the various computational problems with a view to improving the system representation.

Much work here has been concerned with two-dimensional simulations and experiments as a simplification of naturally occurring systems. Each approach considered, however, has its limitations. For example, in the 3D froth model, the main difficulties of the MC method lie in the fact that the number of possible configurations of each bubble becomes enormous with a large number of degrees of freedom which must be simultaneously handled. System size limitation could be another problem for all simulation approaches. Further developments for both software and advanced hardware resources are required. Coding methods such as multi-spin coding can normally be extended to the three-dimension problems and

also apply for the froth case. However, the large number of variables, and operations might not provide easy implementation and the memory is another factor.

5.3.4 Limitation of Simulation Methods

Simulations themselves are not necessarily reliable since they also generate different errors intrinsic to the simulation method. For example, statistical errors occur in drawing a finite number of partially correlated samples, numerical errors occur in the algorithms, and round-off errors arise from finite-size effects. In spite of this, the simulated behaviour of the model gives an approximate analogy of a system's actual behaviour. The real difficulty lies in determining the level of error, aggregated from those various causes and the degree to which it affects the realism and accuracy of the system representation. There is, of course, no single answer to this question and for the majority of simulation work, there is a need to perform many trials and repetitions of the same experiment to test the limits of the simulation and observe carefully end effects. Also, of course, to test vs. known results as a control on the simulation veracity.

Considerable effort has been spent in the development of computational problem-solving environments for physical and related systems. Some attempts have been made to integrate various software components into a unified system hiding the underlying complexity from the user. This is an "idealised" improvement, with the goal of solving all aspects of a problem including simulation, data analysis and visualization. Unfortunately, such systems tend to provide very *poor* performance on large problems even if performance is reasonable for commercial applications. Consequently, they are generally unsuitable for scientific computation.

However, the idea of providing integration of simulation and data analysis is an interesting one. The approach must clearly emphasise transparency rather than attempting to create a highly sophisticated package with over-elaborate interfacing. In short, tools should be simple to use, offer high performance, be maintainable across a *wide* variety of machines rather than get in the way of research on a limited subject. In particular, the following features are needed to measure the development of simulation software in scientific applications.

- Performance and memory efficiency
- Extensibility
- Support of existing code

More advanced developments include controlling applications with scripting language, rather than relying solely on compiled languages, such as C or Fortran. The use of interpreted scripting language for dealing and interacting with physics application has been the subject of recent exploratory work by computational science researchers. The idea is quite simple, providing a high-level interface, such as Matlab. Using this package, users can control physics and other applications interactively by entering commands, writing receipts and adding additional function lists in the interface language, *without* having to modify the underlying code. The software package, the Surface Evolver, is one such package which is applicable to a variety of practical problems and has been mentioned earlier in relation to 3D froth work.

3

3

Chapter 6 Conclusions and Comments

6.1 Introduction

Nature provides many examples of systems which have an essentially single or network cellular structure. The statistical properties of their long-term behaviour can be investigated by e.g. monitoring the occurrence of specific "events" or network evolution through time. Insight on changes ranging from the minor to the catastrophic can be gained through computational models.

The goal of scientific investigation is to understand how nature works. Originally, two options were available to do this, namely experiment and theory. The traditional approach consisted of modelling system equations directly and then solving these equations, either manually or by computer routines. Unfortunately, this breaks down where analytical solutions are not available or where technical difficulties prohibit numerical solution or when the system being studied is not theoretically well understood.

Algorithms or computer programs, which directly model the phenomena under investigation have increased in popularity. This thesis presents a general overview of simulation methods for studies of complex physical and related systems which are of current interest. Most importantly, it provides a description and application of some fast and efficient simulation modelling techniques and their potential for further development, together with our implementation of and results on a selection of these cellular system models.

6.2 Techniques Implementation

We have implemented several different computer simulation techniques in this work, including direct methods, cellular automata, Monte Carlo, and have introduced others, such as molecular dynamics, which have not been explicitly used for the work presented here. These provide an overview of current popular methods used in investigating scientific computing problems. Generally speaking, a number of different techniques may be applied to a given problem, but the choice depends on the aspect of interest. In the direct modelling of the 2D froth in 4, for

example, interest focused on the detailed structural changes, as well as on the long-term behaviour, particularly when following the influence of defects. Thus direct simulation methods, for initial studies anyway, provide an obvious choice. However specifying a certain system so precisely incurs penalties, in terms of adaptability of the code, together with limitation on the size of the system which can be simulated, when so much detail is being retained. Consequently, adaptation to other complex systems which share common features, requires additional effort, even though this may well be considered worthwhile. A close analogy to the soap froth, for example, is provided by the metallic grain growth problem, Weaire and McMurry (1996), yet there are distinct differences, notably in the shape of the grain boundaries, which can be far from the ideal minimal surfaces found in the soap froth, and also in the inherent lattice anisotropy. This latter feature is of particular interest, since it influences the rate of transition between order and disorder, which is much slower than for the corresponding froth, Holm et al (1991) and refs therein.

Far less rigidity of coding is evinced for applications which can be reduced to interactions between fundamental and similar elements, where each of these can be in one of a finite number of states. For this type of system, the cellular automata approach is a natural choice. Its flexibility is reflected in the wide range of problems which CA have been used to model. Here we have considered a CA approach to the modelling of dissipative systems, represented by loss of sand grains induced by perturbation of a quiescent sandpile. The sandpile automaton here serves as a model for transport phenomena in general. CA methods may be used to directly model the behaviour of the elements or indirectly to approximate them, e.g. as in immunological CA, Stauffer and Pandey (1992).

Features of the CA coding include its simplicity and massive iteration. The dynamics of a model typically include very few relations, with traditional parallel updating. Additions and multiplication can be represented by arithmetic additions and multiplications with manipulation at bit level, allowing more efficient code to be provided. Examples are given in Appendix B of multi-bit (multi-spin) operation and this has been implemented for the dissipative sandpiles discussed in Chapter 3 and program Appendix E. This represents a "cheap" method of incorporating

parallelism into the implementation but is obviously inadequate for very large and very complex systems. Practical limitations on the use of multi-spin coding do not extend beyond its use for fluid hydrodynamics, although surprisingly good results have been achieved for lattice gas simulation, e.g. Wolf-Gladrow and Vogeler (1992). Unfortunately, massively parallel computers are not generally accessible, so that most researchers have to make do with general purpose computers with only one or at most a few processors. It is worth noting that multi-spin coding (instruction-level) is the lowest of four levels of parallelism, according to Kohring (1991). Others include statement level or chaining, loop level (or strip mining) and process level, where this last separates SIMD and MIMD machines and is a feature of many molecular dynamics simulations. Even at multi-spin level, choice of language and availability of machines limits performance and we have briefly discussed these factors in Chapter 3. Performance tests for lattice gas automata in two or three-dimensions, coded in FORTRAN and C with reference to bit operations and integer arithmetic are also reported upon by Wolf-Gladrow and Vogeler (1992).

Clearly, sandpile models, such as those considered here, are of interest, not only in their own right, but in terms of understanding other complex systems with many degrees of freedom. Sandpile automata have proved surprisingly successful in the investigation of intrinsically puzzling phenomenon, such as SOC.

MC methodology provides a level of further abstraction when compared to CA modelling and is a stochastic method which relies on good statistical measurements. Thus, any problem related to the probability of an event occurring can be investigated through MC in theory. Unfortunately, the abstraction of the fundamental problem is not always straightforward, since the more complex the system, the more information is required for accurate statistics. Thus, knowledge of Hamiltonian components is very important in terms of successful simulation, since otherwise systematic errors rapidly become very large. This is illustrated in the froth case, Chapter 5, where for 2D froth, simulations are fairly successful, whereas for the 3D case, choice of parameter values and level of approximations used, crucially affect simulation performance. One way to overcome these difficulties is clearly to perform an extensive sensitivity analysis across a range of

parameters and parameter values, with a view to estimating the amount of variability and bias. Some recent 3D froth work, Weaire and Phelan (1996), provides guidelines on which such an analysis might be based. In general, the algorithm which we have used involves a more complex Hamiltonian than that used for example by Glazier et al (1990) for the Potts model variant. Nevertheless, Potts model simulations which correspond closely to the grain growth problem (see previously this section), have proved successful and suggest that a sensitivity analysis such as that proposed should provide further insight on the importance of the volume component of the Hamiltonian in Eqn(5.1.8).

With the increasing availability of high speed general-purpose computers, many formerly prohibitively complex problems have become tractable by simulation techniques. However, even fast programs running for many hours still do not yield satisfactory results in all respects for problems in complex systems, due to practical limitations of time and number of events to be simulated. So simulation techniques are inevitably limited at some stage by computer hardware and software. The choice of different language and compiler during simulation may be particularly important.

6.3 Cellular systems and Phenomena Exhibited

6.3.1 SOC and Simple Systems

It is known that laws governing the evolution of "universes" are often similar and simple. Nevertheless, behaviour observed can be highly diverse and several new concepts have been proposed to explain and explore these phenomena, such as chaos, SOC and complexity.

A SOC system is a class of nonequilibrium system which seem to be capable of generating complexity of its own accord. Cellular automata as a computational paradigm in computational sandpiles, (described in Chapter 3), have been used to demonstrate self-organised criticality, (SOC). The nature of the constraints, either global or local has been considered for various model dynamics. Many natural phenomena exhibit SOC, including earthquakes, fractals, extinction events in biological evolution, landscape formation and so on. The characterisation of spatio-

temporal processes in general, has received considerable impetus from the investigation of these simple cellular systems, first introduced by Bak et al (1987) In particular, early interest focused on providing an explanation for $1/f$ noise, through the establishment of scaling laws

Different dynamical rules, reflecting deterministic or stochastic perturbation, on both continuous and discrete systems, have been used to demonstrate the existence of SOC in CA and CML models Several universality classes have been shown to exist Models with different dynamics have been found in our work to exhibit SOC for both local and global conservation laws in continuous CML models, whereas SOC is not observed if the conservation law is violated locally in CA models While investigations are limited, they provide a basis for further work, both in stochastic systems and on deterministic systems where the nature of the dissipation is dependent on the local environment and/or choice of loss function While SOC is widely prevalent, it may not provide a universal picture

6.3.2 Cellular Networks

Cellular patterns, such as froth and foams, are similar in many biological systems, although the underlying dynamics of the pattern formation is completely different Soap froths are of interest because they are considered to evolve by a similar mechanism to that which governs grain growth in metals and other materials (see previous section) It is reasonable to assume that the essential mechanism of this evolution, (intercellular diffusion resulting in a reduction of surface energy), governs the behaviour of the soap froth without any significant additional factors It therefore offers us an ideal model system, the study of which provide fundamental insight to the theory of network evolution A typical bubble growth process begins with a nearly ordered configuration and gradually evolves into a completely disordered pattern with time-invariant topological distributions The studies of froth, in particular, provide an elegant illustration of the evolutionary behaviour of a cellular network Much of the work presented here has concentrated on the problem of the 2D soap froth, where interest has focused in particular on numerical studies of the froth structure and evolution under various levels of order/disorder or defect concentration

Direct simulation methods have proved particularly valuable in terms of obtaining detailed information on changes in the network, although are inevitably limited as to size of system studied. Results on abstraction of the problem, or modelling it indirectly via MC methods have been mixed. In the 2D case, the network information obtained has been useful although system sizes have not been sensibly extended. In 3D, results have been disappointing. In part, this is due to the level of detail retained and in part due to a weaker theoretical background for 3D networks in general. Nevertheless, a prototypical implementation has been achieved, (see programmes, Appendix E), and provides some basis for extension to other network systems, such as the metallic grain growth problem, e.g. Holm et al (1991)

6.3.3 Common Features

We have discussed properties of two different types of cellular-structure models. From the analysis and detailed discussions, it is clear that these systems share some common characteristics. Both are e.g. non-equilibrium systems, which evolve according to internal or external forces. Nevertheless, distinctive differences exist, not least in the level of interaction considered, and consequently, give rise to diverse behaviour. Much of the work here has been concerned with dissipative effects and their influence on the evolution of these many-cell systems having different spatial dependence. It is conjectured that a dissipative system keeps its structure at the expense of energy flowing, either from the local dynamics rule, or from the open boundary, or both. Further, the new structure can possess either coherent or chaotic behaviour i.e. in the long-term, distinctive asymptotic behaviour must occur. One obvious and immediate question arising from the work so far is thus whether SOC can occur in cellular networks? Some early studies on froth rheology have conjectured the existence of SOC on avalanching in froth under stress, Hutzler et al (1995)

Other network models apart from soap froth, also appear to exhibit SOC. For example, considering domain wall motion in disordered ferromagnets driven by an external field, Bak and Flyvbjerg (1991) have presented a random neighbour

model, representing domains in a 2D film, where motion exhibits SOC. Tadic (1996) has also discussed statistical and scaling properties in Barkhausen noise in 2D ferromagnets.

6.4 Suggestions for Future Work

For the sandpile automaton (discussed in Chapter 3), it is relatively easy to incorporate additional features by extending the number of states or changing the dynamics rules, but clearly to be useful these must relate to some class of physical or other systems, i.e. have a real-world application or alternatively, seek to explore the computational mechanics of the CA models and the efficiency of the algorithm. Our studies represent a modest step in exploring these, by incorporating continuous variable selection corresponding to the CML models. These have application to systems with continuous loss function and are further extendable in a number of ways not least in the context of the immunological CA models mentioned in the Section 6.2, where incubation period and progression of disease may be more appropriately represented by sampling from known lifetime distributions, such as the Weibull, Ruskin (1993).

Suggestions for further consideration on the studies of dissipative sandpile models, therefore, include choice of alternative functions to represent the energy loss in dissipative CA and CML models. In addition, different specifications of the board should be considered in order to simulate "sinks" in the environment, i.e. dissipation holes or wells, (Section 3.3.3). These should be considered at different concentrations of holes p on the board and for random and clustered concentrations, (reminiscent of the "seeded" defects for the froth case). This would provide some insight on how global behaviour of the system is affected during both in the short and long term.

Better understanding of SOC systems and their behaviour may help us to explore general principles of complex system dynamics. The physical interaction processes are varied, so that they cannot be ascribed to any single mechanism or force. Instead, there seems to be some underlying "logical dynamics" in charge of the interrelationship of the degree of freedom of the system. Some effort has been made here to examine scaling behaviour in both space and time in an extended

system. The simplest model systems which show power law behaviour can be further elaborated to have more complex internal states, inhomogeneous updated rules, adaptive rules and unfixed spatial coordinated memory or non-local interactions. Many of these find parallels in real-world applications, such as formation of landscapes, Bak (1996)

A clear understanding of the general connection between stationarity and criticality in spatially extended dynamical systems is still lacking, although SOC may provide a partial explanation. However, SOC, as an indicator of $1/f$ noise may be applicable only to certain system classes as noted in Chapter 3. Similarly, network "noise" or topological change provides an interesting basis for further study of complexity via simulation tools. The robustness or otherwise of such features and their accessibility to computer modelling opens up many challenging problems for the future. A current major area is the development of more efficient and sophisticated software to model the structure of solid foams and relate this to the physical properties. The Brakke software, discussed by Weaire and Phelan (1994) has recently been used to look at the modelling of minimal surfaces in this context.

Further work can also be done in the 2D froth case, including e.g. an examination of the computational implications for extending the direct simulation of dry froth to wet froth, investigating the influence of control parameters during evolution, e.g. temperature and stress following the early work of Tam and Szeto (1996). Also, there are sound grounds for examining the indirect approach via MC in more detail, in particular by considering a sensitivity analysis in 2D and 3D of the principal parameters, as indicated earlier in this chapter. Adaptation of the code for analogous 2D problems should also be considered. Of course, 3D froth is currently a "hot topic" and some progress has been made on solid and wet foams, Duran (1995). However, it is clear that the simulation challenge alone is a fascinating one, even before further useful results can be obtained on the statistical and physical properties. In the short term, specific programs developed to investigate froth by MC methods, can hopefully be used to establish the viability of alternative simulation approaches in terms of obtaining reasonable parameter estimates for real froth and analogous cellular networks. Extended work on the 3D froth model is clearly indicated, using 2D as a blueprint to the stability of the approach. Further

comparisons with performance by direct modelling are also required together with implications for parallelism and limitations of the statistics

1
2

3
4

5
6

References

Aboav D A , (1980) *Metallography*, 13, 43-58

Ali, A A (1995) *Phys Rev E*, 52, R4595-4598

Allen M D and Tildesley D J (1990), *Computer Simulation of Liquids*, Oxford Science Publications

Anderson M P , Grest G S and Srolovitz D J (1989), *Phil Mag B*, 59, 293-329

Aste T Boose D and Rivier N (1996), *Phys Rev E*, 53, 6181-6191

Aste T , Szeto K Y and Tam W Y (1996), *Phys Rev E*, 54, 5482-5492

Aste T and Rivier N (1997), *J Shape Modelling*, accepted

Atkinson H V (1988), *Act Met* 36, 469-491

Aveyard R (1995), *J Chem Soc Faraday Trans* , 91, 175-180

Bak P , Tang C and Wiesenfeld K (1987), *Phys Rev Lett* , 59, 381-384

Bak P , Tang C and Wiesenfeld K (1988), *Phys Rev A*, 38, 364-374

Bak P (1994), *Santa Fe Institute Studies in the Sciences of Complexity*, Proc Vol XIX , 477-495, Addison-Wesley

Bak P (1996), *How Nature Works, the Science of Self-Organized Criticality*, Springer-Verlag

Baker G L and Gollub J P (1996), *Chaotic Dynamics An Introduction*, 2nd Edition,

Cambridge University Press

Ball G , and Guertin P (1992), *Int J Wildland Fire*, 2, 47-56

Baxter R J (1982), *Exactly Solved Models in Statistical Mechanics*, Academic Press

Bennett W R (1976), *Scientific and Engineering Problem-Solving with the Computer*,
Prentice Hall

Berkeley G A (1985), *Simulation*, 29, 161-164

Berlekamp E , Conway J H and Guy R (1982), *Winning Ways for Your
Mathematical Plays*, Vol 2, Academic Press

Binder K (1986), *Monte Carlo Methods in Statistical Physics*, 2nd Edition, Springer
Verlag

Binder K (1992), Editor, *The Monte Carlo Method in Condensed Matter Physics*,
Springer Verlag

Blackman J A and Taguena J (1991), *Conf on Disorder in Condensed Matter Physics*
(1989), Oxford, Clarendon

Boots B N. (1982), *Metallography*, 15, 53-62

Brakke K (1992), *Exp Math* 1, 141-165

Brakke K (1995), *Surface Evolver Manual*

Bratley P , Fox B L and Schrage L E (1987), *A guild to Simulation*, 2nd Edition
Springer-Verlag

- Bulkley S R (1693), Phil Trans Roy Soc London, 17, 708-711
- Burks A W (1966), Editor's introduction, in von Neumann (1966)
- Christensen K , Olami Z and Bak P (1992), Phys Rev Lett , 68, 2417-2421
- Christensen K and Olami Z (1993), Phys Rev E, 48, 3361- 3365
- Ciccotti G , Frenkel D , and McDonald I R (1987), eds , Simulation of Liquids and Solids, North-Holland, Amsterdam
- Ciccotti G and Hoover W G (1986), Molecular Dynamics Simulation of Statistical Mechanical Systems, North-Holland, Amsterdam
- Crandall R E (1996), Topics in Advanced Scientific Computation, Springer Telos
- Crandall R E (1994), Projects in Scientific Computing, Springer Telos
- Dana J E (1992), ACM SIGPLAN Notices, 27, 99-106
- De Icaza-Herrera M and Castano V M (1995), Physica A, 217, 140-145
- De Oliverira P M C (1990), Computing Boolean Statistical Models, World Scientific
- Decker J F and Johnson G M (1993), Computational Science an assessment and projection, proceedings of 2nd International Conf on Computational Physics, Beijing Sept 1993, World Scientific
- Derrida B , de Oliverira P M C and Stauffer D (1996), Physica A, 224, 604-612
- DeVries P L (1994), A First Course in Computational Physics, John Wiley

- Dhar D and Ramaswamy R (1989), *Phys Rev Lett* , 63, 1659-1662
- Diaz-Guilera A (1992), *Phys Rev A*, 45, 8551-8558
- Ding E J , Lu Y N and Ouyang H F (1992), *Phys Rev A*, 46, 6136-6139
- Dormer K J (1980), *Fundamental Tissue Geometry for Biologists*, Cambridge University Press
- Drossel B and Schwabl F (1992), *Phys Rev Lett* , 69,1629-1632
- Duarte J A M S , Carvalho J M and Ruskin H J (1992), *Physica A*, 1983, 411- 421
- Fishwick P A (1995), *IEEE Potentials*, 15, 24-27
- Forrest S (1990), *Physica D*, 42,1-11
- Fradkov V E , Glicksman M E , Palmer M , Nordberg J and Rajan K (1993), *Physica D*, 50-60
- Frankel D and Smit B (1996), *Understanding Molecular Simulation*, Academic Press
- Frette V (1993), *Phys Rev Lett* , 70, 2762-2765
- Frost H J , Thompson C V , Howe C H and Wang J (1988) *Scripta Met* , 22, 65-70
- Gaylord R J and Wellin P R (1995), *Computer Simulations with Mathematica Explorations in Complex Physical and Biological Systems*, Springer-Verlag
- Gaylord R J , Kamin S N , and Wellin P R (1996), *Programming with Mathematica*, second edition, Springer-Verlag

- Gibbs W (1994), *Computation in Modern Physics*, World Scientific
- Giordano N (1997), *Computational Physics*, Prentice Hall
- Glazier J A , Gross S P and Stavans J (1987), *Phys Rev A*, 36, 306-312
- Glazier J A and Stavans J (1989) *Phys Rev A*, 40, 7398-7401
- Glazier J A , Anderson M P and Grest G S (1990), *Phil Mag B* 62, 615-645
- Glazier J A and Weaire D (1992), *J Phys Condens Matter*, 4, 1867-1894
- Glazier J A (1993), *Phys Rev Lett* , 70, 2170-2174
- Gould H and Tobochnik J (1996), *Introduction to Computer Simulation Methods*, second edition, Addison-Wesley
- Grassberger P and Manna S S (1990) *J Phys (Paris)* 51,1077
- Grassberger P (1994), *Phys Rev E*, 49, 2436-2444
- Grinstein G , Lee D H , and Sachdev S (1990), *Phys Rev Lett* , 64, 1927-1930
- Gutowitz H A (1990) *Cellular Automata*, Cambridge, MA MIT Press
- Haile J M (1992), *Molecular Dynamics Simulation Elementary Methods*, John Wiley
- Hasegawa M and Tanemura M (1976), *Ann Inst Stat Math* , 28, 509-519
- Heermann D W and Burkitt A N (1991), *Parallel Algorithms in Computational Science*, Springer-Verlag

Heermann D W (1990), Computer Simulation Methods in Theoretical Physics, 2nd Edition, Springer-Verlag

Hegarty D F , Kechadi M T and Dawson K A (1996) Proceeding of Conference on Scientific Computing in Europe Sept 1996, Dublin

Held G A and Solina D H (1990), Phys Rev Lett , 65, 1120-1123

Herdtle T and Aref H (1992), J Fluid Mech , 241, 233-260

Holm E A , Glazier J A, Srolovitz D J , and Grest G S (1991), Phys Rev A, 43, 2622-2668

Hoover W G (1983), Ann Rev Phys Chem , 34, 103-127

Hoover W G (1991), Computational Statistical Mechanics, Elsevier, Amsterdam.

Hu Y , Ludecke D and Prausnitz J (1984), J Fluid Phase Equilibria, 17, 217-225

Hutzler S , Weaire D and Bolton F (1995), Phil Mag B, 71, 277-289

Ivzhkevich E V (1996), Phys Rev Lett , 76, 3368-3343

Hammersley J M and Handscomb D C (1964), Monte Carlo Methods, John Wiley

Jain S (1992), Monte Carlo Simulations of Disordered Systems, World Scientific

Jiang Y , Mombach J C M and Glazier J A (1995), Phys Rev E 52, R3333-3338

Jong M L D (1991), Introduction to Computational Physics, Addison-Wesley

- Kalos M H and Whitlock P A (1986), Monte Carlo Methods, John Wiley
- Kaneko K (1989), Physica D, 34, 1-41
- Kaplan D and Glass L (1995), Understanding Nonlinear Dynamics, Springer-Verlag
- Kawasaki K, Nagai T and Nakashima K (1989), Phil Mag B, 60, 399-421
- Kelvin L (1887), Philos Mag 24, 503-515
- Kermode J P and Weaire D (1990), Comp Phys Commun, 60, 75-109
- Kohring G A (1990), Inter J of Mod Phys C, 1, 259-277
- Kohring G A (1991), Inter J of Mod Phys C, 2, 755-772
- Koonin S E (1986), Computational Physics, Addison-Wesley
- Koonin S E and Meredith D C (1990), Computational Physics, Addison-Wesley
- Kraynik A M and Reinelt D A (1996), J Coll Int Sci, 181, 511-520
- Landau D (1994), Physica A, 205, 41-64
- Langton C G (1984), Physica D, 10, 135-144
- Langton C G (1990), Physica D, 42, 12-27
- Levitan B (1994), Phys Rev Lett, 72, 4057-4061
- Levitan B and Domany E (1995), Europhys Lett 32, 543-548

Levitan B and Domany E (1996), *Phy Rev E*, 54, 2766-2772

Levitan B and Domany E , *Cond-mat/9702061*

Lewis F T (1925), "A further study of the polyhedral shape of cells" *Proc A A A S*
61, 1-34

Lewis F T (1928), *Anat Rec* , 38, 341-362

Lewis F T (1931), *Anat Rec* , 50, 235-265

Mandelbrot B B (1969), *Int Econ Rev* , 10, 82-111

Manna S S (1990), *J Stat Phys* , 59, 509-517

Manna S S (1991), *Physica A*, 179, 249-268

Manna S S , Kiss L B , and Kertesz J (1990), *J Stat Phys* , 61, 923

Manneville P Boccara N Vichniac G Y and Bidaux R (1989), *Cellular Automata and
Modelling of Complex Physical Systems*, Springer-Verlag

Mehta A and Baker G C (1990), *Rep Prog Phys* , 57, 383-417

Merrill J R (1976), *Using Computers in Physics*, Houghton Mifflin

Metropolis N , Rosenbluth A W , Rosenbluth M N , Teller A H and Teller E (1953),
J Chem Phys , 21, 1087-1092

Middleton A A and Tao C (1995) *Phys Rev Lett* 74, 742-

Mitchell M , Crutchfield J.P and Hraber P T (1994), *Physica D*, 75, 361-391

Mitchell M , Crutchfield J P and Das R (1996), Proceedings of the First Inter Conf on Evolutionary Computation and its Applications, Moscow, Russia, Russia Academy of Science

Nagai T , Ohta S , Kawasaki K and Okuzono T (1990) Phase Trans 28, 177-211

Nagel K and Herrmann H J , (1993), Physica A, 199, 254

Nakanishi H (1990), Phys Rev A, 41, 7086-7093

Naylor J E (1976), Ann Math , 103, 489-539

Nordahl M G (1995), Complex System, 3, 63-78

Okuzono T and Kawasaki K (1995), Phys Rev E, 51, 1246-1253

Olam Z and Christensen K (1992), Phys Rev A, 46, R1720-1723

Olam Z , Feder H and Christensen K (1992), Phys Rev Lett 68, 1244-1250

Mouritsen O G (1984), Computer Studies of Phase Transitions and Critical Phenomena, Springer Verlag

Pietronero L , Tartaglia P , and Zhang Y C (1991), Physica A, 173, 22-

Poundstone W (1985), The Recursive Universe Cosmic Complexity and the Limits of Scientific Knowledge, New York

Puhl H (1992), Physica A, 182, 295-319

Rapaport D (1996), The Art of Molecular Dynamics Simulation, Cambridge

University Press

Rivier N and Lissowski A (1982), J Phys A , 15, L143-148

Rivier N (1985), Phil Mag B, 52, 795-819

Rivier N (1994), Phil Mag Lett 69, 297-303

Rosendahl J , Vekic M and Kelley J (1993), Phys Rev E, 47, 1401-1404

Ruskin H J (1993), J Stat Phys , 73, 389-397

Ruskin H J and Feng Y (1995), J Phys Condens Matter, 7, L553-559

Ruskin H J and Feng Y (1996), Physica A, 230, 455-466

Ruskin H J and Feng Y (1997), Physica A, accepted

Ruskin H J and Feng Y (1997), submitted

Samuel Foley (1694), Phil Trans Roy Soc London, 18, 169-182

Segel D , Mukamel D Krichevsky O and Stavans J (1993), Phys Rev E, 47, 812-819

Smith C S (1952), Metal Interfaces, American Society for Metals Cleveland, 65-108

Smith C S (1954), Sci American, 190, 58-64

Socolar J E S and Grinstein G (1993), Phys Rev E, 47, 2366-2376

Stanley H E and Ostrowsky N (1986), Random Fluctuations and Pattern Growth

Experimental and Models, Kluwer

Stauffer D (1991), *Comp in Phys* Jan/Feb, 62-67

Stauffer D (1991), *J Phys A Math Gen*, 24, 909-927

Stauffer D (1993), *Computer Simulation and Computer Algebra Lectures for Beginners*, Springer-Verlag

Stauffer D , Hehl W, Winkelmann V and Zabolitzky G (1988), *Computer Simulation and Computer Algebra*, Springer-Verlag

Stauffer D and Pandey R (1992), *Computer in Phys* 6, 404-410

Stavans J (1993), *Rep Prog Phys* , 56, 733-789

Stavans J and Glazier J A (1989), *Phys Rev Lett* , 62, 1318-1321

Strocka B , Duarte J A M S and Schreckenberg M (1995), *J Phys I France*, 5, 1233-1238

Tadic B , Nowak U , Usadel K D , Ramaswamy R and Padlewski S (1992), *Phys Rev A* 45, 8536-8555

Takayasu H , Miura H , Hirabayashi T and K Hamada (1992), *Physica A*, 184,127-144

Tam W Y and Szeto K Y (1996), *Phys Rev E*, 53, 877-890

Tam W Y , Zeitak R , Szeto K Y and Stavans J (1997), *Phys Rev Lett* , 78, 1588-

Thompson D (1942), *On Growth and Form*, 2nd Edition, Cambridge University Press

Toffler A (1984), *Science and Change, Forward to Order out of Chaos*, New York

Toffoli T and Margolus N (1987), *Cellular Automata Machines A New Environment for Modelling*, the MIT press

Vesely F J (1994), *Computational Physics*, Plenum Press

Von Neumann J (1952), "discussion" in *Metal Interfaces*, American Society for Metals, Cleveland, 108-110

Von Neumann J (1966), *Theory of Self-Reproducing Automata*, University of Illinois Press

Wagner H M (1975), *principles of Operations Research*, Prentice-Hall

Waldrop M (1992), *Complexity The Emerging Science at the Edge of Order and Chaos*, New York

Weaire D and Kermode J P (1983a), *Phil Mag B*, 47, L29-31

Weaire D and Kermode J P (1983b), *Phil Mag B*, 48, 245-259

Weaire D and Kermode J P (1984), *Phil Mag B*, 50, 379-395

Weaire D and Rivier N (1984), *Contemp Phys*, 25, 59-99

Weaire D and Lei H (1990), *Phil Mag Lett*, 62, 427-430

Weaire and Glazier (1993), *Phil Mag Lett*, 68, 363-365

Weaire D (1994), *Phil Mag Lett*, 69, 99-105

Weaire D and Fortes M A (1994), *Advances in Phys* 43, 685-721

Weaire D and Phelan R (1994), *Phil Mag Lett* 69, 107-110

Weaire D and McMurry S (1996), *Solid State Phys* , 50, 1

Weaire D and Phelan R (1996), *Phil Tran R Soc Lond A*, 354, 1989-1997

Wejchert J , Weaire D and Kermode J P (1986), *Phil Mag B*, 53, 15-24

Wilson K G (1986), *Basic Issues of Computational Science*, Trieste

Wilson K G (1987), *Grand Challenges in Computational Science*, Cornell Univ Press

Wolf D and Vogele A (1992), *Inter J of Mod Phys* , 3, 1179-1187

Wolfram S (1983), *Statistical Mechanics of Cellular Automata*, *Rev of Mod Phys* 55, 601-644

Wolfram S (1984), *Nature*, 311, 419-424

Wolfram S (1986), *Theory and Applications of Cellular Automata*, World Scientific

Wolf-Gladrow D and Vogeler A (1992), *Int J Mod Phys C* 3, 1179-1187

Wong S S M (1992), *Computational Methods in Physics and Engineering*, Prentice Hall

Zapperi S , Lauritsen K B , and Stanley H E , (1995), *Phys Rev Lett* , 75, 4071

Zhang Y C (1989), *Phys Rev Lett* , 63, 470-473

Appendix A
Published Papers

LETTER TO THE EDITOR

The evolution of a two-dimensional soap froth with a single defect

H I Ruskin and Y Feng

School of Computer Applications, Dublin City University, Dublin 9, Ireland

Received 13 September 1995

Abstract. Using the direct simulation method of Weaire and Kermode, we consider the problem raised by Levitan of a 2-D froth with a single defect. We have found that for a single defect in an ideal hexagonal network, the second moment μ_2 of the distribution of the number of cell sides for the region of the defect does not tend to a constant as claimed by Levitan. Some reasons for the varying conclusions drawn by different authors about this problem are also discussed.

The soap froth as an ideal model of a cellular network has attracted considerable attention and has been studied theoretically and experimentally in recent years (see Weaire and Rivier (1984), Glazier *et al.* (1987), Weaire and Lee (1990), Glazier and Weaire (1992), Herdite and Aicl (1992), etc.). Interest has primarily focused on scaling properties obtained through the evolution of the froth with time. Long term behaviour is characterized by system statistics such as the distribution $f(n)$ of the number of cell sides and the second moment of this distribution $\mu_2 = \sum (n-6) f(n)$. There is considerable experimental, theoretical and computational evidence that μ_2 tends to a finite limit (approximately 1.4) which is characteristic of the asymptotic scaling state of the froth.

The initially transient behaviour of a relatively ordered froth has been interpreted in terms of the growth of individual topological defects. The study of this growth has been taken up by Levitan (1994) who considered the insertion of a single local topological defect into a froth of hexagonal cells. He used an approximation which is attractive in that it offers the potential to simulate larger (closer to asymptotic) systems, but results obtained were in disagreement with previous tentative conclusions (Weaire in Blackman and Taguena 1991). We have therefore re-examined this problem by direct simulations which are more extensive than those previously undertaken.

Levitan's method first forces a T1 topological process (neighbour switching) to take place in a group of cells and follows this with a T2 process (cell elimination) for which the probabilities of a triangle, square and pentagon being formed are the same. In fact the first T1 process gives rise to two five sided cells and two seven sided cells in the network (figure 1). Levitan used a mean field theory to show that the topological distribution associated with a single defect approaches a fixed asymptotic form with a high peak $f(6) \approx 0.6$. This implies that μ_2 attains a *difficult* and *stable* value in conflict with previous predictions.

Using the direct simulation approach of Weaire and Kermode (1983b, 1984) and subsequent work, we have implemented a 2-D dry froth with a single topological defect based on a perfect hexagonal network to ensure correspondence with Levitan's original construction. The defect is based on a symmetrical arrangement of two pairs of pentagonal

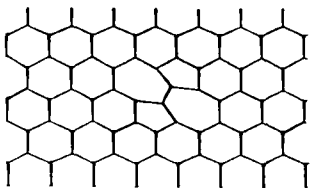


Figure 1 The defective 2-D froth network corresponding to Levitt's method of inserting a single hexagonal defect by forcing a FI process in an ideal hexagonal froth

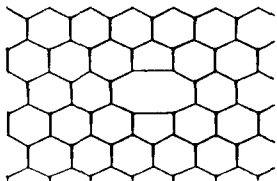


Figure 2 A defective 2-D froth network. The network keeps the hexagonal basis and all the non-defective cells are of the same shape and size

and heptagonal cells with minor discrepancies in the areas of the component cells and with all hexagonal cells surrounding the defect having the same area (figure 1). Additionally we consider another type of topological defect where the distortion is achieved by suppressing an edge in the original network giving an eight-sided cell with two symmetrical five-sided cells amongst its nearest neighbours (figure 2). We have also used an *ordered* Voronoi construction to create a third kind of defect (figure 3) in which the areas of the defect and its neighbouring cells have been adjusted as shown. Periodic boundary conditions are used but for convenience the defective cell is centrally placed in the network. Calculations are not pursued beyond the stage where the defect impacts on the boundary.

We have implemented the froth with single defects as shown (figures 1, 2, and 3) for systems of 100, 400 and 900 cells respectively. We give details of the results for a system of 400 cells as an example. Similar results are found for all system sizes used.

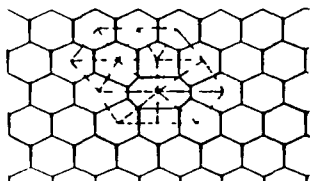


Figure 3 A defective 2-D froth network with an ordered Voronoi set up. (Each vertex of an eight-sided cell and two five-sided cells is a centre of a circumscribed circle that corresponds to the Delaunay cellulation.)

If we define an approximately circular front of disturbance surrounding the large defective cell and including cells which have undergone a single topological change, the circular front will include these (plus other cells which impinge on the circle in part but which have not yet undergone change). Levitt (1994) similarly defines a cluster which refers to the front used in our simulations plus a boundary of hexagonal cells. The slight

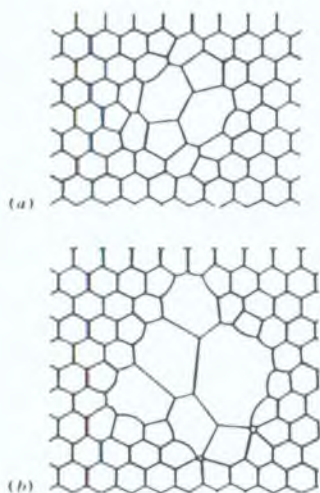


Figure 4. The evolution of a froth with a single defect in a hexagonal network with numbers of time steps of (a) 40 and (b) 100 (Initial structure figure 1)

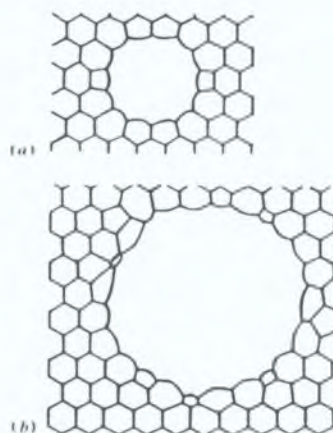


Figure 5. The evolution of a froth with a single defect in a hexagonal network with numbers of time steps of (a) 40 and (b) 100 (Initial structure figure 2)

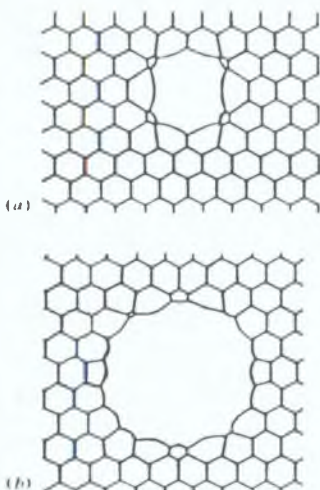


Figure 6. The evolution of a froth with a single defect in a hexagonal network with numbers of time steps of (a) 40 and (b) 100 respectively (Initial structure figure 3)

modification we have used does not affect the behaviour of μ_2 or the side distribution, but enables us to consider separately μ_2 in the front. Figures 4-6 show the evolution within the front at specific time steps for different initial defect types, corresponding to figures 1, 2, and 3 respectively. Here the number of time steps relates to the number of diffusion and equilibration processes which have taken place, with the evolution time, T , measured in units of $\langle A_0 \rangle / K$, where $\langle A_0 \rangle$ is the initial average area over all cells, and K is the constant

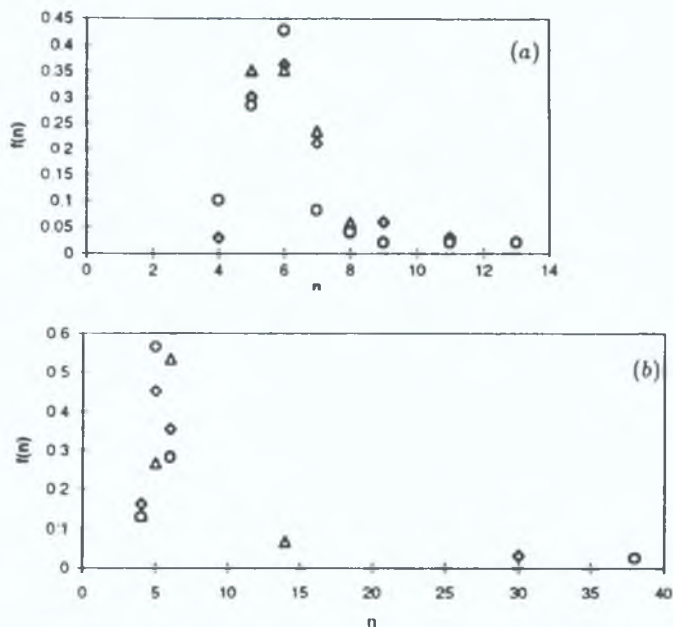


Figure 7. (a) and (b) show the topological distribution $f(n)$ in the front with numbers of time steps of 60 (\circ), 120 (\triangle), and 160 (\square) (Initial set up figures 1 and 2 respectively)

in Von Neumann's law, and may be arbitrarily chosen (Kermode and Weaire 1990). We can see that the number of sides of the large defective cell increases with time, as does the perturbation front area of the disturbance. For the defect formed by edge suppression, starting from the ordered non-Voronoi network set-up (figure 2) and ordered Voronoi network (figure 3), we have observed very similar behaviour in the froth evolution (figures 5 and 6). We give detailed results for the initial structure shown in figures 1 and 2 as follows.

The topological distribution $f(n)$ inside the front, is shown in figures 7(a) and 7(b), at specific numbers of time steps for the different defect topologies (figures 1 and 2 respectively). We find that there tends to be a peak at $n = 5$ in the front as evolution time increases, as opposed to the overall network of a normal froth which has a peak with $n = 5$ and $n = 6$ (Hertle and Aref 1992). However, the distribution $f(n)$ is now, of course, markedly right-skewed. These features are not extraordinary as movement of the front results in continual incrementation of the number of sides of the large defective cell.

From our results, the second moment, μ_2 , continues to change with time without reaching a fixed limit. Figures 8(a) and 8(b) show how the second moment, μ_2 , in the overall network changes versus time, T (for initial set-ups in figures 1 and 2). The range of T includes about 200 diffusion and equilibration processes in our simulation. Topological and diffusive adjustments are made sequentially within each time step and considerable details of the evolution may be observed. Fluctuations in the value of μ_2 around the underlying trend can be explained directly in terms of the T1 and T2 processes, with a high μ_2 corresponding to the defect surrounded by a number of three- or four-sided cells, and

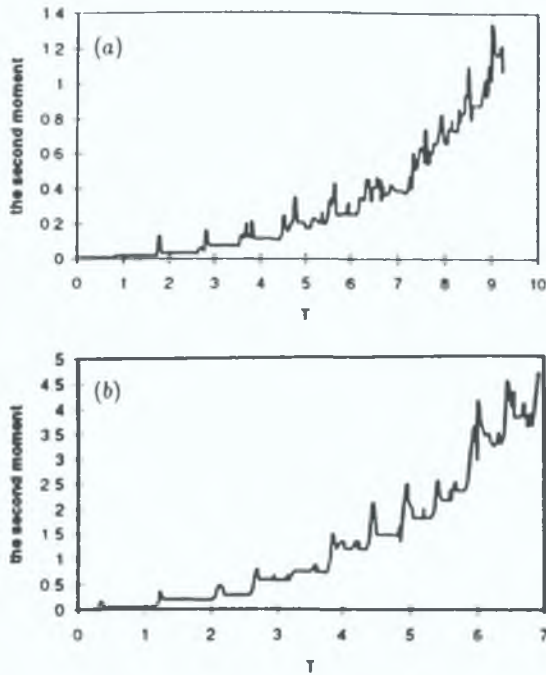


Figure 8. (a) and (b) show μ_2 in the overall network versus time T for a froth of 400 cells (Initial set up figures 1 and 2 respectively)

a sudden decrease in μ_2 associated with the disappearance of one of these cells. During growth in the area of the defect, μ_2 keeps a relatively stable value until the next TI occurs. Clearly, as more cells are involved in the evolution and the number of sides of the defect increases, the value of μ_2 overall changes more rapidly and is dominated by the contribution of the defective cell. Over the whole range of T , $\mu_2 \sim T^\beta$ appears to describe the observed behaviour, with $\beta > 1$. However, few changes take place initially, relative to the evolution as a whole, and for the upper range of T , μ_2 versus T is roughly linear, although it is not clear that a true asymptote is attained.

For a simple theoretical model of a large defect with N sides surrounded by N small cells, newly converted side lengths of the small cells will be characteristic of the whole network, i.e. $N \sim A(d)^{0.5}$, with $A(d)$ the area of the defect. Then, in the asymptotic limit, Von Neumann's law becomes $dA(d)/dt = kA(d)^{0.5}$, i.e. $A(d) \sim T^2$. Similarly, in the front, the topological distribution will be dominated by the defect, so $\mu_2(d) \sim N^2$ with $N \sim T$, i.e. $\mu_2(d) \sim T^2$. Furthermore, the defect gradually involves more and more cells in the overall network, so asymptotically the exponents for the front and the overall network should be the same. From our simulations, we find for the defect that $A(d)$ increases with T at the expense of other cells distorted by topological changes. If we define the increased area $\Delta A(d) = A(d) - A(d)_0$, where $A(d)_0$ is the original area of the defect, for the defect formed by edge suppression (figures 2 and 3), we obtain roughly $\Delta A(d) \sim T^2$ after the initial period of evolution, with the radius of the rough perturbation circle, $r \sim T$

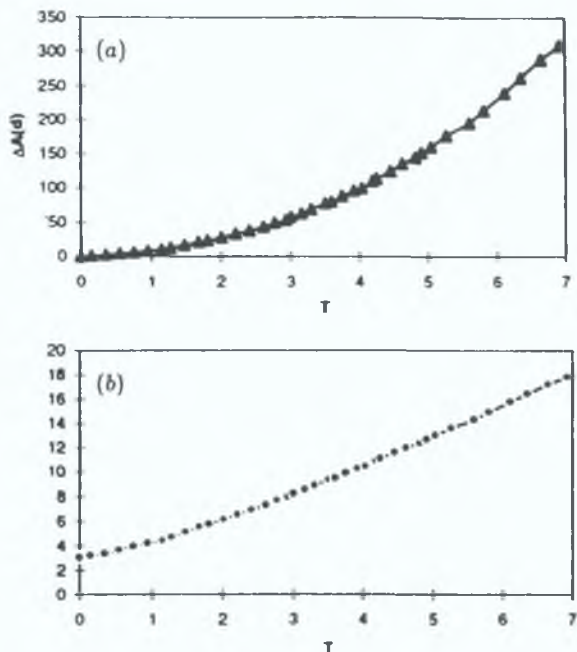


Figure 9. (a) The increase in defective area $\Delta A(d)$ versus time, T . (b) The radius r versus time, T , for a froth of 400 cells. (Initial structure figure 2)

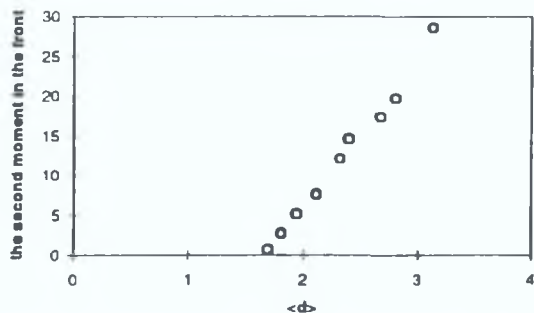


Figure 10. $\mu_2(d)$ in the front versus the average intercept, $\langle d \rangle$. (Initial structure figure 2)

approximately; figures 9(a) and 9(b) illustrate for the set-up of figure 2. Furthermore, we find that $\mu_2(d)$ changes roughly linearly with the average intercept, $\langle d \rangle$, where $\langle d \rangle$ equals the square root of the average cell area in the front (figure 10).

It seems clear that the behaviour of a froth with a single defect in a uniform hexagonal network does *not* lead to a normal scaling state as found for the non-defective froth by

numerical simulation (and as predicted by theory). We find that $f(n)$ in the front tends to develop a long tail extending to large values of n and with a peak at $n = 5$. This is in agreement with Aboav (1980) who also quoted $\alpha = 2$ for the area growth exponent. However, the suggestion that μ_2 overall varies linearly with time (see the comment by Weaire and Kermode (1983a) on Aboav's work) is not wholly supported by our findings and is in conflict with the predictions of the simple model. It is only with hindsight that it has been realized that Aboav was dealing with a transient system with defects characterized by different values of the growth exponents. Our own results are probably not in the asymptotic region since the maximum number of sides achieved by any defect is $N = 44$ (for the set up in figure 2). Nevertheless, they are supported by recent work by Glazier (1995). We also find that there is some similarity between the behaviour of our system and that of Levitan (1994) but we do not agree with a fixed form for $f(n)$ as obtained by Levitan. The value of μ_2 (whether for the front or for the overall network) does not reach a steady state after initial fluctuations at this system size, unlike normal froth evolution.

Our results for the behaviour of the front are in agreement with the original experimental work of Aboav (1980) and recent simulations of Glazier (1995) indicating that a different scaling relation applies there. Regardless of the defect type and initial configuration, there are some grounds for support of the suggested system behaviour put forward by Levitan (1994) but the overall results are in conflict with his predictions for the quantities characterizing the long term evolution.

We should like to thank Professor Denis Weaire for several interesting discussions and for introducing us to the froth problem.

References

- Aboav D A 1980 *Metallography* **13** 43-58
 Blackman J A and Taguena J 1991 *Conf. on Disorder in Condensed Matter Physics (1990)* (Oxford: Clarendon)
 Glazier J A 1995 *Phys. Rev. Lett.* submitted (private communication)
 Glazier J A, Gross S P and Stevens J 1987 *Phys. Rev. A* **36** 306-12
 Glazier J A and Weaire D 1992 *J. Phys.: Condens. Matter* **4** 1867-94
 Herdite T and Arif H 1992 *J. Fluid Mech.* **241** 233-60
 Kermode J P and Weaire D 1990 *Comput. Phys. Commun.* **60** 75-109
 Levitan B 1994 *Phys. Rev. Lett.* **72** 4057-61
 Weaire D and Kermode J P 1983a *Phil. Mag.* **B 47** 129-31
 ——— 1983b *Phil. Mag.* **B 48** 245-59
 ——— 1984 *Phil. Mag.* **B 50** 379-95
 Weaire D and Lei H 1990 *Phil. Mag. Lett.* **62** 277-30
 Weaire D and Rivier N 1984 *Contemp. Phys.* **25** 59-99

Scaling properties for ordered/disordered 2-D dry froths

H.J. Ruskin*, Y. Feng

School of Computer Applications, Dublin City University, Dublin 9, Ireland

Received 15 February 1996

Abstract

We investigate the evolutionary behaviour of a 2-D dry froth with initial ordered/disordered conditions corresponding respectively to monodisperse/polydisperse topological networks. Using the direct simulation approach we discuss the scaling properties of the cell size distribution $f(n)$ and its second moment μ_2 for various system sizes and initial structures. For the case of a highly ordered network the introduction of disorder may be viewed in terms of 'seeding' the froth system with a number of defects d where for $d < 1$ previous work has shown that stable conditions are not achieved. We find that the limiting behaviour here depends on the amount of disorder where this is quantified by the proportion of non-uniform initial cells and the pattern of seeding. Our findings support the view that a quasi-scaling state exists for the highly ordered froth in contrast to the universal scaling state of the disordered and low ordered froth. In the light of these results we briefly reconsider the question of transience for the early results of Aboav (1980).

1. Introduction

Materials with cellular structure appear in many guises in fields of geology, metallurgy, biology and so on. The soap froth as an ideal model of a cellular network has attracted considerable attention providing valuable insight into the behaviour of these complex disordered systems. Original studies of 2-D froth structures are due to Smith [1] and subsequently Aboav [2] and have stimulated much theoretical, experimental and computer simulation work over recent years, e.g. [3-14]. For reviews see [15-18].

*Corresponding author.

A soap froth has all boundaries equivalent with its evolution driven by a transfer of gas between neighbouring bubbles and governed by Von Neumann's law

$$dA/dt = k(n - 6) \quad (1)$$

where A is the area of an n -sided cell and $k > 0$ is a constant. We concentrate on an ideal (or dry) froth with all internal angles of the network equal to 120° and the mean number of sides $\langle n \rangle = 6$ where evolution is through T1 processes (neighbour switching) and T2 processes (cell vanishing). Of interest are the dynamic scaling properties of the system measured by statistics such as the distribution of the number of the cell sides $f(n)$ and its second moment $\mu_2 = \sum f(n)(n - 6)^2$ which is expected to attain a scale invariant value. Other properties such as the correlated side distribution (side distribution of cells next to m -sided cells in the scaling state) also demonstrate universality [13].

On the basis of photographs showing an initial *disordered* froth which evolved from thousands to hundreds of bubbles, Smith [1] suggested that long term asymptotic behaviour was just a change of scale with no change of the side distribution. He also found $\mu_2 \approx 1.5$ after initial transience and the average cell area $\langle A \rangle$ to be dependent on time as $\langle A \rangle \propto t^\gamma$ with the growth exponent $\gamma = 1$. A *different* set of photographs based on an alternative method with initial roughly *uniform* bubbles was analysed by Aboav [2] who found no stable limiting distribution $f(n)$ but $\mu_2 \sim \langle d \rangle$ where $\langle d \rangle \sim \langle l \rangle^2$ is the average linear intercept of all bubbles. Similar experiments have also subsequently been performed for the wet froth [5, 6] and a scaling state achieved ($\mu_2 = 1.4$) irrespective of the amount of ordering described by the initial conditions. Specifically, these authors have suggested that Aboav's findings refer to the froth equilibration period, i.e. that the rapid growth of μ_2 is a transient effect of the early stage of evolution (see also [16, 17]). Aboav also found that the number of sides of an n -sided cell is related to the average number of sides of its neighbours $m(n)$ by $m(n) = (6 - a) + (6a + \mu_2)n$ where a is a constant ($a = 1/2$). This relation is known as Aboav's law [2] or for $a = 1$ the Aboav-Weaire law [15].

Computer simulations of the 2-D dry froth have been performed by a number of authors but initial structures and system sizes have varied considerably [7–14]. Values reported for the second moment were $\mu_2 = 1.42$ and 1.2 respectively for initially disordered froth based on Voronoi structures of size 500 and 1024 cells [12, 14] and while further work generally supports these findings [9, 10, 13] there are some apparent discrepancies. For example, μ_2 vs. time may exhibit a peak before stabilising at a lower value ($\mu_2 = 2.0$) [12] or may approach the asymptote smoothly [14]. Furthermore, a single defect in an otherwise uniform froth network leads to an apparent loss of the normal scaling properties [19–22]. It has also been observed that multiple defects lead to sustained growth in a uniform network with μ_2 reaching a maximum at the final stage of evolution $\mu_2 = 3.45$ [14].

In this paper we consider in more detail the effect of initial conditions on the froth evolution for limited system size. We distinguish especially between systems with

for

local topological dislocations in otherwise uniform networks (monodisperse froths) and those which are intrinsically disordered (polydisperse froths).

1)

2)

2 Order and disorder in a froth

3)

4)

5)

6)

7)

8)

9)

10)

11)

12)

Some confusion appears to exist in the literature as to what is meant by an *ordered* initial condition [2, 6, 12, 14]. Structures may be specified with similar size distribution $f(n)$ and second moment μ_2 but with very different area distributions. Equally, froths with different $f(n)$ may have the same μ_2 . It seems clear that μ_2 alone is insufficient to quantify the degree of disorder and that more specific details of the initial structure are required.

13)

14)

15)

16)

17)

18)

The simplest local *topological dislocation* is defined as a pentagon-heptagon construction in an otherwise hexagonal structure [15] where this construct satisfies Euler's law (see Fig. 1(a)). Alternatively, the dislocation may be formed by forcing a T1 process leading to a paired pentagonal-heptagonal dislocation (Fig. 1(b)). Defining an *ordered* initial froth to be a uniform hexagonal (or monodisperse) network and forcing one or more T1 processes thus systematically increases the amount of seeded disorder present in what is essentially still a regular structure. A *disordered* froth is taken to be a non-uniform (polydisperse) network with random localised topological dislocations which may or may not be of Fig. 1(a) type but are not of Fig. 1(b) type. Voronoi networks (used e.g. in [8, 10, 12, 14]) are in some ways typical of disordered structures and can be constructed by random generation of a set of initial points subject to the condition that these are a certain minimum distance apart.

19)

Froth *reversibility* was discussed by [12, 14] and in mathematical terms involves writing k instead of k in Von Neumann's law (Eq. (1)). Distinction between the so-called *ordered* and *disordered* froths can be made on the basis of this property. In an *ordered* froth the dislocation can be made to disappear through a series of T1

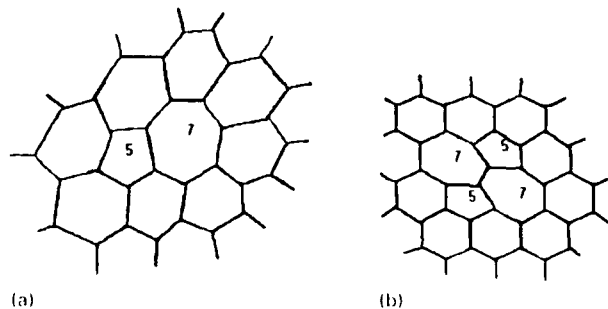


FIG. 1. A topological dislocation (a) with a pentagonal heptagonal dislocation (b) with pentagonal heptagonal cell pair formed by a T1 process.

processes resulting in a final structure which is uniform hexagonal (monodisperse $\mu_2 = 0$). In a *disordered* froth however some topological dislocations *always* exist although their location will change after one or more 11 processes. The froth thus remains a polydisperse network with a minimum value of μ_2 ($\mu_2 = 0$). The irreversibility of a polydisperse froth is implicitly considered in previous work by a number of authors [12–14]. From these definitions of *order* and *disorder* it seems clear that Smith [1] described a highly disordered system whereas Abov [2] investigated one which was highly ordered. Both ordered and disordered initial conditions were considered in [5, 6, 13, 14] whereas disordered systems only were discussed in [12]. Investigations of froth behaviour when a single *defect* (or topological dislocation) is introduced into an otherwise highly ordered network have recently emphasised the importance of the initial structure in achieving stable conditions [19, 21, 22].

In what follows we investigate froth evolution for different initial set-ups and system sizes using direct simulation methods [7, 8]. Information on the froth structure is thus obtained explicitly at each time step during the evolution. Defects which are sparsely seeded in the froth as a whole evolve naturally before impacting on each other after a long period of time. We consider systems of size up to 1600 cells and initial structures which range from highly ordered to highly disordered.

3. Results

From our definition an *ordered* froth is based on the hexagonal network where for any value of n all cells have roughly the same initial area. For a *highly ordered* hexagonal network we have introduced a number of defects: (i) a pair of pentagon–heptagon dislocations ($d = 4$) in a system of size 400 cells ($\mu_2 = 0.05$) and (ii) $d = 7$ in a system of size 900 cells ($\mu_2 \approx 0.03$). For a hexagonal network with *low order* we have introduced (iii) $d = 30$ in a system of 400 cells ($\mu_2 = 0.3$) and (iv) $d = 60$ in a system of 900 cells ($\mu_2 \approx 0.27$). Similar behaviour is observed for examples (i) and (ii) and also for examples (iii) and (iv) results are thus discussed in detail for (ii) and (iv) only.

For the *ordered* froth (initial conditions (ii) and (iv) respectively) the size distribution $f(n)$ is illustrated in Figs. 2(a) and (b) for specific time steps. Here a single time step consists of the number of diffusion and equilibrium processes which have occurred. The evolution time t is measured in units of $\langle l_0 \rangle / k$ with k constant and defined in Eq. (1) (see [11]). The second moment μ_2 vs. time and the average area $\langle l \rangle$ vs. time are shown in Figs. 3 and 4. Agreement with the Abov–Weiner law is shown in Fig. 5 where a is approximately constant ($a \approx 1.05$).

In a *disordered froth* obtained from the Voronoi network the area of an n -sided cell may vary considerably and μ_2 provides an indicator of the degree and nature of disorder arising from increased dispersion in $f(n)$. For a *highly disordered froth* we have considered the evolution of (v) a system of 900 cells with initial $\mu_2 \approx 1.2$ and (vi) a system of 1600 cells with initial $\mu_2 = 1.6$ ($f(4) = 0.12$, $f(5) = 0.25$, $f(6)$

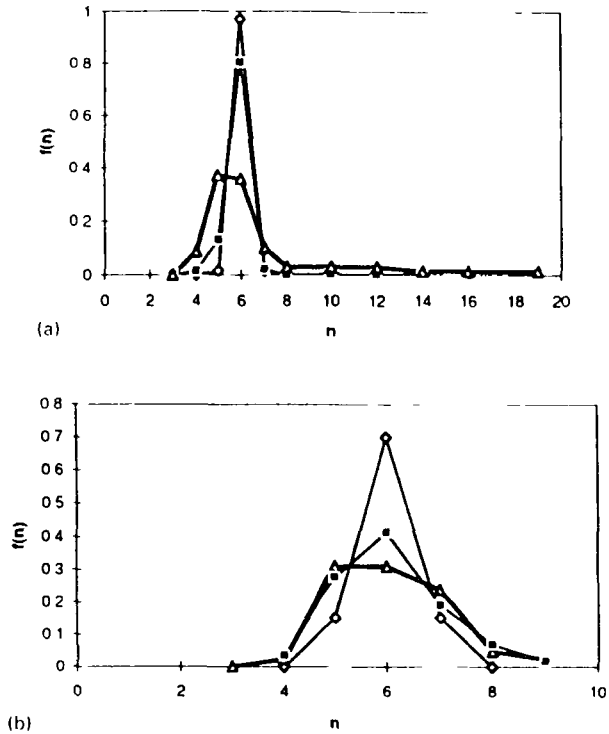


Fig. 2. (a) (b) The topological distribution $f(n)$ at time step of 0.120 200 for (a) a highly ordered and (b) a low ordered froth respectively; the heavier dark line represents $f(n)$ in the quasi-scaling or scaling state.

0.28 $f(7) = 0.09$ $f(9) = 0.02$ $f(10) = 0.01$. For a froth with *less disorder* (formed by reverse diffusion corresponding to low μ) in a polydisperse network, we have considered (vii) a system of 900 cells with initial $\mu \approx 0.22$ (minimum) and (viii) a system of 1600 cells with initial $\mu \approx 0.28$ ($f(5) \approx 0.13$ $f(6) \approx 0.74$ $f(7) \approx 0.12$ $f(8) = 0.01$). Again we give detailed results for examples (vi) and (viii) only, since behaviour is apparently similar under similar initial conditions.

Figs. 6(a) and (b) illustrate the topological distribution $f(n)$ at time steps of 0.120 260 corresponding to the initial, middle and final evolution stage for the disordered Voronoi structure. Figs. 7 and 8(a) and (b) show how the second moment μ^2 and average area $\langle A \rangle$ change with time for examples (vi) and (viii) respectively, and Fig. 9 illustrates the poor agreement with either the Abonyi or Abonyi–Weaire law (μ^2 not constant).

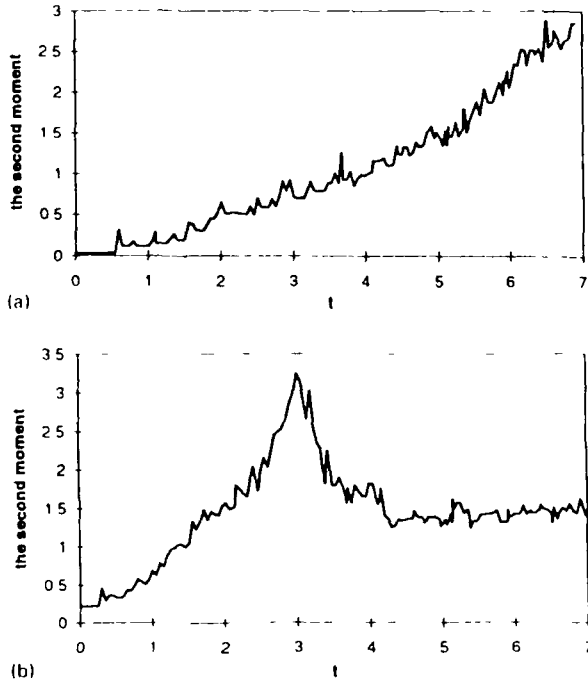
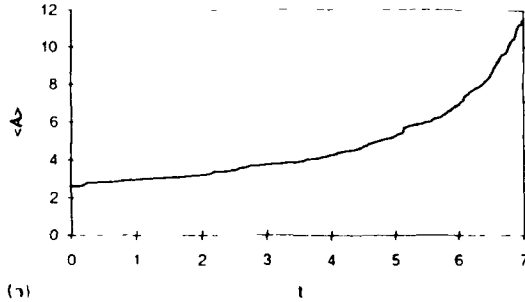


Fig. 3. μ_2 vs. time in a highly ordered froth with initial set up: (a) (b) (c) respectively.

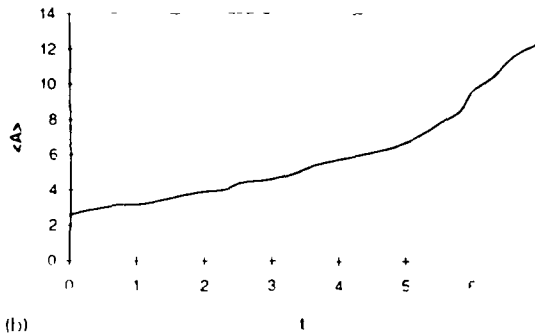
4 Discussion

For a *highly ordered* froth we observe that the side distribution $f(n)$ is markedly right skewed with the long tail reflecting the presence of many sided cells (Fig 2(a)). The second moment grows indefinitely with time $\mu_2 \sim t$ as a result (Fig 3(a)). Therefore if the system size is large enough we expect that μ_2 will continue to increase as larger many sided cells are formed. Our findings for μ_2 vs. t and also for the average area of all cells $\langle A \rangle = t / \nu \approx 2$ are in agreement with those of [2, 14, 20, 21].

The scaling state is reached when both $f(n)$ and μ_2 attain time invariant values and obviously does not apply for a *highly ordered* froth where neither $f(n)$ nor μ_2 tend to a fixed form. However if we truncate $f(n)$ at $n = n_c$ ($n_c^2 = 12$) we find that the side distribution $f(n_c)$ is effectively fixed after the initial period of evolution (see e.g. Fig. 2(c)) $f(4) \approx 0.08$, $f(5) \approx 0.37$, $f(6) \approx 0.35$, $f(7) \approx 0.09$. Such a froth may be said to be in a *quasi scaling state* although clearly μ_2 for all n continues to increase.



(a)



(b)

FIG. 1. The evolution of the expectation value of the operator A for $\beta = 1.7$.

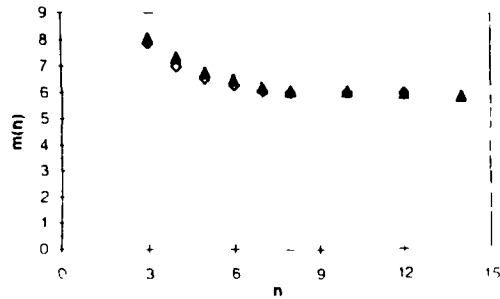


FIG. 1c. Moments of the distribution $P(n)$ for $\beta = 1.7$.

It is also interesting to note that a more appropriate measure of the breadth of the distribution is given by the third or fourth moment of the distribution $P(n)$.

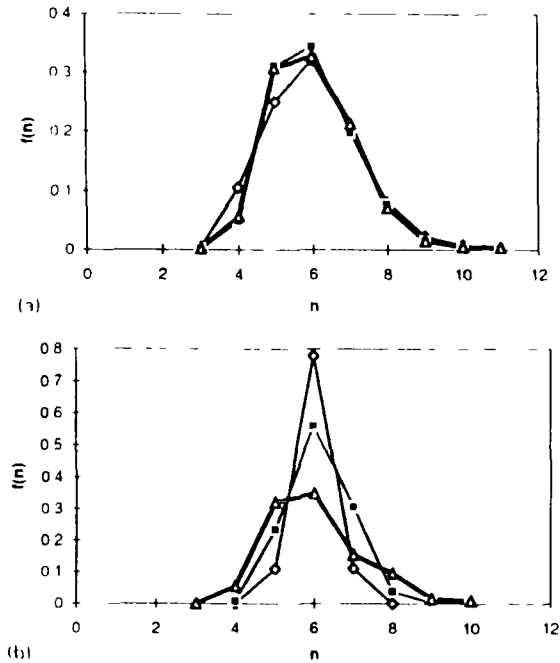


Fig. 3. (a) The side distribution $f(n)$ at time steps of 0.170, 200 for (iv) a high ordered froth and (viii) a low ordered froth through, i.e. the latter (dark line) depicts $f(n)$ in the scaling state.

The emergence of a quasi scaling state in the highly ordered froth, however, does not tend to support the view that Abov's results describe a transient stage [6, 16, 17, 20]. In fact, only 10^5 of initial 5000 cells remained for the value of μ_* given in this work [2]. An alternative explanation, that the long term evolutionary behaviour of a highly ordered froth reaches partial equilibrium, at best, obtains some support from the results presented here.

For the *low ordered* froth (initial conditions as in (iv)) (Fig. 2(b)), the side distribution $f(n)$ does tend to a fixed form, e.g. $f(5) \approx 0.31$, $f(6) \approx 0.30$, $f(7) \approx 0.26$ and the second moment μ_* vs. t exhibits one notable peak before finally reaching a stable value of $\mu_* \approx 1.5$ after initial fluctuations (Fig. 3(b)). The average area of the cells now behaves as $\langle A \rangle \sim t^{-2}$ where $1 < \nu < 2$. These scaling properties are consistent with those obtained by experiment [6]. We also find that there may be two peaks before μ_* reaches a stable value (e.g. in (vi)) with *clustered* defects (figure not shown). Furthermore, the Abov-Abov-Weimer law is obeyed in a *high low ordered* froth, respectively, in Fig. 5.

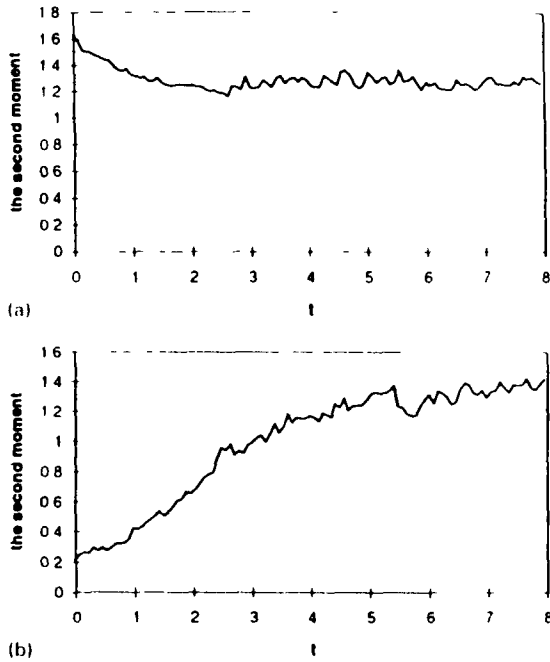


Fig. 6. μ vs. time in a high- and low-disordered froth with initial group $f(n) = (1, 0, 0, 1, 0, 0, 0, 0)$ respectively.

It appears, then, that normal as opposed to quist scaling in an ordered froth depends on the initial side distribution $f(n)$, i.e. the number of defects d with a corresponding threshold or critical value $\mu(d')$ partially determining the degree of disorder. Froths with initial defects of various types [21] either randomly seeded or clustered [14] may correspond to the same μ but exhibit different *evolutionary behaviour* before a final state. For example, one or more peaks may be observed for μ vs. t in the low ordered froth depending, respectively, on whether defects are seeded randomly or clustered. Nevertheless, if the system size is *large*, the ordered froth will tend to either a quist scaling or scaling state, regardless of the initial conditions. Otherwise, transient behaviour will be observed. Moreover, our results suggest that while $\mu(d')$ is around 0.2 for a system up to a thousand cells, this value increases for large system size, indicating that the proportion or density of defects in the overall froth determine the threshold value.

In contrast, for *high* or *low disordered* froths (Figs. 6.8) the side distribution $f(n)$ always tends to a fixed form (e.g. $f(5) = 0.32$, $f(6) = 0.5$, $f(7) = 0.18$) with a stable value of $\mu \approx 1.4$. Thus, the disordered froth in the scaling state, i.e. fixes the average net of all cells with t through $1 - t^{-1}$ with $t = 1$. Neither the

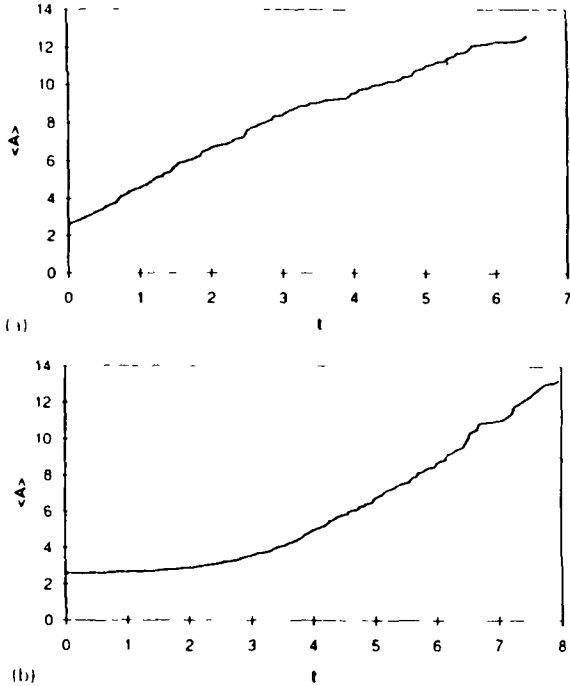


FIG. 5. Evolution of the total number of particles with initial strip (a) (iv) (bottom) and (b) (v).

above nor the Abow-Wentz law apply here according to our simulation results and in agreement with previous work for *disordered* froth evolution [1, 6, 10, 12, 14]. However, the so-called “ordered” initial condition ($\mu = 0.4$) obtained by reverse diffusion [12, 14] in fact is a less *disordered*, not a real *ordered* structure by our definition.

Consequently, our results support the existence of a universal scaling state, irrespective of system size, for a *disordered* froth based on a Voronoi construction. We find that μ vs. t has either a *lower* peak value ($\mu = 2.0$) than that observed for an *ordered* froth (Fig. 3(b)) or increases monotonically (Fig. 7(b)). While there appears to be agreement as to the location of the μ peak during *ordered* and *disordered* froth evolution, it seems likely that it is merely a coincident surface phenomenon since the peak values are different [23, 24]. (For example, we obtain a high peak (such as $\mu = 3.0$) for the *ordered* froth (under condition (iv)), whereas for the *disordered* froth we observe either a small peak ($\mu = 2.0$) or none.) This agrees with former work where μ was found to rise rapidly to a maximum ($\mu = 2.65$ and $\mu = 1.9$, respectively), then dropped to the constant value $\mu = 1.4$ [6, 12]. Furthermore, the phenomenon

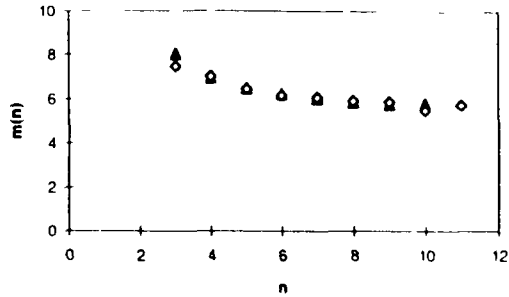


Fig. 2. Abovy-Weinreich distribution $f(n)$ and $f(n) = f(n) - f(n-1)$ for $f(n)$.

of more than one peak for μ vs. time appears to be a peculiarity of the *ordered* froth and we find no evidence for multiple peaks for any *disordered* system we have simulated.

5. Conclusion

By quantifying the amount of *order* (*disorder*) in the initial 2-D froth structure, we have reconciled apparent discrepancies in the scaling properties describing the froth evolution. Our direct simulation results for a *disordered* *highly ordered* froth are in agreement with those of original experiments of Smith [1] and Abovy [2] respectively. Our findings support the view that a quasi scaling state exists in a *highly ordered* froth where the side distribution $f(n)$ ($n < 12$) tends to have a fixed form, whereas $f(n)$ for all n is right skewed with corresponding unlimited growth of μ . However, a universal scaling state is achieved for both the *disordered* and *low ordered* froths where $f(n)$ has a fixed form corresponding to a system invariant asymptotic value of $\mu = 1.4$. Additionally, we suggest an alternative explanation for the curly result of Abovy [2] to the effect that an *ordered* froth does achieve a quasi scaling state as opposed to transience. We also confirm that the Abovy (or Abovy-Weinreich) laws apply only to the *ordered* froth.

References

- [1] C.S. Smith, *Metal Interfaces* (1952) 65.
- [2] D.A. Abovy, *Metallography* 13 (1980) 4.
- [3] H. Eyring, *J. Phys. A* 14 (1981) 298.
- [4] S. Eyring, *Phil. Mag.* B 57 (1988) 795.
- [5] J.A. Glazier, S.L. Glazier and J. Stavim, *Phys. Rev. A* 4 (1981) 90.
- [6] J. Stavim and J.A. Glazier, *Phys. Rev. Lett.* 57 (1986) 1318.
- [7] D. Weinreich and J.P. Kennedy, *Phil. Mag.* B 48 (1983) 248.
- [8] D. Weinreich and J.P. Kennedy, *Phil. Mag.* B 50 (1984) 127.

- [1] J. Weichert, D. Weure and J.J. Kermode, *Phil. Mag.* B 53 (1986) 15.
- [10] E. Fowleski, T. Naito and K. Nishihara, *Phil. Mag.* B 60 (1989) 399.
- [11] H. Kermode and D. Weure, *Comp. Phys. Commun.* 60 (1990) 75.
- [12] D. Weure and H. Lei, *Phil. Mag. Lett.* 62 (1990) 427.
- [13] J.A. Glazier, M.P. Anderson and G.S. Grest, *Phil. Mag. Lett.* (1990) 615.
- [14] I. Herdlic and H. Aref, *J. Fluid Mech.* 244 (1992) 233.
- [15] D. Weure and N. Rivier, *Contemp. Phys.* 25 (1984) 59.
- [16] J.A. Glazier and D. Weure, *J. Phys.: Condens. Matter* 4 (1992) 1867.
- [17] J. Stevens, *Rep. Prog. Phys.* 56 (1993) 733.
- [18] D. Weure and M.A. Fortes, *Adv. Phys.* 43 (1994) 685.
- [19] B. Levitt, *Phys. Rev. Lett.* 72 (1994) 4057.
- [20] D. Weure, *Phys. Rev. Lett.* 74 (1995) 3710.
- [21] H. J. Ruck and Y. Long, *J. Phys.: Condens. Matter* 7 (1995) 1553.
- [22] Y. Long, J.C.M. Mombach and J.A. Glazier, *Phys. Rev. E* 52 (1995) R 3333.
- [23] I. Herdlic, *Ph.D. Thesis* (1995).
- [24] B. Levitt and E. Doming, *Eur. Phys. Lett.* 32 (1995) 543.

Appendix B

This introduces the CA approach to scientific computing problems through a short illustration

Examples of Sequential and Multi-spin coding methods for cellular automata methods are given as follows

Program Sequential uses sequential updating and the most recent value of the neighbour spins and, as such, is not strictly CA methodology as it is generally realised for very many similar elements, since it is inefficient. More usually, cellular automata use simultaneous or parallel updating, where each spin at time $t+1$ takes its neighbour values at time t

Program Multi2 uses multi-spin updating (details see Section 2.2.3.3) for square lattice. A second index J is introduced besides the index I . Many loops run over I and J . A single logical function, OR, is used here to implement that a spin is up if at least one of its four neighbours is up, and the OR rule is over all the four neighbours. This achieved computing speeds which are much improved compared to the sequential method

```
PROGRAM SEQUENTIAL
PARAMETER L=960,LP1=L+1)
INTEGER MAX, ISEED, IP, IBM, I, ITIME, MAG
LOGICAL N(0..LP1)
REAL*4 P
READ(*,*) P, MAX, ISEED
IP=(2.0*P-1.0)*2147483648.0
IBM=2*ISEED-1
DO 10 I=1,L
    IBM=IBM*16807
    N(I)=IBM.LT IP
10 CONTINUE
DO 100 ITIME=1,MAX
    MAG=0
    DO 20 I=1,L
        IF(N(I)) MAG=MAG+1
20 CONTINUE
    WRITE(*,*) ITIME, MAG
    IF(MAG.EQ.L OR MAG.EQ.0) STOP
    N(0)=N(L)
    N(LP1)=N(1)
    DO 30 I=1,L
        N(I)=N(I-1) OR N(I+1)
30 CONTINUE
100 CONTINUE
STOP
END
```

```

PROGRAM MULTI2
INTEGER L, LW1, LW, NBIT, NB, MAX, ISEED, IP, IBM, I,
        J, ITIME, IDOWN, LTEMP1, LTEMP2

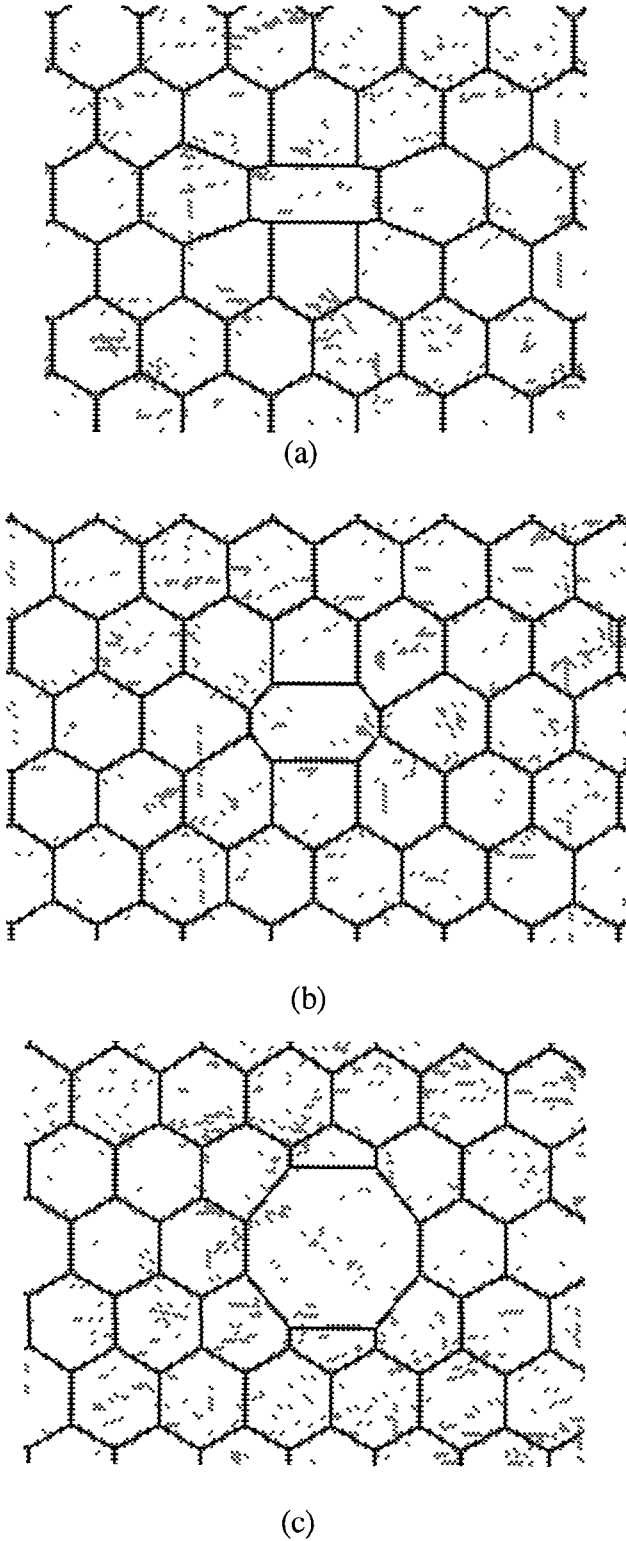
PARAMETER (LW=30, LW1=LW+1, NBIT=32, L=LW*NBIT, LP1=L+1)
INTEGER N(0:LP1, 0:LW1)
INTEGER M(L, LW)
REAL*4 P
ISHFTC(I, K)=IOR(ISHFT(I, K), ISHFT(I, K-NBIT))
READ(*, *) P, MAX, ISEED
IP=(2.0*P-1.0)*2147483648.0
IBM=2*ISEED-1
DO 20 I=1, LW
    DO 10 J=1, L
        N(J, I)=0
10    CONTINUE
20    CONTINUE
DO 50 NB=1, NBIT
    DO 40 I=1, LW
        DO 30 J=1, L
            N(J, I)=ISHFT(N(J, I), 1)
            IBM=IBM*16807
            IF(IBM.LT.IP)N(J, I)=IOR(N(J, I), 1)
30    CONTINUE
40    CONTINUE
50    CONTINUE
DO 200 ITIME=1, MAX
    IDOWN=0
    DO 120 I=1, LW
        DO 110 J=1, L
            IF(NOT(N(J, I)).NE.0) IDOWN=IDOWN+1
            IF(IDOWN EQ 0) STOP
110    CONTINUE
120    CONTINUE
    WRITE(9, *) ITIME, IDOWN
    DO 130 I=1, LW
        N(0, I)=N(L, I)
        N(LP1, I)=N(1, I)
130    CONTINUE
    DO 140 J=1, L
        N(J, 0)=ISHFTC(N(J, LW), NBIT-1)
        N(J, LW1)=ISHFTC(N(J, 1), 1)
140    CONTINUE
    DO 160 I=1, LW
        DO 150 J=1, L
            LTEMP1=IOR(N(J, I-1), N(J, I+1))
            LTEMP2=IOR(N(J-1, I), N(J+1, I))
            M(J, I)=IOR(LTEMP1, LTEMP2)
150    CONTINUE
150    CONTINUE

```

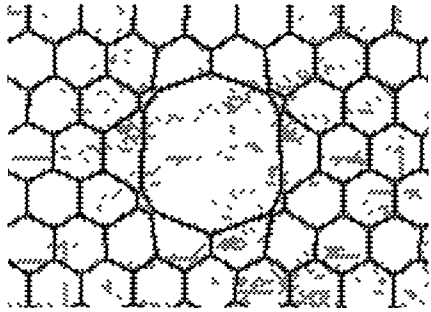
```
160      CONTINUE
        DO 180 I=1,LW
          DO 170 J=1,L
            N(J,I)=M(J,I)
170      CONTINUE
180      CONTINUE
200      CONTINUE
        STOP
        END
```

Appendix C

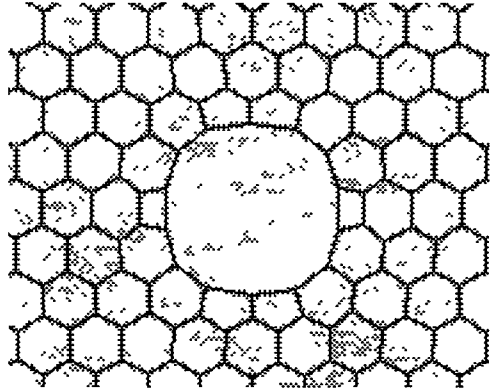
The various initial conditions of 2D froth with a single defect



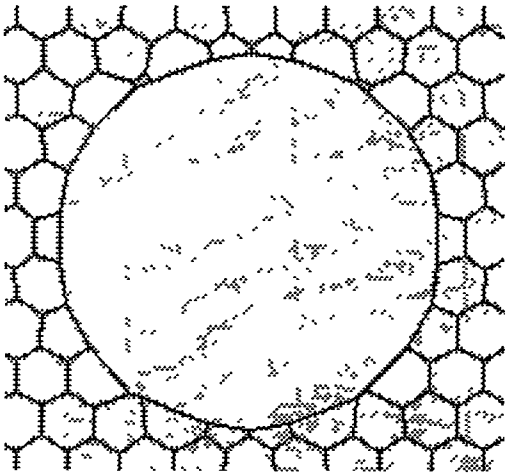
Figs C-1 (a) (b) (c) the various setups of a single defect in a perfect ordered froth



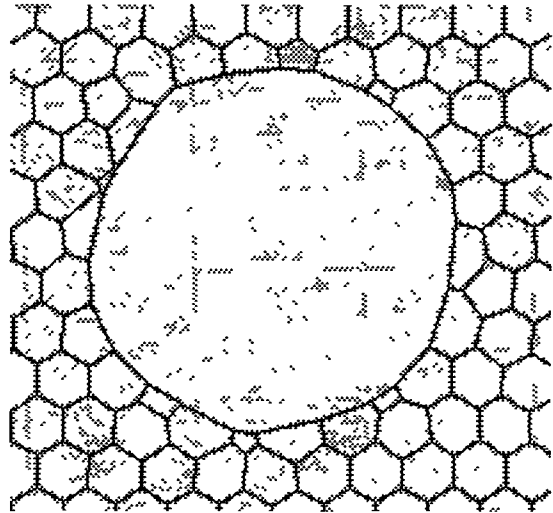
(a)



(b)

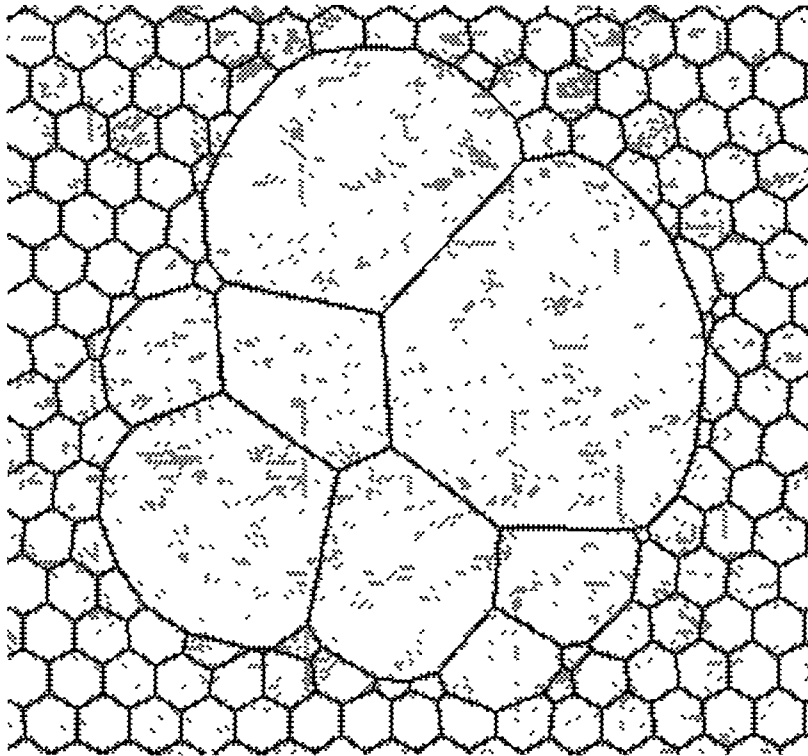


(c)

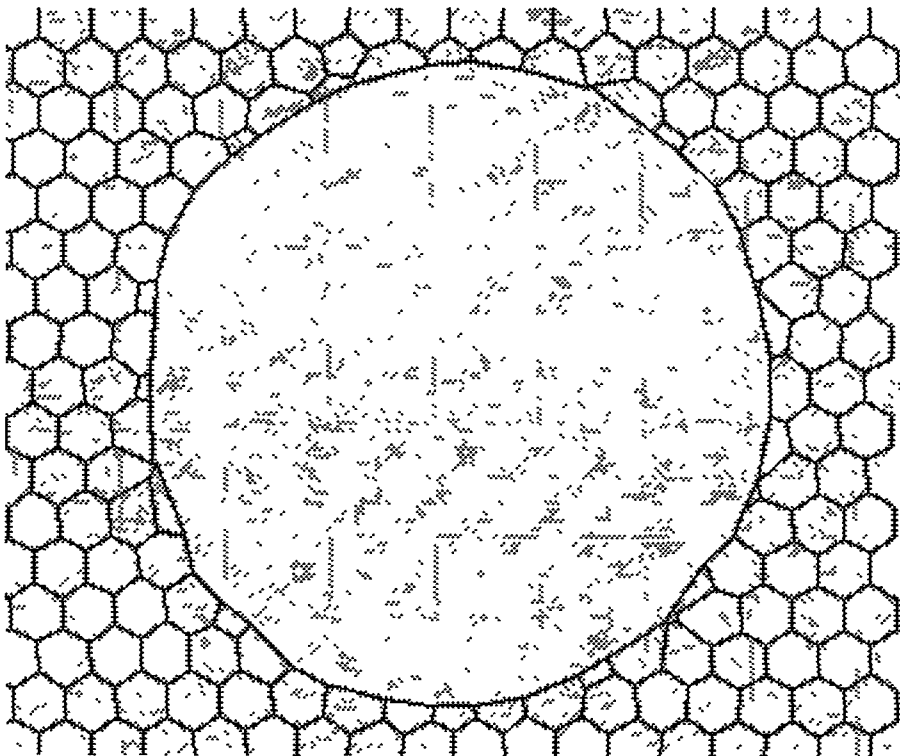


(d)

Figs C-2 (a)(b)(c)(d), the froths evolution at early stage



(a)



(b)

Figs C-3 (a)(b) later stage of froths evolution

Note (a) initial structure is pairs of pentagonal-heptagonal

Appendix D

Some detailed results obtained from direct simulation

We include here example outputs of a system of size 900 cells. After creating a Voronoi network containing 900 cells, the final network is given with statistics showing the distribution of the number of the cell sides with $\mu_2=1.38$. We only give the database obtained during time steps of 80-160, the second moment, μ_2 , is thus approaching its final stable value.

The results we obtained compared well with the results of Kermode and Weaire (1990) and overall agreement on the evolution was achieved with only minor difference in values quoted by those authors. This was partly due to the fact that the values of convergence CNVRMS and CNVRSD and scale factor SCALER were not the same (SCALER is the function of the long diagonal used in the hard-disk formulation in subroutine VSETUP, equivalent to the area perturbation scale in the further subroutine SETUP, see programme disk Appendix E).

D-1 gives the results for vertices of each cell of the network, and the value of pressure and area of each cell and the area change value during the evolution. The total area and pressure are also given.

Tables D-2, D-3 and D-4 show the distribution of the cells with n sides, and calculate the second moment, and show the distributions of average area of n -sided cells and average number of sides of neighbouring cells to n -sided cells. They are used to test correlation laws due to Lewis and Aboav (Aboav-Weaire).

STEP 160

VERTEX

NO	NEAREST	VERTICES	NEAREST	CELLS	FL	X-COORD	Y-COORD
1	66	13	3	1	109	106	14 235785 23 911783
2	613	64	3	109	157	776	14 862444 26 905449
3	4	2	1	109	1	157	15 376797 25 224663
4	359	3	5	1	255	157	16 640196 24 904900
5	59	4	12	1	478	255	16 981863 23 000408
12	5	13	16	82	478	1	16 425505 22 588690
13	15	12	1	1	106	82	14 515132 23 157747
14	16	15	77	691	172	82	14 423850 20 933317
15	13	70	14	691	82	106	13 665382 22 005440
16	19	12	14	82	172	478	16 496382 21 827108
18	24	59	19	478	504	892	17 748842 22 132517
19	18	16	23	172	504	478	16 993984 21 587917
22	28	23	722	172	388	856	15 968502 18 505581
23	18	26	58	216	892	504	18 795813 21 807293
26	24	27	32	145	216	504	19 359312 19 411854
27	23	31	26	145	504	856	18 987633 19 091444
28	29	22	96	388	706	856	16 025360 16 943342
29	30	28	113	706	777	856	17 015610 16 229120
30	29	35	31	42	856	777	19 308083 17 233746
31	27	30	34	42	145	856	19 514824 17 889366
32	44	26	34	145	479	216	20 117775 18 950672
34	32	31	36	42	479	145	19 742060 17 895344
35	124	36	30	42	777	311	19 724100 16 968477
36	39	34	35	42	311	479	19 993668 17 160540
39	36	123	40	250	479	311	21 270674 16 331905
40	41	39	724	250	594	479	22 413256 16 627193
41	44	40	42	594	451	479	22 783489 18.754583
42	46	41	854	594	103	451	23 807703 19 470989
44	48	32	41	479	451	216	21 689426 19 547426
46	42	871	47	36	451	103	23 862827 20 545918
47	48	46	50	36	513	451	23 204538 21 295223
48	53	44	47	451	513	216	21 989862 21 020212
50	51	47	630	36	784	513	23 757202 22 795881
51	50	626	52	376	513	784	22 658482 23 987236
52	51	55	53	122	513	376	20 978910 23 569798
53	48	52	58	122	216	513	20 612053 22 565615
55	623	56	52	122	376	406	19 853817 24 900927
56	60	57	55	122	406	255	19 539135 24 867834
57	59	58	56	122	255	892	18.770424 23 041708
58	53	57	24	892	216	122	19 226286 22 434191
243	242	244	253	8	682	410	6 462644 36 639771
244	1122	1129	243	8	410	736	6 317190 38 433025
246	250	261	241	132	347	16	7 832298 34 237354
250	251	246	242	347	682	16	7 415353 34 471523
251	252	259	250	16	682	316	5 843425 33 604534
252	253	268	251	316	682	463	4 948945 34 118961
253	252	243	1133	8	463	682	4 870450 35 635212
259	265	260	251	16	316	642	5 781813 32 493832

ITERATION 6

NO	NS	PRESSURE	CELL AREA	CHANGE
1	6	- 734571E-01	4 92142	0 537463E-03
3	6	0 446828E-01	2 05785	0 667421E-04
4	5	- 409704E-01	4 24862	- 136337E-02
7	5	0 399777	0 572335	- 104756E-03
8	7	- 140458	9 17200	- 228360E-02
10	4	0 459759	0 926247	- 442702E-03
11	6	- 251900E-01	4 85295	0 578980E-03
12	6	- 780218E-01	4 51595	0 418444E-03
14	6	- 900626E-01	4 48594	0 989777E-04
16	6	- 986054E-01	4 16690	0 419421E-02
22	9	- 226387	11 3768	- 959548E-04
23	5	0 303571	0 723332	0 542479E-03
24	6	- 109859	2 28559	- 175298E-02
26	8	- 244135	11 9532	0 226221E-02
27	5	0 481529E-01	2 10140	- 543950E-04
28	5	0 239352	0 754791	0 102105E-03
30	7	- 186504	10 2727	0 197343E-03
32	7	- 172032	5 22058	- 627232E-05
36	6	- 366451E-01	3 38441	- 101583E-02
39	7	- 190857	9 64751	- 160671E-02
42	5	0 328208	0 428812	- 245296E-03
165	6	- 803328E-01	4 73208	- 130497E-03
167	5	0 186709	1 59137	- 884209E-03
170	7	- 192074	4 67609	- 292118E-03
172	7	- 116524	7 39918	0 331481E-06

260	276	261	259	16	642	377	6	976846	31	596193	
261	321	246	260	16	377	132	7	471171	31	741131	173
265	259	267	271	584	642	316	4	062208	31	711395	
267	274	265	268	316	550	584	3	571759	32	010986	174
268	267	252	269	463	550	316	3	504604	33	205044	
269	1192	268	1188	463	832	550	2	251642	33	828094	175
282	291	284	281	397	880	280	7	775933	27	575993	188
284	285	282	314	280	570	397	8	392872	28	740221	
285	284	321	276	377	397	570	7	526342	30	760241	189
286	281	278	288	773	880	813	5	229830	27	182684	
288	286	298	289	843	880	773	5	346999	25	806343	190
289	288	295	302	840	880	843	6	237485	25	371269	
291	302	315	282	280	880	875	8	284877	26	797705	191
295	301	289	297	843	314	840	6	149061	24	400862	
297	298	299	295	314	843	900	5	215492	23	997952	192
1707	1708	1660	1706	98	744	810	38	056274	12	301379	865
1708	1707	1697	1651	237	810	744	37	854076	12	5219135	
1710	1706	1703	1697	351	744	193	38	452927	13	089301	867
1711	1714	1703	1712	193	656	408	40	351822	15	385736	
1712	1346	1347	1711	656	193	751	41	716499	14	992019	868
1714	1718	1719	1711	408	656	633	40	339657	15	786549	
1716	1703	1719	1694	249	351	408	39	618011	15	544519	869
1718	1714	1347	1720	775	633	656	40	914494	16	150940	
1719	1722	1716	1714	408	633	249	39	928764	15	931385	872
1720	1718	1622	1721	490	633	775	40	756325	17	477066	
1762	1768	995	1763	254	861	491	48	062065	10	641710	
1763	1758	1764	1762	861	254	121	47	406715	11	295651	888
1764	1763	1349	1363	891	861	121	45	128159	11	401845	
1766	1767	1356	1770	527	604	861	45	192154	8	668905	889
1767	1768	1766	1771	604	737	861	46	400455	8	252031	
1768	1767	981	1762	491	861	737	47	965164	9	224290	891
1769	1349	1760	1337	577	189	121	46	919758	14	168591	
1770	1376	1383	1766	604	527	530	44	895882	8	314537	892
1771	1767	1383	1788	348	737	604	46	123409	6	909466	
1774	1212	976	1775	556	720	756	51	883045	4	783600	895
1775	1774	1776	1778	428	720	556	51	064667	4	449310	
1776	982	1779	1775	428	556	737	49	715027	5	390654	896
1778	1211	1775	1468	428	588	720	51	083378	3	990723	
1779	1776	1788	1467	158	428	737	48	259884	4	679558	897
1780	1460	1461	1210	868	588	489	51	105156	0	674767	
1788	1771	1391	1779	158	737	348	46	752892	5	395498	898
1789	1160	1138	1146	63	558	384	51	742752	39	322708	
1794	1797	1380	1670	192	268	447	39	111568	5	948791	900
1797	1387	1794	1674	268	542	447	39	239159	5	429935	

TOTAL AREA 2338 27

TOTAL PRESSURE 0 685453E-06

6 - 127881	6 13436	0 378272E-02
5 0 244289	0 578846	- 283463E-04
6 0 123797E-01	2 51060	0 337373E-03
6 - 172829E-01	3 86964	0 264915E-02
7 - 126857	5 68831	- 479773E-04
5 0 302527	0 389218	- 457808E-04
4 0 490216	0 638784	- 767139E-04
8 - 218788	13 1569	- 713820E-03
5 0 156587	1 16659	- 155696E-04
5 0 403695E-01	2 64290	0 940509E-03
6 - 157173	4 26378	- 387237E-04
8 - 247038	9 62451	- 886680E-03
7 - 143567	8 58892	- 347733E-02
6 - 133162	8 77753	- 214513E-02
6 0 390286E-02	3 99806	0 122788E-02
5 0 218235	0 989011	0 964927E-06
5 0 147794	1 26644	0 913142E-04
8 - 256342	9 02707	0 614685E-03
8 - 189778	11 6216	0 708230E-04
6 - 449861E-01	3 46774	0 715620E-04
6 - 789616E-01	2 36365	0 747760E-03
7 - 155483	11 6688	- 458885E-02

NUMBER CELLS REMAINING 509

* * * * * S T A T I S T I C A L * * * * *

INITIAL CONFIGURATION 60 BY 30 SYSTEM -----> 1800 VERTICES , 900 CELLS

CONVERGENCE (EQUIL) - 0 5000E-02 TOLERANCE (DIFFUS) - 0 0000E+00

OPTIONS -----> 0, 0, 0, 0, 0, 0, 0, 0, 0, 0, 0, 0, 0, 0, 0, 2, 0, 0, 0, 0

NUMBER STEPS PERFORMED - 160 FINAL CELL COUNT - 509 NUMBER OF TOPOLOGICAL CHANGES -----> T1 - 342 T2 -181

PROGRAM ROUTE -----> SYSTEM PERIODIC /INPUT - FOR 31 DAT /EQUIL CALLS - 80 DIFFUS CALLS - 84

STATISTICS - - - - - TABLE A

Distribution of the number of cells with n sides over 160 steps showing 80 points

STEP	3	4	5	6	7	8	9	10	11	12	TOTAL	NO	T1	MU2
81	0	33	209	251	135	45	11	3	1	0	688	3	1	203
82	0	29	214	247	136	43	11	3	1	0	684	5	1	184
83	0	27	214	247	135	43	10	3	1	0	680	4	1	165
119	0	29	190	202	130	39	9	2	1	0	602	14	1	213
120	1	27	188	201	133	39	7	2	1	0	599	7	1	192
121	0	28	187	202	128	42	6	2	1	0	596	7	1	185
122	2	24	188	200	130	39	7	2	1	0	593	6	1	194
123	0	24	190	200	128	41	5	2	1	0	591	0	1	151
124	1	22	192	197	127	42	5	2	1	0	589	5	1	165
125	0	21	192	200	125	42	4	2	1	0	587	1	1	128
126	1	19	191	201	122	42	4	2	0	1	583	6	1	149
127	0	17	193	199	118	42	4	2	1	0	576	7	1	111
128	2	14	194	197	119	42	4	2	1	0	575	3	1	127
154	0	26	160	180	109	37	7	2	0	0	521	3	1	182
155	1	25	160	180	107	38	6	3	0	0	520	2	1	212
156	2	25	158	183	98	39	10	2	0	0	517	16	1	261
157	0	25	158	185	99	37	9	2	0	0	515	0	1	200
158	1	24	157	187	96	38	8	3	0	0	514	2	1	226
159	1	22	159	185	98	36	8	3	0	0	512	3	1	207
160	0	20	161	185	98	34	9	2	0	0	509	2	1	155

STATISTICS - - - - - TABLE B
 Distribution of the average area of n-sided cells over 160 steps showing 80 points

STEP	3	4	5	6	7	8	9	10	11	12
81	0 0000E+00	0 4322	1 428	3 334	5 306	7 366	8 573	10 84	14 09	0 00E+00
82	0 0000E+00	0 4644	1 423	3 369	5 360	7 383	8 617	10 90	14 16	0 00E+00
83	0 0000E+00	0 5677	1 419	3 395	5 373	7 464	8 724	10 94	14 20	0 00E+00
84	0 0000E+00	0 5711	1 409	3 396	5 388	7 630	8 886	10 25	14 31	0 00E+00
89	0 0000E+00	0 6117	1 411	3 424	5 502	7 515	9 641	10 51	14 65	0 0000E+00
138	0 0000E+00	0 4498	1 722	3 975	6 787	9 610	10 30	17 27	0 0000E+00	
139	0 0000E+00	0 3791	1 755	3 975	6 822	9 434	10 39	17 38	0 0000E+00	
140	0 2118E-01	0 5210	1 817	4 014	6 771	8 951	11 53	16 43	0 0000E+00	
141	0 8113E-01	0 4027	1 800	4 040	6 772	9 860	11 46	16 70	0 0000E+00	
142	0 8291E-03	0 5532	1 809	4 049	6 840	9 819	12 29	14 54	0 0000E+00	
143	0 0000E+00	0 6037	1 807	4 065	6 888	9 981	12 06	16 87	0 0000E+00	
144	0 1451E-01	0 6992	1 819	4 028	6 930	10 06	11 63	16 90	0 0000E+00	
151	0 0000E+00	0 7349	1 869	4 072	7 139	10 27	12 86	17 44	0 0000E+00	
152	0 0000E+00	0 7147	1 858	4 072	7 149	10 29	12 89	17 48	0 0000E+00	
153	0 0000E+00	0 8297	1 900	4 060	7 127	10 34	12 51	17 51	0 0000E+00	
154	0 0000E+00	0 8478	1 909	4 063	7 094	10 28	12 94	17 54	0 0000E+00	
155	0 2421E-01	0 8503	1 888	4 096	7 106	10 28	13 23	15 71	0 0000E+00	
156	0 2289E-01	0 7581	1 863	4 211	7 225	9 914	12 38	17 87	0 0000E+00	
157	0 0000E+00	0 7327	1 850	4 221	7 233	10 26	12 81	17 93	0 0000E+00	
158	0 2109E-01	0 7945	1 848	4 247	7 240	10 22	13 26	15 12	0 0000E+00	
159	0 3781E-01	0 8238	1 858	4 245	7 301	10 32	12 84	16 48	0 0000E+00	
160	0 0000E+00	0 8775	1 867	4 254	7 407	10 43	12 94	18 09	0 0000E+00	

STATISTICS - - - - - TABLE C

Distribution of the average number of sides of cells neighbouring n-sided cells over 160 steps showing 80 points

STEP	3	4	5	6	7	8	9	10	11	12
81	0 0000E+00	6 871	6 432	6 203	6 028	5 906	5 808	5 633	5 455	0 0000E+00
82	0 0000E+00	6 879	6 430	6 198	6 034	5 881	5 798	5 633	5 455	0 0000E+00
83	0 0000E+00	6 926	6 417	6 198	6 031	5 890	5 789	5 567	5 455	0 0000E+00
84	0 0000E+00	6 955	6 415	6 200	6 024	5 905	5 815	5 550	5 455	0 0000E+00
85	0 0000E+00	6 963	6 413	6 197	6 026	5 902	5 815	5 550	5 455	0 0000E+00
86	0 0000E+00	6 972	6 413	6 194	6 020	5 909	5 840	5 600	5 455	0 0000E+00
87	0 0000E+00	6 963	6 416	6 195	6 020	5 899	5 833	5 600	5 455	0 0000E+00
88	7 000	6 944	6 424	6 196	6 025	5 905	5 889	5 600	5 455	0 0000E+00
132	0 0000E+00	7 021	6 399	6 193	5 989	5 938	5 762	5 900	5 545	0 0000E+00
133	8 000	7 115	6 409	6 210	5 992	5 936	5 778	5 800	5 545	0 0000E+00
134	0 0000E+00	7 000	6 393	6 202	5 992	5 908	5 764	5 833	0 0000E+00	0 0000E+00
135	0 0000E+00	7 021	6 391	6 200	5 992	5 902	5 764	5 833	0 0000E+00	0 0000E+00
150	0 0000E+00	6 912	6 444	6 184	5 990	5 896	5 762	5 850	0 0000E+00	0 0000E+00
151	0 0000E+00	6 893	6 456	6 180	5 999	5 878	5 746	5 800	0 0000E+00	0 0000E+00
152	0 0000E+00	6 893	6 456	6 180	5 999	5 878	5 746	5 800	0 0000E+00	0 0000E+00
153	0 0000E+00	6 927	6 465	6 181	6 004	5 879	5 750	5 800	0 0000E+00	0 0000E+00
154	0 0000E+00	6 904	6 466	6 183	6 008	5 878	5 762	5 800	0 0000E+00	0 0000E+00
155	8 333	6 940	6 466	6 187	6 011	5 885	5 741	5 833	0 0000E+00	0 0000E+00
156	7 833	6 960	6 470	6 211	6 016	5 865	5 744	5 800	0 0000E+00	0 0000E+00
157	0 0000E+00	6 930	6 462	6 199	6 006	5 865	5 741	5 800	0 0000E+00	0 0000E+00
158	8 000	6 979	6 464	6 198	6 010	5 875	5 764	5 733	0 0000E+00	0 0000E+00
159	8 000	6 943	6 459	6 196	6 013	5 865	5 750	5 800	0 0000E+00	0 0000E+00
160	0 0000E+00	6 938	6 448	6 186	6 009	5 860	5 765	5 800	0 0000E+00	0 0000E+00

Appendix E

Diskette A

Sandpile for --Sandpile Model program

Dissand for ---Dissipative Sandpile Model program

Zz for -----Direct Simulation program

Plan c -----Graphics program

Mc for -----MC method program

12

13

14